


November 2023

CHEMICAL MODIFICATION AND EVALUATION OF CELLS TOWARDS USE AS DELIVERY TOOLS

Bishnu Prasad Joshi
University of Massachusetts Amherst

Follow this and additional works at: https://scholarworks.umass.edu/dissertations_2

 Part of the [Analytical, Diagnostic and Therapeutic Techniques and Equipment Commons](#), [Laboratory and Basic Science Research Commons](#), and the [Organic Chemicals Commons](#)

Recommended Citation

Joshi, Bishnu Prasad, "CHEMICAL MODIFICATION AND EVALUATION OF CELLS TOWARDS USE AS DELIVERY TOOLS" (2023). *Doctoral Dissertations*. 3000.
<https://doi.org/10.7275/36001760> https://scholarworks.umass.edu/dissertations_2/3000

This Open Access Dissertation is brought to you for free and open access by the Dissertations and Theses at ScholarWorks@UMass Amherst. It has been accepted for inclusion in Doctoral Dissertations by an authorized administrator of ScholarWorks@UMass Amherst. For more information, please contact scholarworks@library.umass.edu.

CHEMICAL MODIFICATION AND EVALUATION OF CELLS TOWARDS USE AS
DELIVERY TOOLS

A Dissertation Presented

By

Bishnu Prasad Joshi

Submitted to the Graduate School of the
University of Massachusetts Amherst in partial fulfillment
of the requirements for the degree of
DOCTOR OF PHILOSOPHY

September 2023

Chemistry

© Copyright by Bishnu Prasad Joshi 2023,
All Rights Reserved

CHEMICAL MODIFICATION AND EVALUATION OF CELLS TOWARDS USE AS
DELIVERY TOOLS

A Dissertation Presented

By

BISHNU PRASAD JOSHI

Approved as to style and content by:

Michelle E. Farkas, Chair

Vincent M. Rotello, Member

Mingxu You, Member

Ashish Kulkarni, Member

Ricardo Metz, Department Head
Department of Chemistry

DEDICATION

In the loving memory of my father, Dhanaraj Joshi.

ACKNOWLEDGEMENTS

My sincere gratitude to my advisor Prof. Michelle E. Farkas for her guidance and support over the years. Starting from her guidance and inspiration for me to apply to UMass-Amherst, I am grateful to her mentoring in academics, communication, writing with timely feedback, and encouragement. In addition to these, her commitment to and advocacy of diversity along with the practices of accepting students in lab from diverse backgrounds has inculcated values of inclusion in me. Apart from her valuable pieces of advice on time management, keeping up deadlines, and personal development, she has shown consideration even to my personal problems outside of academics whenever I approached her with them. So grateful to have such a holistic mentor!

I thank my committee members, Prof. Vincent Rotello, Prof. Mingxu You, and Prof. Ashish Kulkarni for their advice and support. I would especially like to thank Prof. Rotello for the collaborative work of his group for my research. Similarly, I extend my gratitude to Prof. Mingxu You and Prof. Ashish Kulkarni for their encouragement and support I received whenever I approached them.

I am also grateful to all the co-workers of the Farkas group: Dr. Joseph Hardie, Dr. Javier Mas-Rosario, Dr. Sujeewa Sampath L.D., Jeffrey D. Cullen, Kyle J. Winters, and Kaitlyn Chhe for their help and comradeship. I would like to especially thank Jeffrey and Kyle, who worked with me on the material and writing in Chapter 4 and the Appendix. I also thank the junior graduate students of Farkas lab -- Claudia, Emmanuel, and Bhavna. I wish them the best of luck in taking the ongoing projects of the lab forward. Similarly, I

acknowledge the co-operation of the undergraduate students who worked with me on different projects. I thank Cameron Sanders and Ryan Thai in particular.

My sincere gratitude for the support of my family. I thank my parents, brother, and sister-in-law and particularly my wife Ayousha Shahi for bearing with me during the journey of my Ph.D.!

ABSTRACT

CHEMICAL MODIFICATION AND EVALUATION OF CELLS TOWARDS USE AS DELIVERY TOOLS

SEPTEMBER 2023

BISHNU PRASAD JOSHI

M.S., SRI SATHYA SAI INSTITUTE OF HIGHER LEARNING

Ph.D., UNIVERSITY OF MASSACHUSETTS AMHERST

Directed by: Professor Michelle E. Farkas

Endogenous cells are being studied for use in various applications, such as next generation therapeutics and drug delivery vehicles. This is on account of their biocompatibility, amenable distribution profiles, and in many instances, recruitment to and localization at diseased tissues. Multiple cell types have been employed, including macrophages, stem cells, red blood cells, and T cells. Most examples of cell-based delivery utilize phagocytosed entities as cargo. However, uniform, and timely loading and release of phagocytosed agents from the cellular vehicles remains a challenge. In this thesis, I describe the use and study of approaches that circumvent these limitations, while harnessing the beneficial characteristics of cells as targeted agents. Through collaborative work, we combined the inherent homing properties of macrophages with on-site manufacturing capabilities of bio-orthogonal nanozymes (NZs), by incorporating the latter into cells. We were able to show that the NZs can be internalized by macrophages without impacting their behavior, and while internalized, NZs can convert inactive pro-drugs to

their active forms. In the latter half of this thesis, I describe studies involving cell surface modifications, which can be used to append imaging and/or chemotherapeutic agents for delivery applications. I used different types of mild bioconjugation chemistries at native and installed moieties on immortalized, model macrophages. The covalent surface modifications were assessed and their effects on cellular characteristics like viability, motility, chemotaxis, and phenotypic polarization are reported. Further, I showed that the modified cells can be used to evaluate macrophage-cancer interactions in both *in vitro* and *in vivo* models. Continuing this line of work, I expanded the studies to primary and immortalized macrophages and stem cells. I characterized the N-hydroxysuccinimide (NHS) modification in terms of retention at the cell surface over time and determined effects on cellular characteristics like viability and migration. This work now sets the stage for further use of surface-modified cells as diagnostic tools and as delivery agents for therapeutics and molecular probes. In summary, this thesis explores the potential of cells for use in delivery and imaging applications beyond payload internalization, with a focus on facile chemical modifications at their surfaces.

TABLE OF CONTENTS

	Page
ACKNOWLEDGEMENTS.....	v
ABSTRACT.....	vii
LIST OF FIGURES.....	xiv
LIST OF TABLES.....	xvii
CHAPTERS	
1. INTRODUCTION: HARNESSING BIOLOGY TO DELIVER THERAPEUTIC AND IMAGING ENTITIES VIA CELL-BASED METHODS.....	1
1.1. Introduction.....	1
1.2. Cell types used for delivery.....	4
1.2.1. Leukocytes (monocytes/macrophages)	5
1.2.2. Stem cells (mesenchymal and neural)	5
1.2.3. Red blood cells.....	6
1.3. Cellular modifications and cargo loading for delivery applications.....	7
1.3.1. Phagocytosis, internalization, and transfection.....	8
1.4. Covalent and non-covalent cell surface modifications.....	13
1.4.1. Non-covalent surface modifications.....	14
1.4.2. Use of biotin-streptavidin linkage.....	16
1.4.3. Direct conjugation to native amino acids.....	18
1.4.4. Other cellular conjugation strategies.....	19
1.5. Perspectives on cell-based delivery	20

1.6. Dissertation overview.....	22
1.7. References.....	23
2. MACROPHAGE-ENCAPSULATED BIOORTHOGONAL NANOZYMES FOR TARGETING CANCER CELLS.....	33
2.1. Introduction.....	33
2.2. Materials and methods.....	35
2.2.1. Preparation of engineered macrophages (RAW_NZ).....	36
2.2.2. Chemotaxis/Boyden chamber assay procedure.....	36
2.2.3. Coculture of NZ with HeLa Cells.....	37
2.2.4. Cytotoxicity measurements of prodrug and drug.....	38
2.2.5. Viability comparison following prodrug activation by RAW_NZ	38
2.3. Results and discussion.....	39
2.3.1. Fabrication of nanozymes.....	39
2.3.2. Loading of nanozymes into macrophages.....	39
2.3.3. Catalytic activity of nanozymes in living cells.....	40
2.3.4. Efficient chemotactic migration of RAW_NZ.....	41
2.3.5. RAW-NZ kills cancer cells in co-culture models.....	43
2.4. Conclusion.....	46
2.5. References.....	46

3. SURFACE-MODIFIED MACROPHAGES FACILITATE TRACKING OF BREAST CANCER-IMMUNE INTERACTIONS	52
3.1. Introduction.....	52
3.2. Materials and methods.....	55
3.2.1. Reagents and cell lines.....	55
3.2.2. Biotin-(strept)avidin modification of macrophages.....	56
3.2.3. Direct NHS-ester modification of macrophages.....	56
3.2.4. Metabolic labeling/Staudinger ligation modification of macrophages.....	57
3.2.5. Wound healing/scratch assay.....	58
3.2.6. Chemotaxis/Boyden chamber assay.....	58
3.2.7. Coculture assays.....	59
3.2.8. Generation of <i>in vivo</i> tumor models and macrophage biodistribution studies.....	59
3.3. Results and discussion.....	60
3.3.1. Modification of macrophages to install fluorescent molecules.....	60
3.3.2. Macrophage migration and chemotaxis.....	66
3.3.3. Macrophage association with <i>in vitro</i> models of breast cancer.....	68
3.3.4. Chemically modified macrophages show tumor homing capabilities in a mouse model of cancer.....	71
3.4. Conclusion.....	73
3.5. References.....	73
4. EFFECTS OF FACILE CHEMICAL SURFACE MODIFICATIONS ON PRIMARY AND IMMORTALIZED MACROPHAGES AND STEM CELLS	78
4.1. Introduction.....	78

4.2. Materials and methods.....	83
4.2.1. Materials.....	83
4.2.2. Cell culture.....	83
4.2.3. Generation of conditioned media.....	84
4.2.4. Isolation of progenitor cells and differentiation into BMDMs and primary MSCs.....	85
4.2.5. NHS-biotin/avidin-FITC modification of cells	86
4.2.6. Confocal microscopy of modified cells.....	87
4.2.7. Assessment of changes in surface fluorescence over time.....	87
4.2.8. Viability studies.....	88
4.2.9. Chemotaxis assays.....	89
4.3. Results and discussion.....	90
4.3.1. Cell surface engineering with NHS-biotin chemistry.....	90
4.3.2. Tracking retention of cell-surface fluorescence over time	91
4.3.3. Viability studies.....	94
4.3.4. Motility studies.....	95
4.4. Conclusion and future directions.....	97
4.5. References.....	98
5. CONCLUSION AND FUTURE DIRECTIONS.....	103
APPENDIX. CHALLENGES OF BIOCONJUGATION OF AMINES TO OXIDIZED CELL SURFACE SIALIC ACID RESIDUES.....	106
A.1. Introduction.....	106

A.2. Materials and methods.....	108
A.2.1. Synthesis and characterization of biotin hexylamine.....	109
A.2.2. NH ₂ -FL (fluorescein hexylamine) modification of cells.....	111
A.2.3. NH ₂ -biotin/avidin-FITC modification of cells.....	112
A.2.4. NHS-biotin/avidin-FITC modification of cells.....	112
A.2.5. Confocal microscopy of modified cells.....	113
A.2.6. Assessment of changes in surface fluorescence over time.....	113
A.3. Results and discussion.....	114
A.3.1. Cell surface engineering with NH ₂ -sialic acid chemistry.....	114
A.3.2. Tracking retention of cell-surface fluorescence and internalization over time.....	120
A.3.3. Inconsistency in bioconjugation of amine-handles to sialic acid residues.....	123
A.4. Conclusion and future directions.....	125
A.5. References.....	125
 BIBLIOGRAPHY.....	 127

LIST OF FIGURES

Figure	Page
Figure 1.1. Cell types employed as delivery vehicles and locations where they are recruited/used to deliver agents to.....	4
Figure 1.2. Non-covalent cellular modifications for cargo delivery.....	7
Figure 1.3. Strategies for covalent cell surface modifications.....	17
Figure 2.1. Schematic representation of macrophage-mediated delivery of bio-orthogonal nanozymes (TTMA-NZ) for prodrug (pro-5FU) and pro-fluorophore (pro-Rho) activation selectively at tumor cells.....	35
Figure 2.2. Cellular uptake of nanozymes via assessment of Au and Pd components.....	40
Figure 2.3. Confocal images of pro-rhodamine 110 fluorophore (pro-Rho) activation by RAW_NZ as a function of time elapsed between nanozyme preparation and reaction....	41
Figure 2.4. Chemotaxis capabilities are retained by RAW_TTMA-NZ as determined by trans-well membrane assay.....	42
Figure 2.5. 5FU activation in co-culture system with RAW_NZ.....	43
Figure 2.6. Coculture of RAW_NZ with GFP-HeLa cells.....	44
Figure 2.7. Viability of NZ loaded RAW and HeLa cells.....	45
Figure 3.1. Macrophage contributions to cancer and its metastasis.....	53
Figure 3.2. Detailed scheme of three cell surface modification methods including step-by-step reaction conditions.....	61
Figure 3.3. Approaches for chemical modification of macrophages.....	62
Figure 3.4. Cellular fluorescence over time.....	64
Figure 3.5. Specific cellular labeling in the presence of both linkers and dyes applied to different macrophage types.....	64

Figure 3.6. Macrophage polarization following chemical modification.....	65
Figure 3.7. Macrophage phagocytosis following chemical modification.....	65
Figure 3.8. Motility and chemotaxis retained by functionalized macrophages.....	67
Figure 3.9. Similar behavior of modified suspended macrophages to one another and non-labeled cells exposed to CSF-1.....	68
Figure 3.10. Modified macrophage homing and interaction with cancer cells.....	70
Figure 3.11. Macrophage biodistribution in an immune-competent mouse model of breast cancer.....	72
Figure 4.1. Overview of approach used for modification of cells....	82
Figure 4.2. Comparison of conjugations to different cell types.....	90
Figure 4.3. Control experiments for cell modifications with NHS-biotin.....	91
Figure 4.4. Representative quenching images for NHS-biotin/avidin-FITC.....	93
Figure 4.5. Surface fluorescence over time in BMDMs, RAW 264.7 cells, primary MSCs, and hTERT MSCs after modification with NHS-biotin/avidin-FITC.....	93
Figure 4.6. Viability of cells 48 h post-modification with NHS-biotin/avidin-FITC.....	94
Figure 4.7. Migration and chemotaxis of NHS-biotin/avidin-FITC modified and control cells.....	96
Figure A.1. Comparison of NH ₂ -FL and NH ₂ -biotin/avidin-FITC bioconjugations at cell surface glycans.....	107
Figure A.2. Detailed scheme comparing cell surface lysine and glycan modification methods.....	108
Figure A.3. Synthesis of biotin hexylamine from D-biotin.....	109
Figure A.4. Comparison of attachment methods for sialic acid modifications.....	115
Figure A.5. Control experiments for amine modifications of sialic acids.....	116

Figure A.6. Representative images of multiple modification types in macrophages and stem cells.....118

Figure A.7. Examples of unsuccessful bioconjugations using NH₂-biotin/avidin-FITC and NH₂-FL.....119

Figure A.8. Representative quenching images for macrophages and stem cells after modification with NH₂-biotin/avidin-FITC or NH₂-FL.....121

Figure A.9. Surface fluorescence over time in macrophages and stem cells after modification with NH₂-biotin/avidin-FITC or NH₂FL.....122

Figure A.10. Viability of NH₂-biotin/avidin-FITC and NH₂-FL modified macrophages and stem cells 48 h post-modification.....123

LIST OF TABLES

Table	Page
Table 1.1. Cellular vehicles and their applications.....	4
Table 1.2. Cell surface modification methods.....	14

CHAPTER 1

HARNESSING BIOLOGY TO DELIVER THERAPEUTIC AND IMAGING ENTITIES VIA CELL-BASED METHODS

Reprinted (adapted) with permission from “Joshi, BP., Hardie, J., Farkas, ME., "Harnessing Biology to Deliver Therapeutic and Imaging Entities via Cell-Based Methods." *Chem. Eur. J.*, 24, (2018), 8717-8726.” Copyright (2018) European Chemical Societies Publishing.

1.1. Introduction

A variety of drug-delivery systems are in development and in use clinically as aids for the transportation of therapeutic entities to diseased sites within the human body. The administration of biologic and/or small molecule drugs via encapsulation or conjugation to a delivery vehicle can result in improved therapeutic characteristics by increasing the drug quantity transported to and retained at the targeted site. Cargo-bearing vehicles based on nanoparticles,¹ liposomes,² polymeric micelles,³ and hydrogels⁴ have been employed to improve the net efficacy of drugs delivered. The circulation half-lives and toxicity profiles of these entities can vary widely, depending on their composition and cargo. However, these traditional strategies generally rely upon passive targeting of disease areas,⁵ and often face various systemic and disease-specific biological barriers to delivery. For example, access to hypoxic areas, typically located within tumors,⁶ and crossing of the blood–brain barrier (BBB) to reach brain cells and tissue⁷ are both significant challenges. Even those entities that are “targeted “must first reach the site of interest in order for the targeting ligand (e.g. antibody, aptamer, peptide, or small molecule) to bind its receptor.⁸

While nanoparticles represent one of the most widely used vehicles, a recent statistical analysis of the literature revealed that only 0.7 % (median) of administered doses

reach solid tumors, indicating “a delivery problem.”⁹ Independently transported functionalized nanoparticles (NPs) can accumulate in non-desired locations, leading to unwanted reactivity and toxicity, or be cleared from circulation without reaching the tissue of interest.¹⁰ Depending on their size, systemically administered agents are generally cleared via the renal (kidney) or mononuclear phagocytic system (MPS, including the liver and spleen). These issues are generally the result of nanoparticles’ reliance on passive accumulation to reach their site of action, referred to as enhanced permeability and retention (EPR). Cell based delivery systems can mitigate these shortcomings via active recruitment of the cellular carrier to the diseased site. Hence, recruited (or “actively targeted”) vehicles are desirable for improved disease-specific treatment paradigms, and represent the next generation in drug delivery system development.

Cell-based therapeutic strategies have been used in the clinic and are being developed for the treatment of a variety of ailments, including Crohn's and other inflammatory diseases,¹¹ stroke,¹² cancer,¹³ and osteoarthritis.¹⁴ Taking these approaches as inspiration, drug delivery systems where circulatory cells are used as biological vehicles are emerging as active therapeutic carriers. Cellular delivery systems have several distinct advantages over others in terms of circulation time, inherent biocompatibility, and excellent *in vivo* distribution characteristics. But perhaps most importantly, cells are actively recruited and able to accumulate in particular tissues and at targets of interest.

Cellular delivery vehicles respond to chemotactic markers and cytokines present in disease microenvironments, facilitating the design of optimal cell vehicle-drug combinations.¹⁵ As a result, therapeutics carried by cells have a greater propensity to accumulate at the targeted tissues compared to those using no delivery or passively

targeting vehicles. With this increased specificity, the biological efficacy of the cargo is enhanced, and there is a reduction in off-target toxicity. Various cell types, including erythrocytes (red blood cells, or RBCs),¹⁶ stem cells (SCs),¹⁷ and phagocytic leukocytes (monocytes and macrophages),¹⁸ have been used for the specific delivery of genes,¹⁹ nanoparticles,²⁰ proteins,²¹ polymers,²² and small molecules.¹⁸ Similarly diverse are the applications they are used in, which include the imaging and/or treatment of cancer,²³ neurodegenerative,²¹ and cardiovascular diseases²⁰ (Table 1.1). Some cellular delivery systems have also been fine-tuned for the controlled release of therapeutics via external stimulus (e.g., light),²⁴ or environmental cues (e.g. pH).¹⁷ The unique properties of cell-based delivery systems have made them a focus of current research toward the development of novel drug delivery systems, with some already being tested in clinical trials.²⁵⁻²⁷

In this introductory chapter I will discuss cell-based vehicles, with a particular focus on modification methods as applied to different cell types. In addition, I will describe their applications, including cargo types and disease targets. I will also consider future work and remaining challenges toward the broad application of these actively targeted platforms.

Table 1.1. Cellular vehicles and their applications.

Cell types	Loading methods	Target tissues	Cargo
Leukocytes	phagocytosis, surface deposition/ modification	plaques, various tumors	genes, nanoparticles, small molecules
RBCs	phagocytosis, surface deposition/ modification	lungs, various tumors	enzymes, nanoparticles, small molecules
SCs	phagocytosis, surface deposition/ modification	brain, various tumors	genes, nanoparticles, small molecules

1.2. Cell Types Used for Delivery

After briefly introducing the main cell types being used and studied for delivery applications (Figure 1.1), I will discuss the methods utilized to modify these cells, along with cargo types, and conditions where they are being employed.

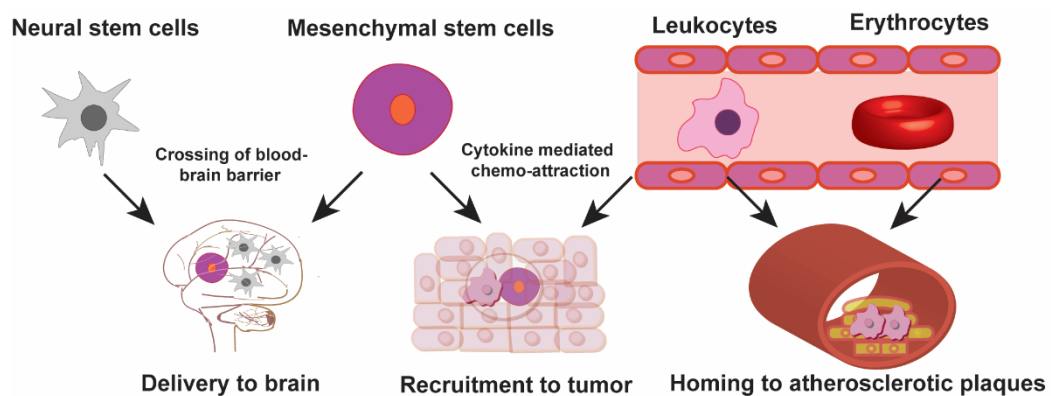


Figure 1.1. Cell types employed as delivery vehicles and locations where they are recruited/used to deliver agents to.

1.2.1. Leukocytes (monocytes/macrophages)

Leukocytes represent the largest category of cells used as delivery vehicles. Also referred to as white blood cells, they are cells of the innate immune system that originate from bone marrow and are involved in host defense. Monocytes are a class of leukocytes that circulate in the bloodstream and migrate to sites of infection or inflammation following chemotactic signals from cytokines. Once recruited, they differentiate into macrophages, which fulfill niche-specific functions.²⁸ Apart from their roles in the phagocytic engulfment of pathogens and clearance of apoptotic cell debris, macrophages are also involved in maintenance of homeostasis and tissue repair.²⁹

Both monocytes and macrophages inherently home to hypoxic, ischemic, and necrotic environments, which are often associated with disease. The mechanisms for hypoxia-mediated accumulation of macrophages at tumors³⁰ and ischemic areas of atherosclerotic plaques³¹ have been well studied.^{32,33} Monocytes and macrophages are often recruited to tumor sites via directed chemotactic migrations induced by signaling proteins. Many cancer types secrete chemo-attractants, such as macrophage colony stimulating factor (referred to as M-CSF or CSF-1)³⁴ and chemokine (C-C motif) ligand 2 (CCL2).³⁵ These homing mechanisms have been taken advantage of for the delivery of small molecule drugs,¹⁸ biological entities,³⁶ imaging agents,³⁷ and supramolecular constructs (NPs, polymers, etc.),²³ among others.

1.2.2. Stem cells (mesenchymal and neural)

Stem cells are pluripotent, plastic cells that can be differentiated in an inducible, tissue-specific manner.³⁸ As such, they have been broadly utilized in regenerative

medicine.³⁹ Two specific types of SCs are most prevalently used in cell-based delivery—mesenchymal stem cells (MSCs) and neural stem cells (NSCs). MSCs, which are also referred to as multipotent stem cells, are present in almost all types of tissue. They can differentiate into a variety of cell types including adipocytes, osteocytes, and muscle cells.⁴⁰ NSCs are self-regenerating cells of the central nervous system that can differentiate into neurons and brain cells.⁴¹

Both types of stem cells have the ability to migrate to specific tissues, tracking various cytokines that act as signals.⁴²⁻⁴⁶ For example, in liver injury, MSCs home toward the site via chemo-attraction mediated by stromal cell-derived factor 1 (SDF-1) and hepatocyte growth factor (HGF).⁴⁵ MSCs home to cancers via interactions with cytokines including interleukins IL-6 and IL-1 β , and growth factors such as transforming factor- β 1 (TGF- β 1) and SDF-1, secreted by the tumor stroma.⁴⁶ NSCs also show tumor-tropic behavior on account of their chemotaxis toward cytokines including IL-6 and VEGF, among others.⁴⁷ These characteristics have made SCs attractive carriers for specific delivery to tumors and CNS tissues. They are especially important in crossing the blood–brain barrier to access brain tissues, an application of which has progressed to clinical trials²⁵ (described in further detail below).

1.2.3. Red blood cells

Red blood cells (RBCs) are the most abundant non-nuclear blood cell type in vertebrates and have a circulation lifetime of approximately four months. RBCs can reach most internal tissues of physiological systems; their vascular access and membrane permeation abilities make them ideal carriers of drug molecules in sustained release

treatments.¹⁶ RBCs bearing particles on their cell surfaces have been reported to shield their cargo from hepatic and spleen filtration,⁴⁷ and have been used as nanoparticle vehicles.⁴⁸ While RBCs are non-phagocytic cells, methods have been developed for their internalization of cargo, facilitating another means of delivery.⁴⁹ Red blood cell-based agents have also been used clinically^{26,27} (described in further detail below).

1.3. Cellular modifications and cargo loading for delivery applications

There are several critical factors in the selection of a cell type for use as a delivery vehicle. These include compatibility of the carrier with the target site, and desired cargo loading strategy and release mechanisms. In this section, we provide an overview of cellular modification methods, along with specific examples of payloads and cell types employed (Figure 1.2).

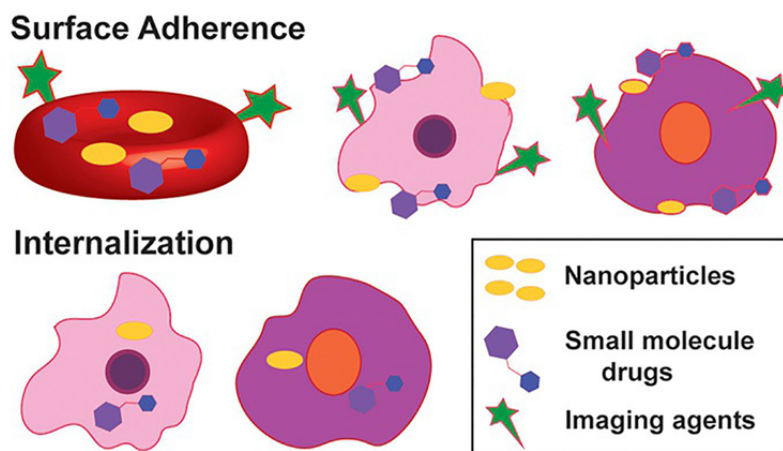


Figure 1.2. Non-covalent cellular modifications for cargo delivery. (Above) Red blood cells (red), leukocytes (pink) and stem cells (purple) have been noncovalently modified at the cell surface to display various agent types shown. (Below) Stem cells and leukocytes have the innate ability to internalize cargo shown. Specialized methods must be used for RBCs (not shown) to uptake therapeutic entities.

1.3.1. Phagocytosis, internalization, and transfection

The two general means of converting cells into delivery agents are via internalization of cargo (via various methods) or exterior modification of cells to display therapeutic entities. Phagocytosis (engulfment by the carrier cell) is perhaps the most straight-forward method of loading cargo into cells. Phagocytosis is dependent both on the size⁵⁰ and geometry⁵¹ of the entities being engulfed. Different strategies for efficient loading via this method have been explored, using nanoparticles,⁵² and polymeric micelles⁵³ and bubbles,⁵⁴ in addition to the encasement of small molecules.¹⁸⁻²³ While examples exist where cells are used as delivery intermediates *in situ*, including uptake of single-walled carbon nanotubes by circulating monocytes,⁵⁴ and nano-therapeutic engulfment and release by tumor-associated macrophages,⁵⁵ our focus here is on systems that include cells as part of the dosing regimen.

The phagocytic loading of monocytes, macrophages, and stem cells has been extensively used to deliver nanoparticles and other entities (Figure 1.2). In what is commonly referred to as a “Trojan horse” strategy,⁵² the imaging and/or therapeutic entity is encased within a biocompatible covering (in this case, a cell). Monocytes carrying gold nanoparticles have been used to image atherosclerosis using computed tomography (CT), with no effect on the viability or cytokine release by the cells.²⁰ Similarly, magnetic resonance imaging (MRI) has been employed to visualize macrophages bearing silica-coated, magnetic NPs in acute inflammation⁵⁶ and cancer⁵³ applications. However, the most widespread application of cellular vehicles is disease therapy.

Various gold-based agents have been internalized and used in photodynamic therapies, including MSCs with hollow gold nanoparticles,⁵⁶ macrophages with

nanoshells,⁵² and NSCs with gold nanorods.⁵⁷⁻⁶⁰ All of these entities have been shown to target tumor cells without significant undesired toxicity, and where assessed, were more effective than analogous agents utilizing only the EPR effect. In a multi-modality treatment, monocytes bearing super-paramagnetic iron oxide nano-particles, photosensitizers, and oxygen-loaded polymer bubbles were used to treat hypoxic areas of tumors.⁶¹

Cells have also been used to deliver chemotherapeutics, including macrophages directly loaded with doxorubicin (DOX)¹⁸ or paclitaxel (PAX),²³ or via internalization of nanoparticles or other entities bearing small molecules.^{23,53,62} In one example, following loading of 100 mg of DOX into 1 million macrophages, >80% of the cells remained viable for up to 72 h; cell-based delivery resulted in increased rates of survival in cancer models versus free DOX treatment.¹⁸ Similarly, liposomal-DOX delivered via macrophages outperformed DOX-liposomes alone.⁵³

While few examples exist, responsive systems have been developed for the specific release of drugs. Echogenic polymer bubbles and DOX-loaded vesicles susceptible to focused ultra-sound liberation, co-delivered in macrophages, resulted in substantial tumor uptake, while free NP-DOX largely accumulated in the liver; the cell-based agents penetrated 150 mm from the nearest blood vessel, however NPs were limited to 10–15 mm.²² Photo-release of drugs has been used with red, far-red, and near-IR light in erythrocytes,^{24,63} which can uptake entities as described in further detail below. Iron oxide nanoparticles phagocytosed by macrophages can also assist in “directing” cellular delivery via magnetic resonance imaging⁶⁴ or electromagnetic actuation.⁶⁵

Cargo-bearing cells loaded in this manner have been utilized to cross the blood–brain-barrier. In the delivery of drug-laden nanoparticles for the treatment of glioma, macrophage viability was not affected at doxorubicin concentrations up to $25 \mu\text{g mL}^{-1}$ and drug-loaded nanoparticles exhibited better tumor targeting efficiency and penetration.⁶² For a nano-formulated version of the therapeutic anti-oxidant enzyme catalase for Parkinson’s disease, the unidirectional influx rate of nanozyme was 0.026 in monocyte-loaded nanozyme versus $0.014 \mu\text{Lg}^{-1}$ every min for free nanozyme, indicating improved BBB penetration, in addition to superior half-life (3.3 versus 2.5 h).²¹

In some instances, phagocytic cell-based delivery systems have been compared to one another. In a direct assessment, doxorubicin- or paclitaxel-nanoparticle conjugates phagocytosed by macrophages were found to have greater efficacy than the small molecules internalized alone, or NP- or free-drugs independently dosed.²³ NSCs used to deliver platinum loaded silica nanoparticles, either loaded into or conjugated to cells were shown to result in higher levels of Pt in ovarian tumors compared to free drug or nanoparticle-drug conjugates, with substantially deeper tissue penetration.⁶⁶ Furthermore, no evidence of localization to normal tissue was observed. Choi and co-workers similarly showed that gold NPs engulfed by macrophages reach tumor sites more efficiently than NPs administered using other methods that access tumor interiors via leaky vasculature reliant EPR.⁵² In the discussion section below, we describe the necessity to perform additional comparative analyses for the field to move forward.

Since RBCs are inherently a non-phagocytic cell type, specialized strategies must be employed for encapsulation of cargo. In a hypotonic buffer of osmolarity less than 160 m-osm/L, RBCs undergo reversible membrane expansion, creating pores large enough for

macromolecules to permeate through.⁴⁹ This passive diffusion-mediated drug loading and subsequent release in isotonic environments is referred to as hypotonic dialysis (HD). HD has been employed to load therapeutic enzymes,^{27,67} nanoparticles,⁴⁸ and drugs.^{63,68} These same (“blood-banking”) conditions are also used for blood storage and transfusion. An apparatus, termed a “Red Cell Loader” (Sorin Group, Italy) has been developed to automate the process, and used to encapsulate a variety of drugs.⁶⁸ RBCs loaded with therapeutic enzymes and small molecule drugs for treatment of leukemia²⁷ and neurodegenerative diseases,²⁶ respectively, are in clinical trials. RBCs bearing l-asparaginase (GRASPA) are in Phase II for the treatment of Philadelphia chromosome-negative acute lymphoblastic leukemia, and have been shown to result in a 70% complete remission rate with limited toxicity.²⁷ Similarly, intra-erythrocyte administration of Dexamethasone (EryDex) was well-tolerated, and alleviated neurological symptoms of ataxia teleangiectasia, a rare neurodegenerative disease, in patients.²⁶ While most (including clinical) studies have utilized the HD method of cell loading, others exist, including chlorpromazine (cpz) treatment and liposomal fusion, which have been shown to be superior to HD in terms of loading efficiency, induction of hemolysis, and cellular deformation post-loading.⁶⁹

As living, actively targeted vehicles, cells have been used as generators of biological entities at targeted locations (referred to here as gene delivery). Because nucleic acid-based material cannot permeate the cell membrane and DNA cannot result in protein production independently, specialized methods for transfection are typically employed. These often require lenti- or adeno-viruses, although new techniques are being developed.⁷⁰ Stem cells and macrophages are the two cell types that have been most commonly used in these approaches.

Macrophages, which home to atherosclerotic plaques, have been used to generate Apolipoprotein E (ApoE), in order to reduce the size and presence of lesions.⁷¹ They have also been used to kill cancer cells via production of the therapeutic human protein cytochrome P4502B6 under hypoxic conditions.¹⁹ MSCs have been used to express anti-proliferative, angiogenesis-inhibiting matrix metalloproteinase C-terminal hemopexin-like domain fragments (PEX)⁷⁰ and immune proapoptotic molecules^{72,73} in a site-specific manner, while retaining cellular viability. Significant toxicities were not observed and improved anti-cancer effects were shown versus purified proteins alone and delivered via other means. Tumor-tropic NSCs have been genetically modified to secrete the anti-HER2 immunoglobulin Herceptin (trastuzumab) to inhibit the growth of HER2-expressing cancers.⁷⁴ The antibody produced *in situ* was shown to be functionally equivalent to the standard drug. While independently injected trastuzumab distribution was heterogeneous and localized near tumor vasculature, the NSC-produced antibody was distributed throughout the tumor.

Cells expressing an enzyme that converts a pro-drug into its active form for treatment of glioma, have recently undergone a first-in-human study.^{25,75} The NSCs generated cytosine deaminase to produce 5-fluorouracil from 5-fluorocytosine in the brain and were able to migrate to distant tumor sites. No dose-dependent toxicity or immunologic response was observed. Also prevalent in the development of this strategy toward cancer treatment is the use of cells to deliver several types of oncoviruses, including macrophages used to deliver/produce adenoviruses in prostate cancers,^{36,76} and MSCs with herpes simplex virus for breast cancer⁷⁷ and metastases,⁷⁸ measles virus for ovarian cancer,⁷⁹ and

adenovirus for pancreatic cancer,⁸⁰ all of which have been shown to significantly affect tumor burden with few side-effects.

1.4. Covalent and non-covalent cell surface modifications

Surface modification (also referred to as surface engineering) of carrier cells is emerging as a more frequently employed cargo loading method due to various factors (Table 1.2). By comparison with cargo internalization methods, it facilitates greater control over cellular loading and cargo release. There is also a diminished likelihood of the intracellular environment affecting and/or trapping the cargo itself. Surface modifications are amenable for use with any cell type, including non-phagocytic cells, which otherwise must undergo rigorous and sometimes toxic methods (e.g. electroporation) for membrane permeabilization to load cargo.⁸¹ Modifications where an entity is adhered to cell surface physically (via electrostatic forces or lithographic deposition) are here referred to as non-covalent surface modifications or adherence (Figure 1.2). While these methods are facile, there is little control over payload release. On the other hand, when cargo is covalently conjugated to the cellular vehicle, it is robustly attached,⁸² but these methods may require more involved chemical manipulation, including design of linkers for therapeutic release. While few direct comparisons have been made, surface functionalization does not generally result in dramatic changes to the modified cells, leaving their intrinsic properties, including homing capability, largely intact.

Table 1.2. Cell surface modification methods

Method	Modified Sites	Advantages	Disadvantages
cellular hitchhiking	non-specific	mild attachment conditions	weak adherence
cellular backpacks	local patches on cell surface	more stable adherence	complexity of deposition methods
biotin-avidin	variable thiols,	strong linkage, modular	large protein conjugation
native amino acids	primary amines	single step modification	internalization by cells, synthetic cargo modification
click chemistry	incorporated azido-sugars	chemically orthogonal	long incubation times, multi-step

1.4.1. Non-covalent surface modifications

Among non-covalent surface engineering strategies, one straight-forward method is via “cellular hitchhiking”—particle adhesion to cell surfaces via electrostatic, van der Waals, hydrogen bonding, and hydrophobic interactions.⁸³ Cationic entities can be immobilized on the hydrophobic cell surfaces mainly through interactions between these opposite charges.⁸⁴ Other weaker interactions, like van der Waals and hydrogen bonding assist this adherence, and displacement of water molecules at the interface gives an entropic advantage for NP assembly and stability at the surface.⁸⁵ Spherical polystyrene NPs adhered to red blood cells via this method have not been shown to affect RBC bio-distribution, avoiding splenic and hepatic filtration.⁴⁷ At the same time, the RBC-nanoparticles showed a threefold increase in blood circulation time, and sevenfold increased accumulation in the lungs versus free nanoparticles. Polymeric nanoparticles

similarly attached possessed extended circulatory lifetimes of almost 24 h compared to non-adhered NPs, greater than 95% of which were cleared in less than 30 min. As long as the particles remained attached to the cells, they stayed in circulation, however shear forces and cell-cell interactions result in passive removal followed by clearance via the liver and spleen.⁸²⁻⁸³

In another non-covalent surface modification method, the cargo is confined to a local vesicle (a “cellular backpack”) on the cell membrane.⁸⁶ These backpacks can be fabricated using layer-by-layer spray deposition of films consisting of alternating hydrogen bond donor-acceptor pairs, for example, PLGA/FITC-BSA [(PLGA = polylactic-*co*-glycolic acid), BSA = bovine serum albumin]. Particles delivered in this manner were shown to accumulate in inflamed tissues, while avoiding clearance organs; free particles showed threefold increased levels in the liver and spleen, and were almost undetectable in areas of inflammation.⁸⁶ Similarly, backpacks bearing the antioxidant enzyme catalase on macrophages were shown to facilitate blood brain barrier crossing in targeting brain inflammation *in vivo*.⁸⁷ While the presence of backpacks slowed cellular trafficking across the BBB, neither catalase alone nor unconjugated backpacks reached the brain. Cellular backpacks have also been employed by Rubner and co-workers to load monocytes with doxorubicin, which were viable for over 72 h, in order to target cancer.⁸⁸ Cells can also be non-covalently modified via small-molecule lipid association. For example, macrophages have been labeled with DiR (1,1-dioctadecyl-3,3,3,3-tetramethylindotricarbocyanine iodide) for tracking via fluorescence-mediated tomography (FMT) in the visualization and quantification of inflammatory responses *in vivo*.³⁷ Cell viability and function (phagocytosis, nitric oxide production, and adherence) were not affected.

1.4.2. Use of biotin-streptavidin linkage

Several different methods have been used to modify cell surfaces in a covalent manner for the conjugation of traceable and/or therapeutic entities for imaging and delivery applications (Figure 1.3). Biotin-streptavidin-based cargo loading methods take advantage of one of the strongest non-covalent interactions known in biology,⁸⁹ and are the most commonly employed. Biotin is a water-soluble, small biomolecule with high affinity for streptavidin-related proteins (dissociation constant (K_d) $\approx 10^{-15}$ M).⁹⁰ It can be conjugated to cell surfaces via various chemical reactions, resulting in display of streptavidin-linked entities following association. This method is biocompatible in the sense that it does not appear to affect cell viability, tissue tropism, or other characteristics. N-hydroxysuccinimide (NHS)-ester-biotin is a common, commercially available biotinylation reagent that can introduce biotin on membranes containing primary amines by forming a stable amide bond within hours at room temperature.⁹¹ This surface functionalization has found varied applications from cell targeting⁹² to loading drugs or therapeutic particles.⁹³

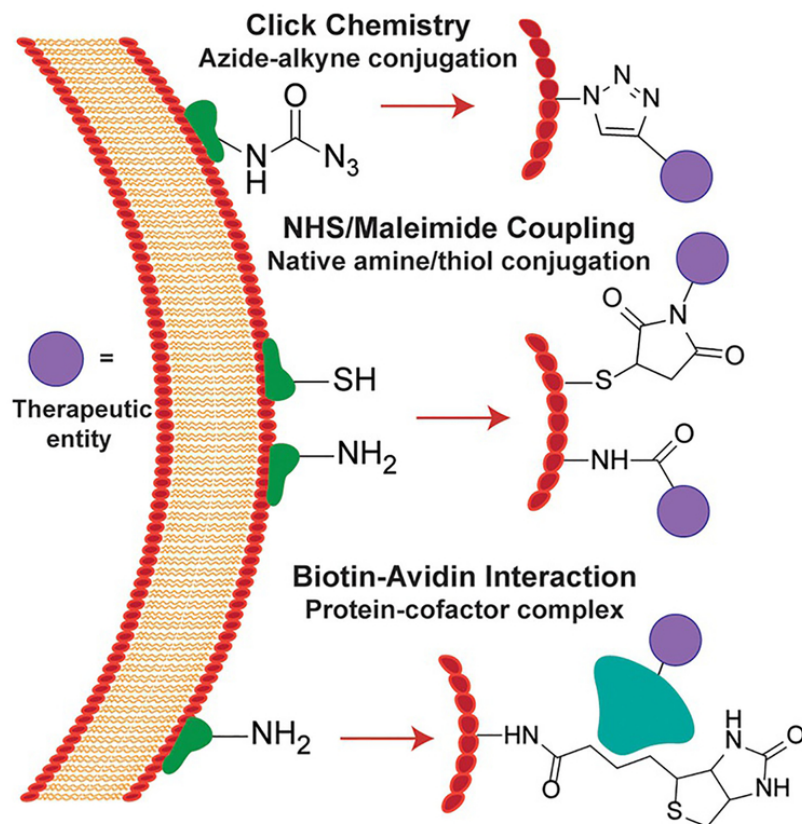


Figure 1.3. Strategies for covalent cell surface modifications. Click chemistry methods involve coupling of metabolically incorporated azides to phosphines or alkynes for cargo delivery. NHS esters and maleimides can be used for conjugations to amines and thiols, respectively. Biotin can be linked to the cell membrane via several means, and then associate with streptavidin-related proteins linked to chemical moieties.

Streptavidin-like proteins conjugated to biotinylated NPs on NSCs and MSCs have been shown to facilitate tumor-selective distribution in intracranial⁹⁴ and tumor tropic⁹³ drug delivery, respectively. In both cases, cell viability was not affected, and NSC-NP conjugates studied in the glioma model had improved distribution and retention versus NPs alone.⁹⁴ RBCs can also be conveniently modified at the surface via biotin–streptavidin conjugation. They have been modified in this manner with insulin and IgG to facilitate targeting for directed delivery of albumin to endothelial cells,⁹⁵ and plasminogen-

activating NPs as prophylactic measures for fibrinolysis, which were shown to persist in the bloodstream for tenfold longer than non-conjugated entities.⁹² In a stimuli-responsive example by Berlin et al., cell surfaces were biotinylated via acid-labile hydrazine linkages, and connected to pH-responsive nanoparticles through an avidin protein.¹⁷ NSC viability and tumor tropism were not affected, and the efficacy of docetaxel-NPs was improved when incorporated with the cell-based vehicle. It has been noted that in addition to streptavidin-biotin interactions, contributions from streptavidin-integrin and passive adsorption of nanoparticles to the cell surface may occur.⁹⁴ However, non-specifically adsorbed NPs have not been shown to be retained following cellular migration.¹

1.4.3. Direct conjugation to native amino acids

As an alternative to the display of a large protein on the cell surface, as in biotin–streptavidin methods (avidin is 66–69 kDa), direct linking of cargo to membranes has been employed. In limited cases, endogenous cell surface protein–ligand combinations are used. For example, monoclonal anti bodies for CD73 and CD90 have been used to link doxorubicin-anchored silica nano-rattles to MSCs for tumor tropic migration.⁹⁶ Cell-based delivery here resulted in better tumor distribution and retention, and improved induction of apoptosis versus free doxorubicin and non-attached nano-rattles. MSC viability was 85% or greater up to 50 mg mL⁻¹ drug. Strategies to modify exposed amines and thiols on cell membranes are more prevalent. N-hydroxysuccinimide (NHS) ester-based cross-linkers are the most frequently employed to link therapeutic payloads to accessible amines in this approach. In proof of concept work, Rossi and co-workers attached polyglycerol-NHS moieties to the surfaces of RBCs, showing that the modification resulted in significant

reduction in Rh antigen immunogenicity,⁹⁷ with good cell viability up to 4 mM. Maleimide based cross-linkers have been utilized to conjugate bio-active molecules to accessible thiols present on carrier cell surfaces. Cytokines (IL-15R α and IL-21) bearing maleimide-functionalized polymeric NPs have been conjugated to stem cells, and were found to be more stable than particles adsorbed to the cell surface.⁹⁸ The cell-conjugated NP-drugs were almost sixfold more effective than free drug, and the NPs did not result in an immune reaction or alter the tumor-tropic movements of the cells. In another case, covalent surface modifications of RBCs were shown to have no detrimental effects on their structure, function, and in vivo circulation and survival, which were akin to non-modified cells.⁹⁹

1.4.4. Other cellular conjugation strategies

Additional chemical reactions are also amenable for use as cell modification methods, although these have not yet been broadly employed in the generation of delivery vehicles. While copper-catalyzed Huisgen cycloadditions between azides and alkynes can be used to label cells,¹⁰⁰ they often result in residual toxicity. This can be mitigated via use of tris(hydroxypropyltriazolyl)methylamine (THPTA), yielding improved cell viability after labeling. Other click-type reactions that use metabolically installed azides to link functionalities to cells include the Staudinger ligation with phosphines¹⁰¹ and strain-promoted copper-free cycloadditions developed by Bertozzi and coworkers, neither of which result in appreciable cellular toxicity.¹⁰² As an example, paclitaxel-loaded diarylcyclooctyne-functionalized nanoparticles linked to glyco-modified MSCs have been shown to result in significant tumor growth inhibition in an orthotopic metastatic ovarian cancer model. The viability of glyco-engineered cells was unaffected up to a week, and the

system resulted in significant reduction in tumor size and improved survival versus nanoparticles alone.¹⁰³ Tetrazines and alkenes can also be ligated together in a biorthogonal manner,¹⁰⁴ which can be applied to cells by appending either an alkene or tetrazine moiety prior to conjugation.^{105,106}

1.5. Perspectives on cell-based delivery

Cellular vehicles have been used for the delivery of various nanoparticles and molecules via direct attachment or internalization of cargo. These systems have several advantages over their non-cellular counterparts in terms of circulation, site-specific recruitment and delivery, and bio-compatibility. However, the use of a biological system as a vehicle is also accompanied by several complexities. Specialized laboratory equipment and protocols are required, and unlike super-molecular entities (e.g., nanoparticles), cells cannot simply be “pulled off of the shelf.” Furthermore, issues of consistency and generalizability have not yet been addressed. Likely due to the platform’s nascence, quantitative studies involving the direct comparison of delivery efficiency, specificity, bio-compatibility, and other characteristics are generally lacking. Experiments assessing the impact of cell type and modification method would enrich the existing knowledge in the field and contribute towards optimization of cell-based delivery vehicles. For the successful translation of these approaches toward use as clinically viable tools, several additional issues need to be overcome.

Except for red blood cells, vector cells are generally scarce on account of the difficulty in their harvest and low natural abundance. Following FDA approval of cellular immunotherapy for cancer treatment,¹⁰⁷ there has been much industrial investment in the

commercialization of cell-based products, which should lead to developments in methods for producing and harvesting these cells at higher yields.

A general concern for using cell-based vehicles is potential immunogenicity. Most studies described here do not evaluate the immune responses that may be generated by the cells themselves, and it is likely that internalized cargo will result in different profiles from those displayed on the surface. Additional modifications, including use of PEG, may be required. PEGylation of RBCs⁹⁹ and pancreatic islets¹⁰⁸ has been shown to be compatible with cells, non-toxic *in vivo*, and can temper immunogenicity.

Another limitation associated with cell-based delivery vehicles is that many current loading strategies do not facilitate control over cargo release. Cleavable linkers between therapeutics and carriers can facilitate specific delivery to target tissues, leading to even greater treatment efficacy, and decreased risk of off-target effects. A potential strategy for development of such a system could involve the use of a moiety between the cell and therapeutic, labile under conditions present in the tissue or disease microenvironment, or a cellular “kill switch” resulting in release of payload from within the cell interior. Polymers and linkers that respond to subtle changes in pH and temperature^{109,110} and undergo degradation-based controlled release are being developed for drug delivery.¹¹¹ Similarly, disulfide bonds have also been used as linkers,¹¹² as have peptides that are cleaved by enzymes present in specific disease and/or tissue microenvironments.

With increasing research and clinical applications of both cellular therapies¹²⁻¹⁴ and vehicles,²⁵⁻²⁷ the foundation has been laid for further development of cell-based delivery agents. It is likely that any of the issues described here will be addressed in the near future. The field of cell-based delivery is one that continues to expand, with new modification

strategies, cargo types, and health applications being explored. This platform has the potential to improve efficacy and reduce undesirable effects of many existing therapies, and lead to a new generation of therapeutics and imaging agents.

1.6. Dissertation overview

In the backdrop of cellular vehicles showing great promise in imaging and therapeutic applications, in this thesis, I describe the chemical modification and evaluation of cells towards use as imaging agents and delivery vehicles. In **Chapter 2**, through collaborative work, we combined the inherent homing properties of macrophages with on-site manufacturing capabilities of bio-orthogonal nanozymes (NZs), by incorporating the latter in cells. I was able to show that the NZs can be internalized by macrophages without impacting the cells, and while internalized, inactive pro-drugs can be converted to the active forms. Taken together, this strategy integrates the targeting ability of cell-based drug delivery with on-site generation of therapeutics, providing a new approach for targeted drug delivery systems.

Since the phagocytic loading of nanoparticles as a therapeutic strategy has shortcomings, with phagocytosis and release being difficult to control, I have focused on surface modifications of cells toward future use in delivery applications. In **Chapter 3**, I demonstrate proof-of-concept modifications of macrophages under physiological conditions, without inhibiting the normal functioning of the cells. I showed that fluorescent probes can be appended to macrophages to monitor their chemotactic responses, interactions with cancer cells *in vitro*, and accumulation in tumors *in vivo*. Further expanding the toolbox of bioconjugation to other cell types that can be used, in **Chapter**

4, I expanded the N-hydroxysuccinimide (NHS) modification to primary and immortalized macrophages and stem cells. The modified cells were further studied to quantify the retention of the fluorophore at the cell surface over time. Then cellular characteristics like viability and migration were accessed. This work demonstrates the feasibility of using exterior modifications for use in cellular vehicles. I also attempted additional reactions to modify glycans present on the cell surface and performed comparative studies between glycan and protein modifications and the attachment of small molecule fluorophores and large avidin proteins complexes, which are described in the **Appendix**. I compared effects on cellular characteristics including viability and migration, and also quantified the extents of modifications and their cell-surface retention.

In summary, the results presented in this thesis set the stage to use cells as diagnostic tools and/or delivery platforms. This approach can be used with therapeutics and/or probes in applications ranging from regenerative medicine to studies of tumor microenvironments. This fundamental work to optimize chemical reactions on live cells will benefit their use as next generation functional agents.

1.7. References

- (1) Parveen, S.; Mishra, R.; Sahoo, S. K. Nanoparticles: A Boon to Drug Delivery, Therapeutics, Diagnostics and Imaging. *Nanomed. Nanotechnol. Biol. Med.* **2012**, *8*, 147–166.
- (2) Allen, T. M.; Cullis, P. R. Liposomal Drug Delivery Systems: From Concept to Clinical Applications. *Adv. Drug Deliv. Rev.* **2013**, *65*, 36–48.
- (3) Matsumura, Y.; Kataoka, K. Preclinical and Clinical Studies of Anticancer Agent-incorporating Polymer Micelles. *Cancer Sci.* **2009**, *100*, 572–579.

- (4) Ashley, G. W.; Henise, J.; Reid, R.; Santi, D. V. Hydrogel Drug Delivery System with Predictable and Tunable Drug Release and Degradation Rates. *Proc. Natl. Acad. Sci. U. S. A.* **2013**, *110*, 2318–2323.
- (5) Brannon-Peppas, L.; Blanchette, J. O. Nanoparticle and Targeted Systems for Cancer Therapy. *Adv. Drug Deliv. Rev.* **2004**, *56*, 1649–1659.
- (6) Bottaro, D. P.; Liotta, L. A. Out of Air Is Not out of Action. *Nature* **2003**, *423*, 593–595.
- (7) Neuwelt, E.; Abbott, N. J.; Abrey, L.; Banks, W. A.; Blakley, B.; Davis, T.; Engelhardt, B.; Grammas, P.; Nedergaard, M.; Nutt, J.; Pardridge, W.; Rosenberg, G. A.; Smith, Q.; Drewes, L. R. Strategies to Advance Translational Research into Brain Barriers. *Lancet Neurol.* **2008**, *7*, 84–96.
- (8) Muro, S. Challenges in Design and Characterization of Ligand-Targeted Drug Delivery Systems. *J. Control. Release* **2012**, *164*, 125–137.
- (9) Wilhelm, S.; Tavares, A. J.; Dai, Q.; Ohta, S.; Audet, J.; Dvorak, H. F.; Chan, W. C. W. Analysis of Nanoparticle Delivery to Tumours. *Nat. Rev. Mater.* **2016**, *1*, 16014.
- (10) De Jong, W. H.; Borm, P. J. A. Drug Delivery and Nanoparticles: Applications and Hazards. *Int. J. Nanomed.* **2008**, *3*, 133–149.
- (11) Duran, N. E.; Hommes, D. W. Stem Cell-Based Therapies in Inflammatory Bowel Disease: Promises and Pitfalls. *Therap. Adv. Gastroenterol.* **2016**, *9*, 533–547.
- (12) Steinberg, G. K.; Kondziolka, D.; Wechsler, L. R.; Lunsford, L. D.; Coburn, M. L.; Billigen, J. B.; Kim, A. S.; Johnson, J. N.; Bates, D.; King, B.; Case, C.; McGrogan, M.; Yankee, E. W.; Schwartz, N. E. Clinical Outcomes of Transplanted Modified Bone Marrow-Derived Mesenchymal Stem Cells in Stroke: A Phase 1/2a Study. *Stroke* **2016**, *47*, 1817–1824.
- (13) Newick, K.; O'Brien, S.; Moon, E.; Albelda, S. M. CAR T Cell Therapy for Solid Tumors. *Annu. Rev. Med.* **2017**, *68*, 139–152.
- (14) Burke, J.; Hunter, M.; Kolhe, R.; Isales, C.; Hamrick, M.; Fulzele, S. Therapeutic Potential of Mesenchymal Stem Cell Based Therapy for Osteoarthritis. *Clin. Transl. Med.* **2016**, *5*, 1–8.
- (15) Su, Y.; Xie, Z.; Kim, G. B.; Dong, C.; Yang, J. Design Strategies and Applications of Circulating Cell-Mediated Drug Delivery Systems. *ACS Biomater. Sci. Eng.* **2015**, *1*, 201–217.
- (16) Muzykantov, V. R. Drug Delivery by Red Blood Cells: Vascular Carriers Designed by Mother Nature. *Expert Opin. Drug Deliv.* **2010**, *7*, 403–427.
- (17) Mooney, R.; Weng, Y.; Garcia, E.; Bhojane, S.; Smith-Powell, L.; Kim, S. U.; Annala, A. J.; Aboody, K. S.; Berlin, J. M. Conjugation of PH-Responsive Nanoparticles to Neural Stem Cells Improves Intratumoral Therapy. *J. Control. Release* **2014**, *191*, 82–89.

- (18) Fu, J.; Wang, D.; Mei, D.; Zhang, H.; Wang, Z.; He, B.; Dai, W.; Zhang, H.; Wang, X.; Zhang, Q. Macrophage Mediated Biomimetic Delivery System for the Treatment of Lung Metastasis of Breast Cancer. *J. Control. Release* **2015**, *204*, 11–19.
- (19) Griffiths, L.; Binley, K.; Iqball, S.; Kan, O.; Maxwell, P.; Ratcliffe, P.; Lewis, C.; Harris, A.; Kingsman, S.; Naylor, S. The Macrophage – a Novel System to Deliver Gene Therapy to Pathological Hypoxia. *Gene Ther.* **2000**, *7*, 255–262.
- (20) Chhour, P.; Naha, P. C.; O’Neill, S. M.; Litt, H. I.; Reilly, M. P.; Ferrari, V. A.; Cormode, D. P. Labeling Monocytes with Gold Nanoparticles to Track Their Recruitment in Atherosclerosis with Computed Tomography. *Biomaterials* **2016**, *87*, 93–103.
- (21) Zhao, Y.; J. Haney, M. Active Targeted Macrophage-Mediated Delivery of Catalase to Affected Brain Regions in Models of Parkinson's Disease. *J. Nanomed. Nanotechnol.* **2011**, *4*, 1-8.
- (22) Huang, W.-C.; Chiang, W.-H.; Cheng, Y.-H.; Lin, W.-C.; Yu, C.-F.; Yen, C.-Y.; Yeh, C.-K.; Chern, C.-S.; Chiang, C.-S.; Chiu, H.-C. Tumortropic Monocyte-Mediated Delivery of Echogenic Polymer Bubbles and Therapeutic Vesicles for Chemotherapy of Tumor Hypoxia. *Biomaterials* **2015**, *71*, 71–83.
- (23) Li, S.; Feng, S.; Ding, L.; Liu, Y.; Zhu, Q.; Qian, Z.; Gu, Y. Nanomedicine Engulfed by Macrophages for Targeted Tumor Therapy. *Int. J. Nanomed.* **2016**, *11*, 4107–4124.
- (24) Gao, M.; Hu, A.; Sun, X.; Wang, C.; Dong, Z.; Feng, L.; Liu, Z. Photosensitizer Decorated Red Blood Cells as an Ultrasensitive Light-Responsive Drug Delivery System. *ACS Appl. Mater. Interfaces* **2017**, *9*, 5855–5863.
- (25) Portnow, J.; Synold, T. W.; Badie, B.; Tirughana, R.; Lacey, S. F.; D’Apuzzo, M.; Metz, M. Z.; Najbauer, J.; Bedell, V.; Vo, T.; Gutova, M.; Frankel, P.; Chen, M.; Aboody, K. S. Neural Stem Cell-Based Anticancer Gene Therapy: A First-in-Human Study in Recurrent High-Grade Glioma Patients. *Clin. Cancer Res.* **2017**, *23*, 2951–2960.
- (26) Leuzzi, V.; Micheli, R.; D’Agnano, D.; Molinaro, A.; Venturi, T.; Plebani, A.; Soresina, A.; Marini, M.; Ferremi Leali, P.; Quinti, I.; Pietrogrande, M. C.; Finocchi, A.; Fazzi, E.; Chessa, L.; Magnani, M. Positive Effect of Erythrocyte-Delivered Dexamethasone in Ataxia-Telangiectasia. *Neurol. Neuroimmunol.* **2015**, *2*, 3.
- (27) Hunault-Berger, M.; Leguay, T.; Huguet, F.; Leprêtre, S.; Deconinck, E.; Ojeda-Urbe, M.; Bonmati, C.; Escoffre-Barbe, M.; Bories, P.; Himberlin, C.; Chevallier, P.; Rousselot, P.; Reman, O.; Boulland, M.-L.; Lissandre, S.; Turlure, P.; Bouscary, D.; Sanhes, L.; Legrand, O.; Lafage-Pochitaloff, M.; Béné, M. C.; Liens, D.; Godfrin, Y.; Ifrah, N.; Dombret, H.; Group for Research on Adult Acute Lymphoblastic Leukemia (GRAALL). A Phase 2 Study of L-Asparaginase Encapsulated in Erythrocytes in Elderly Patients with Philadelphia Chromosome Negative Acute Lymphoblastic Leukemia: The GRASPALL/GRAALL-SA2-2008 Study: L-Asparaginase within Erythrocytes in Elderly ALL Patients. *Am. J. Hematol.* **2015**, *90*, 811–818.
- (28) Ginhoux, F.; Williams, M.; Naik, S. H. Editorial: Dendritic Cell and Macrophage Nomenclature and Classification. *Front. Immunol.* **2016**, *7*, 168.

- (29) Eming, S. A.; Krieg, T.; Davidson, J. M. Inflammation in Wound Repair: Molecular and Cellular Mechanisms. *J. Invest. Dermatol.* **2007**, *127*, 514–525.
- (30) Vaupel, P.; Rallino, F.; Okunieff, P. Blood Flow, Oxygen and Nutrient Supply, and Metabolic Microenvironment of Human Tumors: A Review. *Cancer Res.* **1989**, *49*, 6449–6465.
- (31) Björnheden, T.; Levin, M.; Evaldsson, M.; Wiklund, O. Evidence of Hypoxic Areas Within the Arterial Wall In Vivo. *Arterioscl. Thromb. Vasc. Biol.*, **1999**, *19*, 870–876.
- (32) Murdoch, C.; Giannoudis, A.; Lewis, C. E. Mechanisms Regulating the Recruitment of Macrophages into Hypoxic Areas of Tumors and Other Ischemic Tissues. *Blood* **2004**, *104*, 2224–2234.
- (33) Brown, J. M. Exploiting the Hypoxic Cancer Cell: Mechanisms and Therapeutic Strategies. *Mol. Med. Today* **2000**, *6*, 157–162.
- (34) Pixley, F. J.; Stanley, E. R. CSF-1 Regulation of the Wandering Macrophage: Complexity in Action. *Trends Cell Biol.* **2004**, *14*, 628–638.
- (35) Qian, B.-Z.; Li, J.; Zhang, H.; Kitamura, T.; Zhang, J.; Campion, L. R.; Kaiser, E. A.; Snyder, L. A.; Pollard, J. W. CCL2 Recruits Inflammatory Monocytes to Facilitate Breast-Tumour Metastasis. *Nature* **2011**, *475*, 222–225.
- (36) Muthana, M.; Giannoudis, A.; Scott, S. D.; Fang, H.-Y.; Coffelt, S. B.; Morrow, F. J.; Murdoch, C.; Burton, J.; Cross, N.; Burke, B.; Mistry, R.; Hamdy, F.; Brown, N. J.; Georgopoulos, L.; Hoskin, P.; Essand, M.; Lewis, C. E.; Maitland, N. J. Use of Macrophages to Target Therapeutic Adenovirus to Human Prostate Tumors. *Cancer Res.* **2011**, *71*, 1805–1815.
- (37) Eisenblätter, M.; Ehrchen, J.; Varga, G.; Sunderkötter, C.; Heindel, W.; Roth, J.; Bremer, C.; Wall, A. In Vivo Optical Imaging of Cellular Inflammatory Response in Granuloma Formation Using Fluorescence-Labeled Macrophages. *J. Nucl. Med.* **2009**, *50*, 1676–1682.
- (38) Wagers, A. J.; Weissman, I. L. Plasticity of Adult Stem Cells. *Cell* **2004**, *116*, 639–648.
- (39) Bianco, P.; Robey, P. G. Stem Cells in Tissue Engineering. *Nature* **2001**, *414*, 118–121.
- (40) Chamberlain, G.; Fox, J.; Ashton, B.; Middleton, J. Concise Review: Mesenchymal Stem Cells: Their Phenotype, Differentiation Capacity, Immunological Features, and Potential for Homing. *Stem Cells* **2007**, *25*, 2739–2749.
- (41) Rakic, P. Evolution of the Neocortex: A Perspective from Developmental Biology. *Nat. Rev. Neurosci.* **2009**, *10*, 724–735.
- (42) Liu, S.; Ginestier, C.; Ou, S. J.; Clouthier, S. G.; Patel, S. H.; Monville, F.; Korkaya, H.; Heath, A.; Dutcher, J.; Kleer, C. G.; Jung, Y.; Dontu, G.; Taichman, R.; Wicha, M. S.

Breast Cancer Stem Cells Are Regulated by Mesenchymal Stem Cells through Cytokine Networks. *Cancer Res.* **2011**, *71*, 614–624.

(43) Zhao, D.; Najbauer, J.; Annala, A. J.; Garcia, E.; Metz, M. Z.; Gutova, M.; Polewski, M. D.; Gilchrist, M.; Glackin, C. A.; Kim, S. U.; Aboody, K. S. Human Neural Stem Cell Tropism to Metastatic Breast Cancer. *Stem Cells* **2012**, *30*, 314–325.

(44) Perrigue, P. M.; Silva, M. E.; Warden, C. D.; Feng, N. L.; Reid, M. A.; Mota, D. J.; Joseph, L. P.; Tian, Y. I.; Glackin, C. A.; Gutova, M.; Najbauer, J.; Aboody, K. S.; Barish, M. E. The Histone Demethylase Jumonji Coordinates Cellular Senescence Including Secretion of Neural Stem Cell–Attracting Cytokines. *Mol. Cancer Res.* **2015**, *13*, 636–650.

(45) Chen, Y.; Xiang, L.-X.; Shao, J.-Z.; Pan, R.-L.; Wang, Y.-X.; Dong, X.-J.; Zhang, G.-R. Recruitment of Endogenous Bone Marrow Mesenchymal Stem Cells towards Injured Liver. *J. Cell. Mol. Med.* **2009**, *14*, 1494–1508.

(46) Guan, J.; Chen, J. Mesenchymal Stem Cells in the Tumor Microenvironment. *Biomed. Rep.* **2013**, *1*, 517–521.

(47) Anselmo, A. C.; Gupta, V.; Zern, B. J.; Pan, D.; Zakrewsky, M.; Muzykantov, V.; Mitragotri, S. Delivering Nanoparticles to Lungs While Avoiding Liver and Spleen through Adsorption on Red Blood Cells. *ACS Nano* **2013**, *7*, 11129–11137.

(48) Wang, C.; Sun, X.; Cheng, L.; Yin, S.; Yang, G.; Li, Y.; Liu, Z. Multifunctional Theranostic Red Blood Cells for Magnetic-Field-Enhanced in Vivo Combination Therapy of Cancer. *Adv. Mater.* **2014**, *26*, 4794–4802.

(49) Hoffman, J. F. On Red Blood Cells, Hemolysis and Resealed Ghosts. In The Use of Resealed Erythrocytes as Carriers and Bioreactors. *Adv. Exp. Med. Biol.* **1992**, *326*, 1–15.

(50) Champion, J. A.; Walker, A.; Mitragotri, S. Role of Particle Size in Phagocytosis of Polymeric Microspheres. *Pharm. Res.* **2008**, *25*, 1815–1821.

(51) Champion, J. A.; Mitragotri, S. Role of Target Geometry in Phagocytosis. *Proc. Natl. Acad. Sci. U. S. A.* **2006**, *103*, 4930–4934.

(52) Choi, M.-R.; Stanton-Maxey, K. J.; Stanley, J. K.; Levin, C. S.; Bardhan, R.; Akin, D.; Badve, S.; Sturgis, J.; Robinson, J. P.; Bashir, R.; Halas, N. J.; Clare, S. E. A Cellular Trojan Horse for Delivery of Therapeutic Nanoparticles into Tumors. *Nano Lett.* **2007**, *7*, 3759–3765.

(53) Choi, J.; Kim, H.-Y.; Ju, E. J.; Jung, J.; Park, J.; Chung, H.-K.; Lee, J. S.; Lee, J. S.; Park, H. J.; Song, S. Y.; Jeong, S.-Y.; Choi, E. K. Use of Macrophages to Deliver Therapeutic and Imaging Contrast Agents to Tumors. *Biomaterials* **2012**, *33*, 4195–4203.

(54) Smith, B. R.; Ghosn, E. E. B.; Rallapalli, H.; Prescher, J. A.; Larson, T.; Herzenberg, L. A.; Gambhir, S. S. Selective Uptake of Single-Walled Carbon Nanotubes by Circulating Monocytes for Enhanced Tumour Delivery. *Nat. Nanotechnol.* **2014**, *9*, 481–487.

(55) Miller, M. A.; Zheng, Y.-R.; Gadde, S.; Pfirschke, C.; Zope, H.; Engblom, C.; Kohler, R. H.; Iwamoto, Y.; Yang, K. S.; Askevold, B.; Kolishetti, N.; Pittet, M.; Lippard, S. J.;

Farokhzad, O. C.; Weissleder, R. Tumour-Associated Macrophages Act as a Slow-Release Reservoir of Nano-Therapeutic Pt(IV) pro-Drug. *Nat. Commun.* **2015**, *6*, 8692.

(56) Kang, S.; Lee, H. W.; Jeon, Y. H.; Singh, T. D.; Choi, Y. J.; Park, J. Y.; Kim, J. S.; Lee, H.; Hong, K. S.; Lee, I.; Jeong, S. Y.; Lee, S.-W.; Ha, J.-H.; Ahn, B.-C.; Lee, J. Combined Fluorescence and Magnetic Resonance Imaging of Primary Macrophage Migration to Sites of Acute Inflammation Using Near-Infrared Fluorescent Magnetic Nanoparticles. *Mol. Imaging Biol.* **2015**, *17*, 643–651.

(57) Encabo-Berzosa, M. M.; Gimeno, M.; Lujan, L.; Sancho-Albero, M.; Gomez, L.; Sebastian, V.; Quintanilla, M.; Arruebo, M.; Santamaria, J.; Martin-Duque, P. Selective Delivery of Photothermal Nanoparticles to Tumors Using Mesenchymal Stem Cells as Trojan Horses. *RSC Adv.* **2016**, *6*, 58723–58732.

(58) Baek, S.-K.; Makkouk, A. R.; Krasieva, T.; Sun, C.-H.; Madsen, S. J.; Hirschberg, H. Photothermal Treatment of Glioma; an in Vitro Study of Macrophage-Mediated Delivery of Gold Nanoshells. *J. Neurooncol.* **2011**, *104*, 439–448.

(59) Schnarr, K.; Mooney, R.; Weng, Y.; Zhao, D.; Garcia, E.; Armstrong, B.; Annala, A. J.; Kim, S. U.; Aboody, K. S.; Berlin, J. M. Gold Nanoparticle-Loaded Neural Stem Cells for Photothermal Ablation of Cancer. *Adv. Health. Mater.* **2013**, *2*, 976–982.

(60) Mooney, R.; Roma, L.; Zhao, D.; Van Haute, D.; Garcia, E.; Kim, S. U.; Annala, A. J.; Aboody, K. S.; Berlin, J. M. Neural Stem Cell-Mediated Intratumoral Delivery of Gold Nanorods Improves Photothermal Therapy. *ACS Nano* **2014**, *8*, 12450–12460.

(61) Huang, W.-C.; Shen, M.-Y.; Chen, H.-H.; Lin, S.-C.; Chiang, W.-H.; Wu, P.-H.; Chang, C.-W.; Chiang, C.-S.; Chiu, H.-C. Monocytic Delivery of Therapeutic Oxygen Bubbles for Dual-Modality Treatment of Tumor Hypoxia. *J. Control. Release* **2015**, *220*, 738–750.

(62) Pang, L.; Qin, J.; Han, L.; Zhao, W.; Liang, J.; Xie, Z.; Yang, P.; Wang, J. Exploiting Macrophages as Targeted Carrier to Guide Nanoparticles into Glioma. *Oncotarget* **2016**, *7*, 37081–37091.

(63) Hughes, R. M.; Marvin, C. M.; Rodgers, Z. L.; Ding, S.; Oien, N. P.; Smith, W. J.; Lawrence, D. S. Phototriggered Secretion of Membrane Compartmentalized Bioactive Agents. *Angew. Chem. Int. Ed.* **2016**, *55*, 16080–16083.

(64) Muthana, M.; Kennerley, A. J.; Hughes, R.; Fagnano, E.; Richardson, J.; Paul, M.; Murdoch, C.; Wright, F.; Payne, C.; Lythgoe, M. F.; Farrow, N.; Dobson, J.; Conner, J.; Wild, J. M.; Lewis, C. Directing Cell Therapy to Anatomic Target Sites in Vivo with Magnetic Resonance Targeting. *Nat. Commun.* **2015**, *6*, 8009.

(65) Han, J.; Zhen, J.; Du Nguyen, V.; Go, G.; Choi, Y.; Ko, S. Y.; Park, J.-O.; Park, S. Hybrid-Actuating Macrophage-Based Microrobots for Active Cancer Therapy. *Sci. Rep.* **2016**, *6*, 28717.

(66) Cao, P.; Mooney, R.; Tirughana, R.; Abidi, W.; Aramburo, S.; Flores, L.; Gilchrist, M.; Nwokafor, U.; Haber, T.; Tiet, P.; Annala, A. J.; Han, E.; Dellinger, T.; Aboody, K.

- S.; Berlin, J. M. Intraperitoneal Administration of Neural Stem Cell–Nanoparticle Conjugates Targets Chemotherapy to Ovarian Tumors. *Bioconjug. Chem.* **2017**, *28*, 1767–1776.
- (67) Ihler, G. M.; Glew, R. H.; Schnure, F. W. Enzyme Loading of Erythrocytes. *Proc. Natl. Acad. Sci. U. S. A.* **1973**, *70*, 2663–2666.
- (68) Magnani, M.; Rossi, L.; D’Ascenzo, M.; Panzani, I.; Bigi, L.; Zanella, A. Erythrocyte Engineering for Drug Delivery and Targeting. *Biotechnol. Appl. Biochem.* **1998**, *28*, 1–6.
- (69) Favretto, M. E.; Cluitmans, J. C. A.; Bosman, G. J. C. G. M.; Brock, R. Human Erythrocytes as Drug Carriers: Loading Efficiency and Side Effects of Hypotonic Dialysis, Chlorpromazine Treatment and Fusion with Liposomes. *J. Control. Release* **2013**, *170*, 343–351.
- (70) Haber, T.; Baruch, L.; Machluf, M. Ultrasound-Mediated Mesenchymal Stem Cells Transfection as a Targeted Cancer Therapy Platform. *Sci. Rep.* **2017**, *7*, 42046.
- (71) He, W.; Qiang, M.; Ma, W.; Valente, A. J.; Quinones, M. P.; Wang, W.; Reddick, R. L.; Xiao, Q.; Ahuja, S. S.; Clark, R. A.; Freeman, G. L.; Li, S. Development of a Synthetic Promoter for Macrophage Gene Therapy. *Hum. Gene Ther.* **2006**, *17*, 949–959.
- (72) Yan, F.; Li, X.; Li, N.; Zhang, R.; Wang, Q.; Ru, Y.; Hao, X.; Ni, J.; Wang, H.; Wu, G. Immunoproapoptotic Molecule ScFv-Fdt-TBid Modified Mesenchymal Stem Cells for Prostate Cancer Dual-Targeted Therapy. *Cancer Lett.* **2017**, *402*, 32–42.
- (73) Cai, Y.; Xi, Y.; Cao, Z.; Xiang, G.; Ni, Q.; Zhang, R.; Chang, J.; Du, X.; Yang, A.; Yan, B.; Zhao, J. Dual Targeting and Enhanced Cytotoxicity to HER2-Overexpressing Tumors by Immunoapoptotin-Armored Mesenchymal Stem Cells. *Cancer Lett.* **2016**, *381*, 104–112.
- (74) Frank, R. T.; Edmiston, M.; Kendall, S. E.; Najbauer, J.; Cheung, C.-W.; Kassa, T.; Metz, M. Z.; Kim, S. U.; Glackin, C. A.; Wu, A. M.; Yazaki, P. J.; Aboody, K. S. Neural Stem Cells as a Novel Platform for Tumor-Specific Delivery of Therapeutic Antibodies. *PLoS ONE* **2009**, *4*, e8314.
- (75) Aboody, K. S.; Najbauer, J.; Metz, M. Z.; D’Apuzzo, M.; Gutova, M.; Annala, A. J.; Synold, T. W.; Couture, L. A.; Blanchard, S.; Moats, R. A.; Garcia, E.; Aramburo, S.; Valenzuela, V. V.; Frank, R. T.; Barish, M. E.; Brown, C. E.; Kim, S. U.; Badie, B.; Portnow, J. Neural Stem Cell–Mediated Enzyme/Prodrug Therapy for Glioma: Preclinical Studies. *Sci. Transl. Med.* **2013**, *5*, 184.
- (76) Muthana, M.; Rodrigues, S.; Chen, Y.-Y.; Welford, A.; Hughes, R.; Tazzyman, S.; Essand, M.; Morrow, F.; Lewis, C. E. Macrophage Delivery of an Oncolytic Virus Abolishes Tumor Regrowth and Metastasis after Chemotherapy or Irradiation. *Cancer Res.* **2013**, *73*, 490–495.
- (77) Leng, L.; Wang, Y.; He, N.; Wang, D.; Zhao, Q.; Feng, G.; Su, W.; Xu, Y.; Han, Z.; Kong, D.; Cheng, Z.; Xiang, R.; Li, Z. Molecular Imaging for Assessment of Mesenchymal Stem Cells Mediated Breast Cancer Therapy. *Biomaterials* **2014**, *35*, 5162–5170.

- (78) Leoni, V.; Gatta, V.; Palladini, A.; Nicoletti, G.; Ranieri, D.; Dall’Ora, M.; Grosso, V.; Rossi, M.; Alviano, F.; Bonsi, L.; Nanni, P.; Lollini, P.-L.; Campadelli-Fiume, G. Systemic Delivery of HER2-Retargeted Oncolytic-HSV by Mesenchymal Stromal Cells Protects from Lung and Brain Metastases. *Oncotarget* **2015**, *6*, 34774–34787.
- (79) Mader, E. K.; Butler, G.; Dowdy, S. C.; Mariani, A.; Knutson, K. L.; Federspiel, M. J.; Russell, S. J.; Galanis, E.; Dietz, A. B.; Peng, K.-W. Optimizing Patient Derived Mesenchymal Stem Cells as Virus Carriers for a Phase I Clinical Trial in Ovarian Cancer. *J. Transl. Med.* **2013**, *11*, 20.
- (80) Kaczorowski, A.; Hammer, K.; Liu, L.; Villhauer, S.; Nwaeburu, C.; Fan, P.; Zhao, Z.; Gladkich, J.; Groß, W.; Nettelbeck, D. M.; Herr, I. Delivery of Improved Oncolytic Adenoviruses by Mesenchymal Stromal Cells for Elimination of Tumorigenic Pancreatic Cancer Cells. *Oncotarget* **2016**, *7*, 9046–9059.
- (81) Baron, S.; Poast, J.; Rizzo, D.; McFarland, E.; Kieff, E. Electroporation of Antibodies, DNA, and Other Macromolecules into Cells: A Highly Efficient Method. *J. Immunol. Methods* **2000**, *242*, 115–126.
- (82) Chambers, E.; Mitragotri, S. Long Circulating Nanoparticles via Adhesion on Red Blood Cells: Mechanism and Extended Circulation. *Exp. Biol. Med.* **2007**, *232*, 958–966.
- (83) Chambers, E.; Mitragotri, S. Prolonged Circulation of Large Polymeric Nanoparticles by Non-Covalent Adsorption on Erythrocytes. *J. Control. Release* **2004**, *100*, 111–119.
- (84) Gribova, V.; Auzely-Velty, R.; Picart, C. Polyelectrolyte Multilayer Assemblies on Materials Surfaces: From Cell Adhesion to Tissue Engineering. *Chem. Mater.* **2012**, *24*, 854–869.
- (85) Kinge, S.; Crego-Calama, M.; Reinhoudt, D. N. Self-Assembling Nanoparticles at Surfaces and Interfaces. *Chem. Phys. Chem.* **2008**, *9*, 20–42.
- (86) Anselmo, A. C.; Gilbert, J. B.; Kumar, S.; Gupta, V.; Cohen, R. E.; Rubner, M. F.; Mitragotri, S. Monocyte-Mediated Delivery of Polymeric Backpacks to Inflamed Tissues: A Generalized Strategy to Deliver Drugs to Treat Inflammation. *J. Control. Release* **2015**, *199*, 29–36.
- (87) Klyachko, N. L.; Polak, R.; Haney, M. J.; Zhao, Y.; Gomes Neto, R. J.; Hill, M. C.; Kabanov, A. V.; Cohen, R. E.; Rubner, M. F.; Batrakova, E. V. Macrophages with Cellular Backpacks for Targeted Drug Delivery to the Brain. *Biomaterials* **2017**, *140*, 79–87.
- (88) Polak, R.; Lim, R. M.; Beppu, M. M.; Pitombo, R. N. M.; Cohen, R. E.; Rubner, M. F. Liposome-Loaded Cell Backpacks. *Adv. Healthcare Mater.* **2015**, *4*, 2832–2841.
- (89) Livnah, O.; Bayer, E. A.; Wilchek, M.; Sussman, J. L. Three-Dimensional Structures of Avidin and the Avidin-Biotin Complex. *Proc. Natl. Acad. Sci. U. S. A.* **1993**, *90*, 5076–5080.
- (90) Wilchek, M.; Bayer, E. A. Introduction to Avidin-Biotin Technology. *Methods Enzymol.* **1990**, *184*, 5–13.

- (91) Abbina, S.; Siren, E. M. J.; Moon, H.; Kizhakkedathu, J. N. Surface Engineering for Cell-Based Therapies: Techniques for Manipulating Mammalian Cell Surfaces. *ACS Biomater. Sci. Eng.* **2018**, *4*, 3658–3677.
- (92) Murciano, J.-C.; Medinilla, S.; Eslin, D.; Atochina, E.; Cines, D. B.; Muzykantov, V. R. Prophylactic Fibrinolysis through Selective Dissolution of Nascent Clots by TPA-Carrying Erythrocytes. *Nat. Biotechnol.* **2003**, *21*, 891–896.
- (93) Cheng, H.; Kastrup, C. J.; Ramanathan, R.; Siegwart, D. J.; Ma, M.; Bogatyrev, S. R.; Xu, Q.; Whitehead, K. A.; Langer, R.; Anderson, D. G. Nanoparticulate Cellular Patches for Cell-Mediated Tumor-tropic Delivery. *ACS Nano* **2010**, *4*, 625–631.
- (94) Mooney, R.; Weng, Y.; Tirughana-Sambandan, R.; Valenzuela, V.; Aramburo, S.; Garcia, E.; Li, Z.; Gutova, M.; Annala, A. J.; Berlin, J. M.; Aboody, K. S. Neural Stem Cells Improve Intracranial Nanoparticle Retention and Tumor-Selective Distribution. *Future Oncol.* **2014**, *10*, 401–415.
- (95) Sternberg, N.; Georgieva, R.; Duft, K.; Bäuml, H. Surface-Modified Loaded Human Red Blood Cells for Targeting and Delivery of Drugs. *J. Microencapsul.* **2012**, *29*, 9–20.
- (96) Li, L.; Guan, Y.; Liu, H.; Hao, N.; Liu, T.; Meng, X.; Fu, C.; Li, Y.; Qu, Q.; Zhang, Y.; Ji, S.; Chen, L.; Chen, D.; Tang, F. Silica Nanorattle–Doxorubicin-Anchored Mesenchymal Stem Cells for Tumor-Tropic Therapy. *ACS Nano* **2011**, *5*, 7462–7470.
- (97) Rossi, N. A. A.; Constantinescu, I.; Kainthan, R. K.; Brooks, D. E.; Scott, M. D.; Kizhakkedathu, J. N. Red Blood Cell Membrane Grafting of Multi-Functional Hyperbranched Polyglycerols. *Biomaterials* **2010**, *31*, 4167–4178.
- (98) Stephan, M. T.; Moon, J. J.; Um, S. H.; Bershteyn, A.; Irvine, D. J. Therapeutic Cell Engineering with Surface-Conjugated Synthetic Nanoparticles. *Nat. Med.* **2010**, *16*, 1035–1041.
- (99) Murad, K. L.; Mahany, K. L.; Brugnara, C.; Kuypers, F. A.; Eaton, J. W.; Scott, M. D. Structural and Functional Consequences of Antigenic Modulation of Red Blood Cells with Methoxypoly(Ethylene Glycol). *Blood* **1999**, *93*, 2121–2127.
- (100) Hong, V.; Steinmetz, N. F.; Manchester, M.; Finn, M. G. Labeling Live Cells by Copper-Catalyzed Alkyne–Azide Click Chemistry. *Bioconjug. Chem.* **2010**, *21*, 1912–1916.
- (101) Laughlin, S. T.; Bertozzi, C. R. Metabolic Labeling of Glycans with Azido Sugars and Subsequent Glycan-Profilng and Visualization via Staudinger Ligation. *Nat. Protoc.* **2007**, *2*, 2930–2944.
- (102) Jewett, J. C.; Sletten, E. M.; Bertozzi, C. R. Rapid Cu-Free Click Chemistry with Readily Synthesized Biarylazacyclooctynones. *J. Am. Chem. Soc.* **2010**, *132*, 3688–3690.
- (103) Layek, B.; Sadhukha, T.; Prabha, S. Glycoengineered Mesenchymal Stem Cells as an Enabling Platform for Two-Step Targeting of Solid Tumors. *Biomaterials* **2016**, *88*, 97–109.

- (104) Blackman, M. L.; Royzen, M.; Fox, J. M. Tetrazine Ligation: Fast Bioconjugation Based on Inverse-Electron-Demand Diels–Alder Reactivity. *J. Am. Chem. Soc.* **2008**, *130*, 13518–13519.
- (105) Devaraj, N. K.; Weissleder, R.; Hilderbrand, S. A. Tetrazine-Based Cycloadditions: Application to Pretargeted Live Cell Imaging. *Bioconjug. Chem.* **2008**, *19*, 2297–2299.
- (106) Ni, Z.; Zhou, L.; Li, X.; Zhang, J.; Dong, S. Tetrazine-Containing Amino Acid for Peptide Modification and Live Cell Labeling. *PLoS ONE* **2015**, *10*, e0141918.
- (107) Salgaller, M. L.; Tjoa, B. A.; Lodge, P. A.; Ragde, H.; Kenny, G.; Boynton, A.; Murphy, G. P. Dendritic Cell-Based Immunotherapy of Prostate Cancer. *Crit. Rev. Immunol.* **1998**, *18*, 109–119.
- (108) Scott, M. D.; Chen, A. M. Beyond the Red Cell: Pegylation of Other Blood Cells and Tissues. *Transfus. Clin. Biol.* **2004**, *11*, 40–46.
- (109) Schmaljohann, D. Thermo- and pH-Responsive Polymers in Drug Delivery. *Adv. Drug Deliv. Rev.* **2006**, *58*, 1655–1670.
- (110) Lu, J.; Jiang, F.; Lu, A.; Zhang, G. Linkers Having a Crucial Role in Antibody–Drug Conjugates. *Int. J. Mol. Sci.* **2016**, *17*, 561.
- (111) Xie, Z.; Zhang, Y.; Liu, L.; Weng, H.; Mason, R. P.; Tang, L.; Nguyen, K. T.; Hsieh, J.-T.; Yang, J. Development of Intrinsically Photoluminescent and Photostable Polylactones. *Adv. Mater.* **2014**, *26*, 4491–4496.
- (112) Patil, U. S.; Qu, H.; Caruntu, D.; O’Connor, C. J.; Sharma, A.; Cai, Y.; Tarr, M. A. Labeling Primary Amine Groups in Peptides and Proteins with *N*-Hydroxysuccinimidyl Ester Modified Fe₃O₄@SiO₂ Nanoparticles Containing Cleavable Disulfide-Bond Linkers. *Bioconjug. Chem.* **2013**, *24*, 1562–1569.

CHAPTER 2

MACROPHAGE-ENCAPSULATED BIOORTHOGONAL NANOZYMES FOR TARGETING CANCER CELLS

Reprinted (adapted) with permission from “Das, R., Hardie, J., Joshi, BP., Zhang, X., Gupta, A., Luther, DC., Fedeli, S., Farkas, ME., Rotello, VM. "Macrophage-Encapsulated Bioorthogonal Nanozymes for Targeting Cancer Cells." *JACS Au*, 2, (2022), 1679–1685.” Copyright (2022) American Chemical Society.

2.1. Introduction

Drug targeting can reduce off-target toxicity, improving survival time and quality of life for cancer patients.¹⁻⁴ Recent metanalyses, however, have shown that the tumor targeting efficiency of most delivery systems is quite low,⁵⁻⁸ and that much of the delivered therapeutic payloads are taken up by tumor-associated macrophages rather than the targeted tumor cells.⁹⁻¹¹ Cell-based therapies provide a potential strategy for the enhanced targeting of tumors.¹²⁻¹⁸ However, commonly used cellular vehicles such as red blood cells (RBCs) and mesenchymal stem cells (MSCs), however, may not be effective for tumor targeting due to lack of targeting ability and low percentage at the tumor site (~3-11%), respectively.^{19,20} Macrophages are inherently attracted to specific tissue environments, including hypoxic, ischemic, and necrotic areas associated with tumors.²¹⁻²³ Concurrently, this homing ability is complemented by the secretion of macrophage chemo-attractants by many cancer cell types to recruit macrophages to tumors,^{24,25} resulting in their contributing up to 50% of tumor mass.²⁶ Taken together, these characteristics make macrophages particularly attractive for use as cell-based delivery vehicles for treating solid tumors that are difficult to reach using conventional targeting strategies.^{14,15,27}

Previous therapeutic delivery studies using macrophages as cell-based carriers have loaded them with nanoparticle-drug conjugates or free chemotherapeutics.^{14,16,17} These agents provided greater efficacy and reduced off-target toxicity when compared with free drugs.^{18,21} The direct loading of therapeutics into macrophages is challenging, however, due to limitations in the amounts of therapeutics that can be loaded into the cells before compromising their viability and/or homing efficiency.²⁸ To a certain extent, these issues can be addressed by utilizing macrophages bearing stimuli-responsive nanoparticles that control the release of therapeutics.^{29,30} In these approaches, external stimuli such as thermal energy, light, or ultrasound can be used to trigger the release of drug molecules from nanoparticles specifically at the tumor site. While this strategy is promising, limited loading and increased complexity of the release process remain challenges.

Bioorthogonal catalysis³¹⁻³⁷ provides a strategy for creating drug ‘factories’ for on-site activation of pro-imaging agents and prodrugs,³⁸⁻⁴⁰ providing essentially unlimited quantities of active entities at desired cells, tissues, and organs.⁴¹⁻⁴⁴ We report here the integration of on-site manufacturing capability with the inherent homing properties of macrophages using cell-internalized bioorthogonal nanozymes (NZs).^{45,46} These nanozymes use gold nanoparticles (AuNPs) to solubilize and stabilize transition metal catalysts (TMCs) through encapsulation in the AuNP monolayer. The TMCs can then generate imaging and therapeutic agents via bioorthogonal uncaging of inactive small molecule precursors in cells.⁴⁷⁻⁵⁴ NZs were delivered into RAW 264.7 macrophages to provide NZ-loaded macrophages (RAW_NZ). The efficacy of RAW-NZ for pro-fluorophore and prodrug activation was demonstrated in a co-culture model with HeLa (human cervical cancer) cells (Figure 2.1). Macrophages retain their migratory behavior towards Colony

Stimulating Factor-1 (CSF), a major chemoattractant secreted by cancer cells to recruit macrophages at tumor sites.⁵⁵ Significant cancer cell toxicity was achieved in the presence of nanozyme-bearing macrophages, even at the lowest concentration of the prodrug administered. Taken together, this strategy integrates the targeting ability of cell-based drug delivery with the on-site generation of therapeutics, providing a new approach for targeted drug delivery systems.

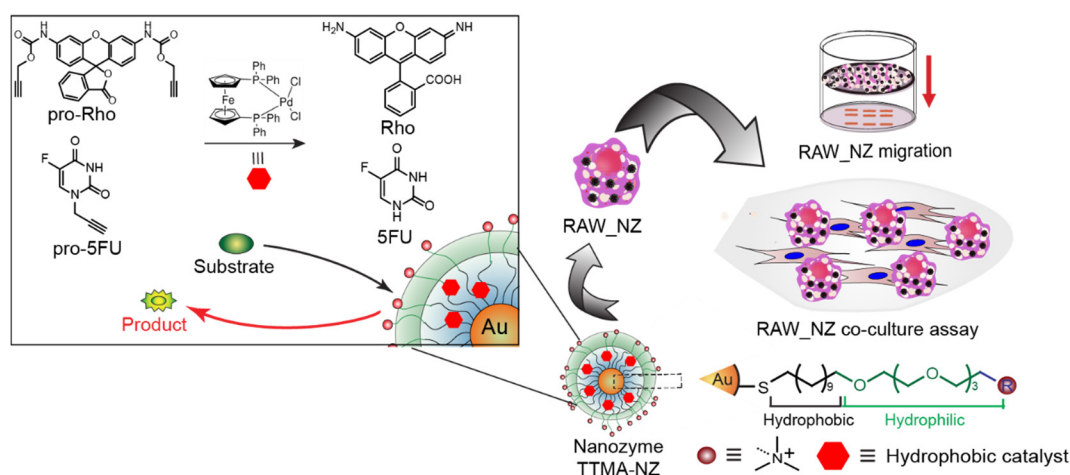


Figure 2.1. Schematic representation of macrophage-mediated delivery of bioorthogonal nanozymes (TTMA-NZ) for prodrug (pro-5FU) and pro-fluorophore (pro-Rho) activation selectively at tumor cells.

2.2. Materials and methods

All chemicals and materials used in the experiments were obtained from Sigma Aldrich or Fisher Scientific. HeLa and RAW 264.7 cells were purchased from ATCC. U2OS-GFP cells were obtained from Prof. Patricia Wadsworth (Biology, UMass Amherst). Dulbecco's modified Eagle's medium (DMEM), fetal bovine serum (Fisher Scientific) was used in cell culture.

2.2.1. Preparation of engineered macrophages (RAW_NZ)

Macrophages (RAW 264.7) were seeded at a concentration of 20,000 cells/well in a 24 well plate, and allowed to attach overnight (at 37 °C in a humidified atmosphere of 5% CO₂). After 24 h, cells were washed three times with PBS to remove any dead cells. NZ solution (100 nM) in macrophage growth media was added to the cells and incubated together for 24 h (at 37 °C in a humidified atmosphere of 5% CO₂), except where otherwise noted for specific experiments. After, the cells were washed with PBS three times to remove any excess NZ, to provide RAW_NZ. RAW_NZ was detached via treatment with trypsin, depending on the nature of the experiment to follow.

2.2.2. Chemotaxis/Boyden Chamber assay procedure

Cell migration towards Colony Stimulating Factor 1 (CSF-1) was investigated by a Boyden Chamber Assay following previously described protocols.²³ Briefly, a trans-well membrane with 8 mm pore size was coated with 10 mg/mL fibronectin. After 4 hours, the excess fibronectin was rinsed with PBS and left to dry overnight. The next day, designated wells of a 24 well plate received 650 µL serum-free growth media supplemented with 40 ng/mL rCSF-1; control wells received serum-free growth media only. The fibronectin-coated inserts were then placed onto the wells. 100 µL of RAW_NZ (100,000 cells/well) solution was added into each insert and incubated for 12 h at 37 °C and 5% CO₂. Non-migratory cells were removed with a Q-tip and migratory cells at the bottoms of the inserts were fixed in 4% formaldehyde and stained with a 0.1% crystal violet solution in 25% methanol. Membranes were removed precisely, mounted onto cover-glass, and visualized under a Zeiss Axio Observer Z1 with an Axio Cam 506 Color attachment under a 20x

objective lens. The cells were counted from three random, non-overlapping fields of view per membrane, with three membranes per condition ($n = 3 \times 3 = 9$). Box and whisker plots were generated using OriginPro 2017.

2.2.3. Coculture of RAW_NZ with HeLa cells and viability evaluation

Glass slides were coated with poly-lysine solution, washed with PBS, and dried overnight. Each of the dry glass slides was placed onto each well of a 6-well plate. Macrophages (RAW 264.7) (100,000/well) in standard growth media were seeded in designated wells with glass slides; 3 mL of media was used in each well to ensure that the glass slides remained fully immersed in solution. The cells were treated with 100 nM NZs for wells designated as RAW_NZ. In parallel, HeLa cells (100,000/well) were seeded in separate 6-well plates. All plates were stored under 5% CO₂ at 37 °C for 24 h. HeLa cells were washed three times with PBS followed by adding fresh, standard growth media. The glass slides coated with RAW 264.7/RAW_NZ were thoroughly washed with PBS to remove any non-adhered cells and/or excess NZ. The slides were then removed carefully with a tweezer from their designated wells and placed within wells containing HeLa cells (atop the cells) for coculture. As a result, both HeLa cells and RAW 264.7/RAW_NZ were in the same wells and solution. For control experiments with only HeLa cells, blank glass slides were placed on top of the cells. For control experiments with only RAW 264.7 cells, the slides coated with RAW 264.7 cells were placed in wells containing only media. The cells were incubated with the prodrug/drug for 24 h, followed by washing three times with PBS. The glass slides were removed and placed in separate 6-well plates. All wells (with cells now separated) were thoroughly washed with PBS three times. Finally, 10% Alamar

blue assay in serum-containing media was performed separately for HeLa and RAW 264.7 cells.

2.2.4. Cytotoxicity measurements of prodrug and drug

HeLa cells were seeded at a concentration of 10,000 cells/well in a 96 well plate overnight. The next day, the cells were treated with pro-5FU and 5FU at various concentrations for 24 h. After the incubation period, the cells were washed three times with PBS to remove dead cells and excess pro-5FU/5FU. 10% Alamar blue in serum-containing media was added to each well (220 μ L) and incubated for 2 h further at 37 °C and 5% CO₂. Cell viability was then determined by measuring the fluorescence intensity at $\lambda_{ex} = 560\text{nm}$ $\lambda_{em} = 590 \text{ nm}$ using a SpectraMax M2 microplate spectrophotometer.

2.2.5. Viability comparison following prodrug activation by RAW_NZ and free NZ

A comparative study was performed to evaluate the abilities of RAW_NZ and free NZ activated prodrug to kill HeLa cells. The co-culture with RAW_NZ was done following the protocol in *Section 2.2.3*. For the experiments with free NZ and AuNPs, HeLa cells (100,000/well) were seeded in 6 well plates and were treated with 100 nM NZs/100 nM AuNPs. Blank glass slides were placed on top of the cells to simulate the co-culture wells. All plates were stored under 5% CO₂ at 37 °C for 24 h. The cells were washed three times with PBS followed by adding fresh standard growth media. The cells were incubated with prodrug for 24 h, followed by washing three times with PBS. The glass slides were removed and 10% Alamar blue assay in serum-containing media was performed.

2.3. Results and discussion

2.3.1. Fabrication of nanozymes

The NZ scaffold was provided by 2 nm cationic AuNP functionalized with thioalkyl tetra(ethylene glycol) trimethylammonium (TTMA), previously shown to have both high cellular uptake and low toxicity.⁵⁶⁻⁶¹ The ligand monolayer of TTMA contains a crucial hydrophobic alkane interior for catalyst encapsulation and a tetra(ethylene glycol) spacer to provide biocompatibility and improve stability in aqueous intracellular environments. We then tested the ability of nanozyme (NZ) to catalytically convert pro-fluorophore and pro-drug into their corresponding active counterparts.

2.3.2. Loading of nanozymes into macrophages

For cellular uptake studies, macrophages were incubated with TTMA-NZ for 24 h and then washed thoroughly to remove non-internalized nanozyme (Figure 2.2). The use of additional washes has been shown to completely remove externally adsorbed NZ. This process did not affect the effective internalization of NZ. The NZ content up-taken by cells can be readily tuned through variation in TTMA-NZ concentrations during incubation, providing a ~four-fold difference in the NZ level for RAW_NZ-0 nM versus RAW_NZ 250 nM. Significantly, retention of catalytically active NZ was observed over extended (48 and 72 h) periods.

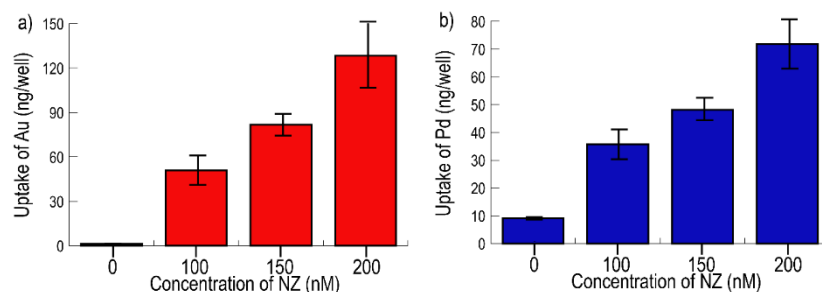


Figure 2.2. Cellular uptake of nanozymes via assessment of a) Au (ng/well) and b) Pd (ng/well) components. Following 24 h incubation of NZs of increasing concentrations with RAW 264.7 macrophages (20,000 cells/well), cells were washed 5 times with PBS prior to digestion to remove all externally bound NZs. The data shown are averages of triplicates; error bars indicate standard deviations.

2.3.3. Catalytic activity of nanozymes in living cells

Effective application of nanozyme-based cell therapy requires the intracellular activation of substrates. The cell-internalized catalysts of RAW_NZ were used to uncage non-fluorescent di(propargyloxycarbonyl)-caged rhodamine 110 (pro-Rho)⁶² as a pro-fluorophore. RAW_NZ was cultured in serum-containing media for 24, 48 or 72 h, followed by addition of pro-Rho and incubation for a further 24 h. Confocal microscopy imaging indicated that RAW_NZ successfully activated pro-Rho to rhodamine 110, independent of RAW_NZ generation time (Figure 2.3). Efficient nanozyme activity was observed even after 72 h of cell internalization, indicating that NZs in RAW_NZ both remain inside of macrophages and retain their activity for prolonged periods.

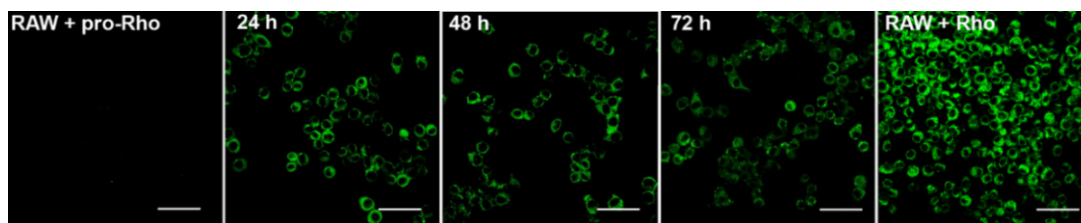


Figure 2.3. Confocal images of pro- rhodamine 110 fluorophore (pro-Rho) activation by RAW_NZ as a function of time elapsed between nanozyme preparation and reaction. RAW_NZ was generated and treated with pro-Rho for 24 h, 48 h and 72 h afterwards. In each case, images were acquired 24 h following exposure of nanozyme to pro-fluorophore. Pro-Rho was used as the negative control and Rho was used as the positive control. The scale bars are 15 μm .

2.3.4. Efficient chemotactic migration of RAW_NZ

We next investigated the effects of nanozyme internalization on macrophage response to chemotactic signals. Colony Stimulating Factor-1 (CSF-1) was used as the chemoattractant, and migration was evaluated by transwell membrane (Boyden Chamber) assay²³ (Figure 2.4). We compared the abilities of non-modified macrophages (RAW 264.7) without NZ versus those loaded with NZ (RAW_NZ) to traffic through a membrane in response to CSF-1 presence. Macrophages were stained with crystal violet at the conclusion of the experiment to visualize and quantify the migrated cells. No significant differences were observed in the behaviors of macrophages (Figure 2.4b) in the presence or absence of CSF-1, indicating that the NZs do not affect the migratory behavior and chemotaxis capabilities of the macrophages.

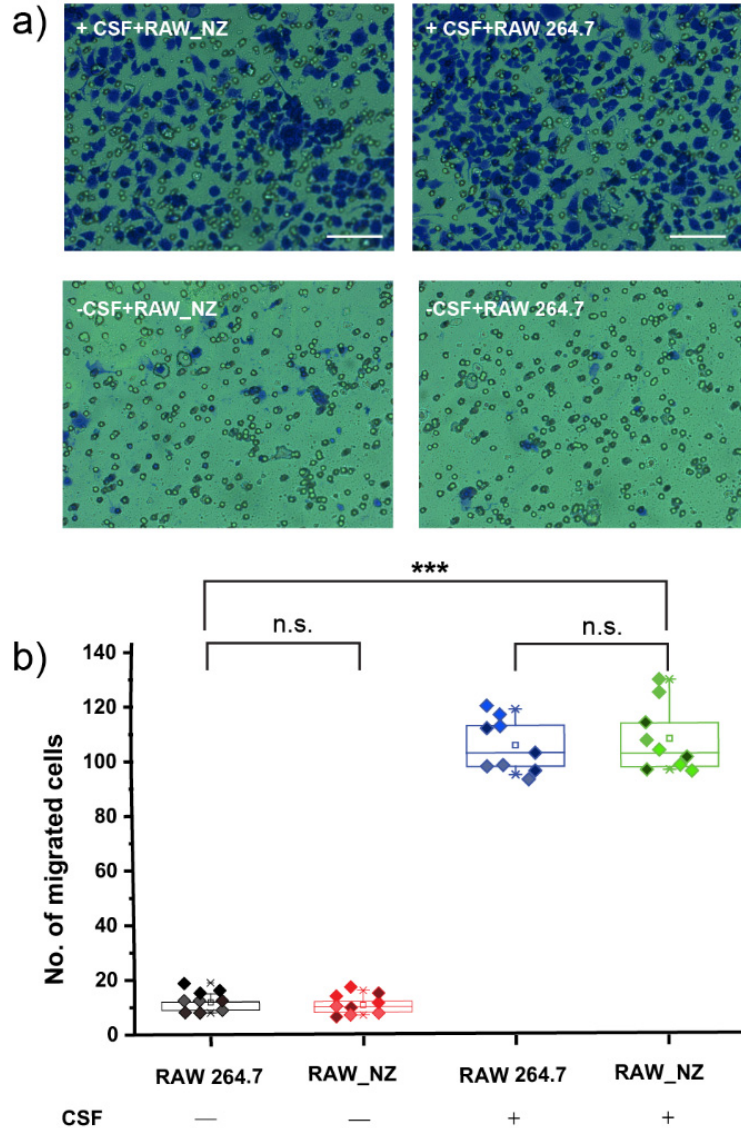


Figure 2.4. Chemotaxis capabilities are retained by **RAW_TTMA-NZ** as determined by transwell membrane assay. a) Confocal imaging of migrated macrophages with NZs (**RAW_TTMA-NZ**) and without NZs (RAW 264.7) in presence and absence of chemoattractant Colony-Stimulating Factor-1 (CSF-1). All cells were stained with crystal violet to facilitate detection. Scale bar = 100 μ m. b) Quantification of migrated RAW 264.7 cells and **RAW_TTMA-NZ** in presence and absence of CSF-1. Nine panels of cells were counted per treatment ($n = 9$, from three biological replicates). Box constitutes the interquartile range (25th to 75th percentile), the intersecting line designates the median, the small square in the center represents the mean, and the bottom and top whiskers specify the 5th and 95th percentiles, respectively. n.s. = not significant, *** $p < 0.0001$.

2.3.5. RAW-NZ kills cancer cells in co-culture models

Having established the stability and retention of inherent chemotactic capabilities of macrophages of RAW_NZs, we next investigated their therapeutic potential in a co-culture model with HeLa cells (Figure 2.5a). RAW_NZ were also co-cultured with green fluorescent protein (GFP) expressing HeLa cells (GFP-HeLa) and separately, U2OS cells (GFP-U2OS) (Figure 2.5b).

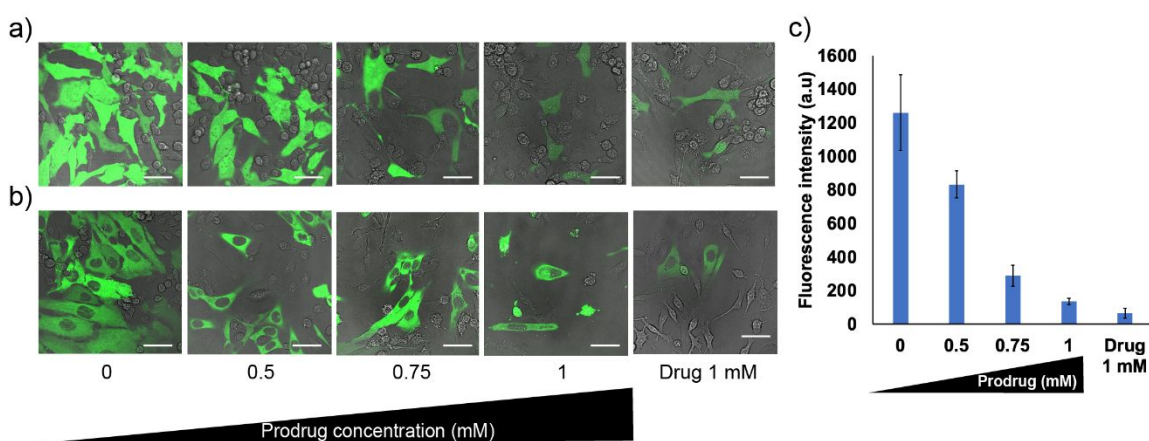


Figure 2.5. Co-culture experiment of RAW_NZ with a) GFP-HeLa cells and b) GFP-U2OS cells to demonstrate toxicity following pro-5FU activation *via* reduction of GFP fluorescence. Scale bar = 15 μ m. c) Fluorescence intensity was quantified ImageJ software.

For this study, propargyl-protected 5-fluorouracil (pro-5FU)⁶³ was chosen as a model prodrug due to the broad application of its active counterpart (5FU; Figure 2.6a).^{64,65} For the co-culture experiment, RAW_NZ or RAW 264.7 cells were seeded on glass slides that were then immersed into wells seeded with HeLa cells (Figure 2.6b).

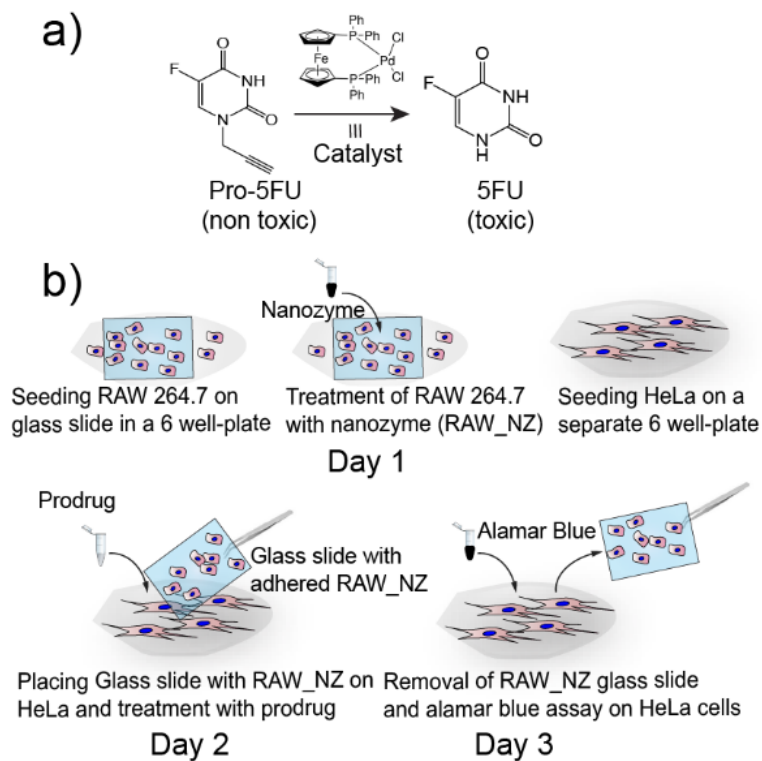


Figure 2.6. 5FU activation in a co-culture system with **RAW_NZ**. a) Pro-5FU activation by TTMA catalysis. b) Graphical scheme of co-culture experiment to evaluate therapeutic efficacy of **RAW_NZ** in HeLa cells.

Macrophage-free slides and HeLa-free wells were used for additional control conditions. Pro-5FU (0 to 1 mM) was added to the co-culture and control wells and incubated for 24 h. Slides with RAW_NZ and controls were removed before performing Alamar blue assays separately on HeLa cells and macrophages to differentiate viabilities by cell type. In the presence of RAW_NZ, the viabilities of both HeLa and RAW 264.7 carrier (Figure 2.7) cells were substantially reduced with increasing concentrations of the prodrug. This dose-dependent cytotoxicity indicates the successful conversion of pro-5FU into the active therapeutic by NZ. The activity against the HeLa cells demonstrates that the uncaged drug was able to diffuse from the macrophages to the target cells. HeLa (and

macrophage) cells that received increasing concentrations of prodrug but were not cultured with RAW_NZ (or TTMA-NZ) did not show any reduction in cell viability, indicating successful caging of 5FU (Figure 2.7).

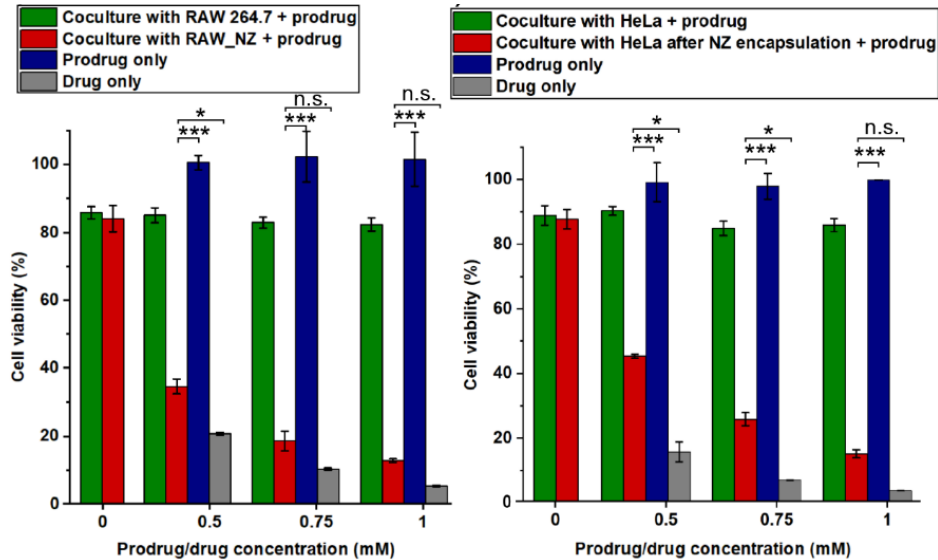


Figure 2.7. Viability of HeLa cells and RAW 264.7 cells following pro-5FU (pro-drug) activation by RAW_NZ in the co-culture experiment, and control conditions. The data are average of triplicates and the error bars indicate standard deviations. n.s. = not significant, * $p < 0.05$, *** $p < 0.001$.

For future *in vivo* applications, nanozyme-loaded macrophages will be injected intravenously due to the macrophages' ability to home towards tumor site. Based on our previous research,²³ we are optimistic about the targeting efficiency of macrophages towards the tumor, however, liver accumulation and nanozyme leakage from the cells should be considered potential challenges. The dose of the prodrug is not expected to be an issue, since a similar prodrug has been used *in vivo* showing no toxicity to the animal.⁶²

2.4. Conclusion

In summary, we have demonstrated a macrophage-based bioorthogonal strategy for tumor imaging and therapy. Macrophages bearing internalized bioorthogonal nanozymes featured catalytic activity extending over days. The carrier macrophages retained chemotactic behavior and exhibited efficient generation of therapeutics in a co-culture model, illustrating the potential of this macrophage-based therapy for therapeutic uses. Coupling the chemotactic ability of macrophages with the ability to generate therapeutic and imaging agents at tumor sites presents a new strategy for reducing off-target effects and extending on-demand delivery, providing the potential to bring drug-activating factories into deep center of tumor. Future studies are underway exploring the use of this platform for specific drug activation in *in vivo* tumor models after optimizing the half-life of catalysts, number of vehicle cells, dose of prodrug, and frequency of the treatment.

2.5. References

- (1) Danhier, F.; Feron, O.; Pr at, V. To Exploit the Tumor Microenvironment: Passive and Active Tumor Targeting of Nanocarriers for Anti-Cancer Drug Delivery. *J. Control. Release* **2010**, *148*, 135–146.
- (2) Byrne, J. D.; Betancourt, T.; Brannon-Peppas, L. Active Targeting Schemes for Nanoparticle Systems in Cancer Therapeutics. *Adv. Drug Deliv. Rev.* **2008**, *60*, 1615–1626.
- (3) Garzon, R.; Marcucci, G.; Croce, C. M. Targeting MicroRNAs in Cancer: Rationale, Strategies and Challenges. *Nat. Rev. Drug Discov.* **2010**, *9*, 775–789.
- (4) Ma, C.; Xia, F.; Kelley, S. O. Mitochondrial Targeting of Probes and Therapeutics to the Powerhouse of the Cell. *Bioconjug. Chem.* **2020**, *31*, 2650–2667.
- (5) Rosenblum, D.; Joshi, N.; Tao, W.; Karp, J. M.; Peer, D. Progress and Challenges towards Targeted Delivery of Cancer Therapeutics. *Nat. Commun.* **2018**, *9*, 1410
- (6) Wilhelm, S.; Tavares, A. J.; Dai, Q.; Ohta, S.; Audet, J.; Dvorak, H. F.; Chan, W. C. W. Analysis of Nanoparticle Delivery to Tumours. *Nat. Rev. Mater.* **2016**, *1*, 16014.

- (7) Lammers, T.; Kiessling, F.; Hennink, W. E.; Storm, G. Drug Targeting to Tumors: Principles, Pitfalls and (Pre-) Clinical Progress. *J. Control. Release* **2012**, *161*, 175–187.
- (8) Sykes, E. A.; Chen, J.; Zheng, G.; Chan, W. C. W. Investigating the Impact of Nanoparticle Size on Active and Passive Tumor Targeting Efficiency. *ACS Nano* **2014**, *8*, 5696–5706.
- (9) Miller, M. A.; Zheng, Y.; Gadde, S.; Pfirschke, C.; Zope, H.; Engblom, C.; Kohler, R. H.; Iwamoto, Y.; Yang, K. S.; Askevold, B.; Kolishetti, N.; Pittet, M.; Lippard, S. J.; Farokhzad, O. C.; Weissleder, R. Tumour-Associated Macrophages Act as a Slow-Release Reservoir of Nano-Therapeutic Pt(IV) pro-Drug. *Nat. Commun.* **2015**, *6*, 8692.
- (10) Dai, Q.; Wilhelm, S.; Ding, D.; Syed, A. M.; Sindhvani, S.; Zhang, Y.; Chen, Y. Y.; Macmillan, P.; Chan, W. C. W. Quantifying the Ligand-Coated Nanoparticle Delivery to Cancer Cells in Solid Tumors. *ACS Nano* **2018**, *12*, 8423–8435.
- (11) Huai, Y.; Hossen, M. N.; Wilhelm, S.; Bhattacharya, R.; Mukherjee, P. Nanoparticle Interactions with the Tumor Microenvironment. *Bioconjug. Chem.* **2019**, *30*, 2247–2263.
- (12) Joshi, B. P.; Hardie, J.; Farkas, M. E. Harnessing Biology to Deliver Therapeutic and Imaging Entities via Cell-Based Methods. *Chem. Eur. J.* **2018**, *24*, 8717–8726.
- (13) Pierigè, F.; Serafini, S.; Rossi, L.; Magnani, M. Cell-Based Drug Delivery. *Adv. Drug Deliv. Rev.* **2008**, *60*, 286–295.
- (14) Choi, M.-R.; Stanton-Maxey, K. J.; Stanley, J. K.; Levin, C. S.; Bardhan, R.; Akin, D.; Badve, S.; Sturgis, J.; Robinson, J. P.; Bashir, R. A Cellular Trojan Horse for Delivery of Therapeutic Nanoparticles into Tumors. *Nano Lett.* **2007**, *7*, 3759–3765.
- (15) Doshi, N.; Swiston, A. J.; Gilbert, J. B.; Alcaraz, M. L.; Cohen, R. E.; Rubner, M. F.; Mitragotri, S. Cell-Based Drug Delivery Devices Using Phagocytosis-Resistant Backpacks. *Adv. Healthc. Mater.* **2011**, *23*, H105–H109.
- (16) Anselmo, A. C.; Mitragotri, S. Cell-Mediated Delivery of Nanoparticles: Taking Advantage of Circulatory Cells to Target Nanoparticles. *J. Control. Release* **2014**, *190*, 531–541.
- (17) Batrakova, E. V.; Gendelman, H. E.; Kabanov, A. V. Cell-Mediated Drug Delivery. *Expert Opin. Drug Deliv.* **2011**, *8*, 415–433.
- (18) Wang, Q.; Cheng, H.; Peng, H.; Zhou, H.; Li, P. Y.; Langer, R. Non-Genetic Engineering of Cells for Drug Delivery and Cell-Based Therapy. *Adv. Drug Deliv. Rev.* **2015**, *91*, 125–140.
- (19) Sun, X.; Wang, C.; Gao, M.; Hu, A.; Liu, Z. Remotely Controlled Red Blood Cell Carriers for Cancer Targeting and Near-Infrared Light-Triggered Drug Release in Combined Photothermal-Chemotherapy. *Adv. Funct. Mater.* **2015**, *25*, 2386–2394.
- (20) Studeny, M.; Marini, F. C.; Champlin, R. E.; Zompetta, C.; Fidler, I. J.; Andreeff, M. Bone Marrow-Derived Mesenchymal Stem Cells as Vehicles for Interferon- β Delivery into Tumors. *Cancer Res.* **2002**, *62*, 3603–3608.

- (21) Murdoch, C.; Giannoudis, A.; Lewis, C. E. Mechanisms Regulating the Recruitment of Macrophages into Hypoxic Areas of Tumors and Other Ischemic Tissues. *Blood* **2004**, *104*, 2224–2234.
- (22) Brown, J. M.; Giaccia, A. J. The Unique Physiology of Solid Tumors: Opportunities (and Problems) for Cancer Therapy. *Cancer Res.* **1998**, *58*, 1408–1416.
- (23) Joshi, B. P.; Hardie, J.; Mingroni, M. A.; Farkas, M. E. Surface-Modified Macrophages Facilitate Tracking of Breast Cancer- Immune Interactions. *ACS Chem. Biol.* **2018**, *13*, 2339–2346.
- (24) Pollard, J. W. Tumour-Educated Macrophages Promote Tumour Progression and Metastasis. *Nat. Rev. Cancer* **2004**, *4*, 71–78.
- (25) Lewis, C. E.; Pollard, J. W. Distinct Role of Macrophages in Different Tumor Microenvironments. *Cancer Res.* **2006**, *66*, 605–612.
- (26) Zhang, Y.; Cheng, S.; Zhang, M.; Zhen, L.; Pang, D.; Zhang, Q.; Li, Z. High-Infiltration of Tumor-Associated Macrophages Predicts Unfavorable Clinical Outcome for Node-Negative Breast Cancer. *PLoS One* **2013**, *8*, e76147.
- (27) Wan, D. H.; Ma, X. Y.; Lin, C.; Zhu, D. H.; Li, X.; Zheng, B. Y.; Li, J.; Ke, M. R.; Huang, J. D. Noncovalent Indocyanine Green Conjugate of C-Phycocyanin: Preparation and Tumor-Associated Macrophages-Targeted Photothermal Therapeutics. *Bioconjug. Chem.* **2020**, *31*, 1438–1448.
- (28) Fu, J.; Wang, D.; Mei, D.; Zhang, H.; Wang, Z.; He, B.; Dai, W.; Zhang, H.; Wang, X.; Zhang, Q. Macrophage Mediated Biomimetic Delivery System for the Treatment of Lung Metastasis of Breast Cancer. *J. Control. Release* **2015**, *204*, 11–19.
- (29) Mura, S.; Nicolas, J.; Couvreur, P. Stimuli-Responsive Nanocarriers for Drug Delivery. *Nat. Mater.* **2013**, *12*, 991–1003.
- (30) Ganta, S.; Devalapally, H.; Shahiwala, A.; Amiji, M. A Review of Stimuli-Responsive Nanocarriers for Drug and Gene Delivery. *J. Control. Release* **2008**, *126*, 187–204.
- (31) Sletten, E. M.; Bertozzi, C. R. Bioorthogonal Chemistry: Fishing for Selectivity in a Sea of Functionality. *Angew. Chemie Int. Ed.* **2009**, *48*, 6974–6998.
- (32) Völker, T.; Meggers, E. Transition-Metal-Mediated Uncaging in Living Human Cells—an Emerging Alternative to Photolabile Protecting Groups. *Curr. Opin. Chem. Biol.* **2015**, *25*, 48–54.
- (33) Völker, T.; Dempwolff, F.; Graumann, P. L.; Meggers, E. Progress towards Bioorthogonal Catalysis with Organometallic Compounds. *Angew. Chemie Int. Ed.* **2014**, *53*, 10536–10540.
- (34) Zhang, X.; Huang, R.; Gopalakrishnan, S.; Cao-milán, R.; Rotello, V. M. Bioorthogonal Nanozymes: Progress towards Therapeutic Applications. *Trends Chem.* **2019**, *1*, 90–98.

- (35) Bai, Y.; Chen, J.; Zimmerman, S. C. Designed Transition Metal Catalysts for Intracellular Organic Synthesis. *Chem. Soc. Rev.* **2018**, *47*, 1811–182.
- (36) van de L’Isle, M. O. N.; Ortega-Liebana, M. C.; Unciti-Broceta, A. Transition Metal Catalysts for the Bioorthogonal Synthesis of Bioactive Agents. *Curr. Opin. Chem. Biol.* **2021**, *61*, 32–42.
- (37) Wang, W.; Zhang, X.; Huang, R.; Hirschbiegel, C. M.; Wang, H.; Ding, Y.; Rotello, V. M. In Situ Activation of Therapeutics through Bioorthogonal Catalysis. *Adv. Drug Deliv. Rev.* **2021**, *176*, 113893.
- (38) Springer, C. J.; Niculescu-Duvaz, I. Prodrug-Activating Systems in Suicide Gene Therapy. *J. Clin. Invest.* **2000**, *105*, 1161–1167.
- (39) Denmeade, S. R.; Mhaka, A. M.; Rosen, D. M.; Brennen, W. N.; Dalrymple, S.; Dach, I.; Olesen, C.; Gurel, B.; Demarzo, A. M.; Wilding, G.; Carducci, M. A.; Dionne, C. A.; Møller, J. V.; Nissen, P.; Christensen, S. B.; Isaacs, J. T. Engineering a Prostate-Specific Membrane Antigen – Activated Tumor Endothelial Cell Prodrug for Cancer Therapy. *Sci. Transl. Med.* **2012**, *4*, 140ra86.
- (40) Heine, D.; Müller, R.; Brüsselbach, S. Cell Surface Display of a Lysosomal Enzyme for Extracellular Gene-Directed Enzyme Prodrug Therapy. *Gene Ther.* **2001**, *8*, 1005–1010.
- (41) Sancho-albero, M.; Rubio-ruiz, B.; Pérez-lópez, A. M.; Sebastián, V.; Martín-duque, P.; Arruebo, M.; Santamaría, J.; Unciti-broceta, A. Cancer-Derived Exosomes Loaded with Ultrathin Palladium Nanosheets for Targeted Bioorthogonal Catalysis. *Nat. Catal.* **2019**, *2*, 864–872.
- (42) Du, Z.; Liu, C.; Song, H.; Scott, P.; Liu, Z.; Ren, J.; Qu, X. Neutrophil-Membrane-Directed Bioorthogonal Synthesis of Inflammation-Targeting Chiral Drugs. *Chem* **2020**, *6*, 2060–2072.
- (43) Das, R.; Landis, R. F.; Tonga, G. Y.; Cao-Milán, R.; Luther, D. C.; Rotello, V. M. Control of Intra-versus Extracellular Bioorthogonal Catalysis Using Surface-Engineered Nanozymes. *ACS Nano* **2018**, *13*, 229–235.
- (44) Gupta, A.; Das, R.; Yesilbag Tonga, G.; Mizuhara, T.; Rotello, V. M. Charge-Switchable Nanozymes for Bioorthogonal Imaging of Biofilm-Associated Infections. *ACS Nano* **2018**, *12*, 89–94.
- (45) Huang, Y.; Ren, J.; Qu, X. Nanozymes: Classification, Catalytic Mechanisms, Activity Regulation, and Applications. *Chem. Rev.* **2019**, *119*, 4357–4412.
- (46) Wu, J.; Wang, X.; Wang, Q.; Lou, Z.; Li, S.; Zhu, Y.; Qin, L.; Wei, H. Nanomaterials with Enzyme-like Characteristics (Nanozymes): Next-Generation Artificial Enzymes (II). *Chem. Soc. Rev.* **2019**, *48*, 1004–1076.
- (47) Tonga, G. Y.; Jeong, Y.; Duncan, B.; Mizuhara, T.; Mout, R.; Das, R.; Kim, S. T.; Yeh, Y.-C.; Yan, B.; Hou, S.; Rotello, V. M. Supramolecular Regulation of Bioorthogonal

Catalysis in Cells Using Nanoparticle-Embedded Transition Metal Catalysts. *Nat. Chem.* **2015**, *7*, 597.

(48) Cao-Milán, R.; He, L. D.; Shorkey, S.; Tonga, G. Y.; Wang, L.-S.; Zhang, X.; Uddin, I.; Das, R.; Sulak, M.; Rotello, V. M. Modulating the Catalytic Activity of Enzyme-like Nanoparticles through Their Surface Functionalization. *Mol. Syst. Des. Eng.* **2017**, *2*, 624–628.

(49) Jeong, Y.; Tonga, G. Y.; Duncan, B.; Yan, B.; Das, R.; Sahub, C.; Rotello, V. M. Solubilization of Hydrophobic Catalysts Using Nanoparticle Hosts. *Small* **2018**, *14*, 1702198.

(50) Zhang, X.; Liu, Y.; Gopalakrishnan, S.; Castellanos-Garcia, L.; Li, G.; Malassine, M.; Uddin, I.; Huang, R.; Luther, D. C.; Vachet, R. W.; Rotello, V. M. Intracellular Activation of Bioorthogonal Nanozymes through Endosomal Proteolysis of the Protein Corona. *ACS Nano* **2020**, *14*, 4767–4773.

(51) Cao-milan, R.; Gopalakrishnan, S.; He, L. D.; Huang, R.; Wang, L.; Castellanos, L.; Luther, D. C.; Landis, R. F.; Makabenta, J. M. V; Li, C. -H.; Zhang, X.; Scaletti, F.; Vachet, R. W.; Rotello, V. M. Thermally Gated Bio-Orthogonal Nanozymes with Supramolecularly Confined Porphyrin Catalysts for Antimicrobial Uses Thermally Gated Bio-Orthogonal Nanozymes with Supramolecularly Confined Porphyrin Catalysts for Antimicrobial Uses. *Chem.* **2020**, *6*, 1–12.

(52) Zhang, X.; Fedeli, S.; Gopalakrishnan, S.; Huang, R.; Gupta, A.; Luther, D. C.; Rotello, V. M. Protection and Isolation of Bioorthogonal Metal Catalysts by Using Monolayer-Coated Nanozymes. *ChemBioChem* **2020**, *21*, 2759–2763.

(53) Zhang, X.; Landis, R. F.; Keshri, P.; Cao-Milán, R.; Luther, D. C.; Gopalakrishnan, S.; Liu, Y.; Huang, R.; Li, G.; Malassiné, M.; Uddin, I.; Rondon, B.; Rotello, V. M. Intracellular Activation of Anticancer Therapeutics Using Polymeric Bioorthogonal Nanocatalysts. *Adv. Healthc. Mater.* **2021**, 2001627.

(54) Huang, R.; Li, C.; Cao-milan, R.; He, L. D.; Makabenta, J. M.; Zhang, X.; Yu, E.; Rotello, V. M. Polymer-Based Bioorthogonal Nanocatalysts for the Treatment of Bacterial Biofilms. *J. Am. Chem. Soc.* **2020**, *142*, 10723–10729.

(55) Pixley, F. J.; Stanley, E. R. CSF-1 Regulation of the Wandering Macrophage: Complexity in Action. *Trends Cell Biol.* **2004**, *14*, 628–638.

(56) Jiang, Y.; Huo, S.; Mizuhara, T.; Das, R.; Lee, Y.; Hou, S.; Moyano, D. F.; Duncan, B.; Liang, X.; Rotello, V. M. The Interplay of Size and Surface Functionality on the Cellular Uptake of Sub-10 Nm Gold Nanoparticles. *ACS Nano* **2015**, *9*, 9986–9993.

(57) Rana, S.; Bajaj, A.; Mout, R.; Rotello, V. M. Monolayer Coated Gold Nanoparticles for Delivery Applications. *Adv. Drug Deliv. Rev.* **2012**, *64*, 200–216.

(58) Saha, K.; Agasti, S. S.; Kim, C.; Li, X.; Rotello, V. M. Gold Nanoparticles in Chemical and Biological Sensing. *Chem. Rev.* **2012**, *112*, 2739–2779.

- (59) Ghosh, P.; Han, G.; De, M.; Kim, C. K.; Rotello, V. M. Gold Nanoparticles in Delivery Applications. *Adv. Drug Deliv. Rev.* **2008**, *60*, 1307–1315.
- (60) Albanese, A.; Tang, P. S.; Chan, W. C. W. The Effect of Nanoparticle Size, Shape, and Surface Chemistry on Biological Systems. *Annu. Rev. Biomed. Eng.* **2012**, *14*, 1–16.
- (61) Yusop, R. M.; Unciti-Broceta, A.; Johansson, E. M. V; Sánchez-Martín, R. M.; Bradley, M. Palladium-Mediated Intracellular Chemistry. *Nat. Chem.* **2011**, *3*, 239–243.
- (62) Li, J.; Yu, J.; Zhao, J.; Wang, J.; Zheng, S.; Lin, S.; Chen, L.; Yang, M.; Jia, S.; Zhang, X.; Chen, P. R. Palladium-Triggered Deprotection Chemistry for Protein Activation in Living Cells. *Nat. Chem.* **2014**, *6*, 352–361.
- (63) Weiss, J. T.; Dawson, J. C.; Macleod, K. G.; Rybski, W.; Fraser, C.; Torres-Sánchez, C.; Patton, E. E.; Bradley, M.; Carragher, N. O.; Unciti-Broceta, A. Extracellular Palladium-Catalysed Dealkylation of 5-Fluoro-1-Propargyl-Uracil as a Bioorthogonally Activated Prodrug Approach. *Nat. Commun.* **2014**, *5*, 3277.
- (64) Longley, D. B.; Harkin, D. P.; Johnston, P. G. 5-Fluorouracil: mechanisms of action and clinical strategies. *Nat. Rev. Cancer* **2003**, *3*, 330–338.
- (65) Cohen, S. S.; Flaks, J. G.; Barner, H. D.; Loeb, M. R.; Lichtenstein, J. The mode of action of 5-fluorouracil and its derivatives. *Proc. Natl. Acad. Sci. U. S. A.* **1958**, *44*, 1004–1012.

CHAPTER 3

SURFACE-MODIFIED MACROPHAGES FACILITATE TRACKING OF BREAST CANCER-IMMUNE INTERACTIONS

Reprinted (adapted) with permission from “Joshi, BP., Hardie, J., Mingroni, MA., Basabrain, AO., Paracha, A., Farkas, ME. "Surface-Modified Macrophages Facilitate Tracking of Breast Cancer-Immune Interactions." *ACS Chem. Biol.*, 13, (2018), 2339-2346.” Copyright (2018) American Chemical Society.

3.1 Introduction

With implications toward the development of new treatments and understanding the nature of the disease, the intersection between cancer and the immune system has become a very busy place.¹ While the immune system is responsible for detecting and removing abnormal cells, many cancers can produce signals and/or undergo transformations to avoid this fate. Macrophages are immune cells that play a major role in facilitating cancer progression (Figure 3.1), leading to the correlation of their presence with disease severity in many cancer types.² In fact, macrophages represent the most abundant leukocyte within the tumor environment, comprising in some instances up to 50% of the tumor mass.³ Tumor associated macrophages (TAMs) have been shown to generate factors that promote tumor angiogenesis,⁴ silence the immune response to tumors,² and contribute to the epithelial to mesenchymal transition (EMT),⁵ a metastatic process where epithelial cells undergo changes that result in an enhanced migratory capability, increased invasiveness, and elevated resistance to apoptosis ascribed to mesenchymal (i.e., stem cell-like) phenotypes via remodeling of the tumor environment and association with tumor cells.⁶ They have also been implicated in the metastasis-enabling processes of intra- and extravasation of migratory tumor cells⁷ and can affect the efficacy of anticancer

therapeutics.⁸ TAMs are not only important in the initial stages of metastasis but have been shown to contribute to the establishment and survival of metastases at sites away from the primary tumor.^{9,10,11} TAMs have been associated with a variety of tumor types, including breast, prostate, glioma, lymphoma, bladder, lung, cervical, and melanoma.¹²

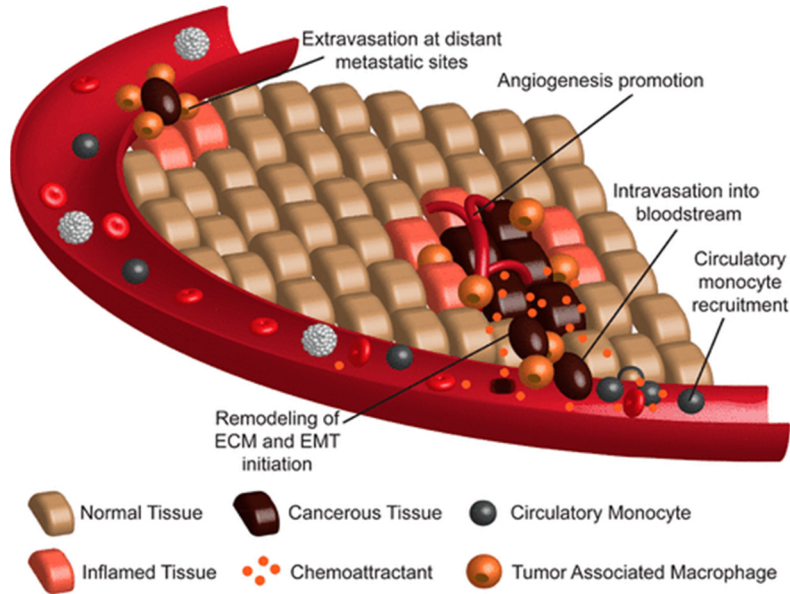


Figure 3.1. Macrophage contributions to cancer and its metastasis.

On account of their roles in cancer progression and metastasis, TAMs have become a target of interest for developing new treatments.¹³ But because macrophages and their monocyte precursors are actively recruited to cancerous tissues,¹⁴ they have also become candidates for use as imaging and therapeutic agent delivery vehicles.¹⁵ A number of tumor types secrete the major macrophage chemoattractants macrophage colony stimulating factor (M-CSF, also known as colony stimulating factor 1, or CSF-1)¹⁶ and monocyte chemoattractant protein like chemokine (C-C motif) ligand 2 (CCL2).¹⁷ Once in the tumor microenvironment, TAMs can traffic into difficult-to-reach hypoxic regions,¹⁴ areas that

are problematic to target with other therapeutic delivery systems.¹⁸ Engineered macrophages are therefore being developed as tools for the diagnosis and treatment of various diseases, from delivering theranostic (therapeutic and diagnostic) agents to tumors¹⁹ to administering antiretroviral therapeutics to HIV infected mice.²⁰ For cancer-based applications, the specific interactions of macrophages with tumor tissue have been exploited to facilitate imaging of tumors and metastases and the delivery of various therapeutics. This has enabled enhanced contrast of tumor boundaries and imaging of metastases, as well as the delivery of nanoparticle-conjugated small molecule and photothermal therapeutics to tumors, showing efficacy *in vitro* and *in vivo*.^{19,21,22,23,24}

The challenge in using nanoparticles as a therapeutic strategy, however, is that their phagocytosis and release are difficult to control, despite modifications to particle surfaces to alter their characteristics.²⁵ Furthermore, because small molecules cannot be engulfed and released in the same manner without additional modifications,²⁶ these platforms are limited to the use of nanoparticle agents. Separately, transgenic animals expressing GFP,²⁷ CFP,²⁸ and RFP²⁹ have been produced and employed in imaging studies of cancer–host cell interactions,³⁰ including in longitudinal studies.³¹ In these cases, tumor cells derived from a fluorescent animal can be distinguished from host cells in or from another animal bearing a different reporter.^{32,33} While cells derived from these systems can be used in the context of imaging, they must be obtained from genetically modified animals, and only fluorescence-detecting platforms may be used. To circumvent various issues associated with macrophage engulfment and release, and to provide a more flexible strategy for imaging, delivery, and studies of macrophage associations with cancer, we have investigated the direct modification of macrophage cell surfaces with small molecules.

The cell membrane contains a diverse array of biomolecules, many of which can be chemically manipulated³⁴ to allow selective noncovalent³⁵ and covalent bioconjugations.³⁶ Successful membrane modification involves linkage of the target molecule to the cell surface under physiological conditions, without inhibiting the normal functioning of the cell. In this report, we demonstrate that fluorescent probes can be appended to macrophages to monitor chemo-sensing, tracking, and interactions with cancer cells. Using either N-hydroxysuccinimide coupling chemistry³⁷ or metabolic incorporation of unnatural azido-sugars,³⁸ we show that modified macrophages chemotaxis to a similar extent as unmodified cells and, more importantly, continue to associate with cancer cells *in vitro* and accumulate in tumors *in vivo*. This work sets the stage for further use of this platform as a diagnostic tool but also as a delivery agent for therapeutics and molecular probes to study the tumor microenvironment.

3.2. Materials and methods

3.2.1. Reagents and cell lines

All reagents were purchased from Thermo-Fisher Scientific except where otherwise noted. Immortalized cell lines were obtained from the ATCC and maintained under ATCC recommended conditions. Primary macrophages were isolated and differentiated from bone marrow of BALB/c mice, as previously reported.³⁹ Following differentiation, cells were used within 7 days.

3.2.2. Biotin-(strept)avidin modification of macrophages

Cells were labeled in either an adherent or suspended manner. For adherent labeling, culture medium was removed and cells rinsed twice with phosphate-buffered saline (PBS). Cells were then incubated in 2 mM Sulfo-NHS-LC-Biotin for 30 min at ambient temperature and then washed twice with 100 mM glycine, once with PBS, and then incubated in 2.5 µg/mL Avidin-FITC or Streptavidin-Dylight for 30 min at 37 °C/5% CO₂. Cells were rinsed once more with PBS before use. For suspended labeling, cells were harvested via trypsinization, centrifugation, and resuspension, followed by counting. For 6 x 10⁶ cells, the cell pellet was rinsed twice with 1 mL of PBS, centrifuging, and removing supernatant for each wash. Cells were resuspended in 2 mL of 2 mM Sulfo-NHS-LC-Biotin and incubated for 30 min at ambient temperature. Cells were then centrifuged at 1500 rpm for 5 min, and the pellet was washed twice with 2 mL of 100 mM glycine and once with 1 mL of PBS. Cells were resuspended in 2 mL of 2.5 µg/mL FITC-Avidin or Streptavidin-Dylight 680 for 30 min at 37 °C and 5% CO₂. Cells were centrifuged at 1500 rpm for 5 min, and the pellet was rinsed once with 1 mL of PBS before use. Images of cells were acquired using a Nikon Point Scanning C2+ confocal microscope with excitation at 488 and 650 nm.

3.2.3. Direct NHS-ester modification of macrophages

Cells were labeled in either an adherent or suspended manner. For adherent labeling, culture medium was removed and cells rinsed twice with phosphate-buffered saline (PBS). Cells were then incubated in 100 µM sulfo-NHS-Cyanine5 (Lumiprobe) for 1 h at 37 °C and 5% CO₂, and then washed twice with 100 mM glycine, once with PBS.

Cells were rinsed once more with PBS before use. For suspended labeling, the cell monolayer was treated with 0.25% trypsin for detachment, centrifuged, resuspended, and counted. For 4×10^6 cells, the pellet was rinsed twice with 1 mL of PBS, centrifuging and removing supernatant for each wash. Then, cells were suspended in 400 μ L of 100 μ M sulfo-NHS-Cyanine5 (Lumiprobe) and incubated for 1 h at 37 °C and 5% CO₂. Cells were centrifuged at 1500 rpm for 5 min, and the pellet was rinsed twice with 2 mL of 100 mM glycine and once with 1 mL of PBS before use. Images of cells were acquired using a Nikon Point Scanning C2+ confocal microscope with excitation at 488 and 650 nm.

3.2.4. Metabolic labeling/Staudinger ligation modification of macrophages

Labeling of cells via this method largely followed previously established protocols.²⁸ In both suspended and adherent modifications, cells were cultured in complete DMEM media supplemented with 40 μ M ManNAz or GlcNAz (0.4% DMSO v/v), for 72 h at 37 °C and 5% CO₂. For adherent labeling, culture medium was removed, and cells rinsed twice with phosphate-buffered saline (PBS). Cells were then incubated in Dylight 650-Phosphine (1% DMSO v/v) and incubated for 3 h at 37 °C and 5% CO₂ and then washed twice with PBS. Cells were rinsed once more with PBS before use. For suspended modification, cells were detached using a cell scraper. For 4×10^6 cells, following additional centrifugation, the pellet was rinsed with 1 mL of 2% fetal bovine serum (FBS) in Hank's Buffered Saline Solution (HBSS), and then resuspended in 400 μ L of 100 μ M Dylight 650-Phosphine (1% DMSO v/v) and incubated for 3 h at 37 °C and 5% CO₂. Cells were centrifuged at 1500 rpm for 5 min, and the pellet was rinsed twice with 1 mL of 2% FBS in HBSS and once with 1 mL of PBS before use. Images of cells were acquired using

a Nikon Point Scanning C2+ confocal microscope with excitation at 488 and 650 nm. For experiments employing a DMSO control, populations of cells were treated with DMSO for analogous times at the same concentrations (0.4% for 72 h and 1% for 3 h).

3.2.5. Wound healing/scratch assay

For the wound healing assay, RAW 264.7 cells were plated at high density (5×10^6 cells per well) in a six-well plate and incubated for 6 h at 37 °C and 5% CO₂ to adhere. The cells were labeled with avidin-FITC according to the protocol in section 3.2.2. A sterile 200 µL pipet tip was used to make a single scratch through the monolayer. The cells were rinsed once with PBS and then incubated in phenol-red free complete DMEM media. Scratch width was monitored using a Zeiss Axio Observer Z1 microscope.

3.2.6. Chemotaxis/Boyden chamber assay

Boyden chamber cell migration assays were largely performed as previously described.⁴⁰ A transwell insert (8 µm pore, 6.5 mm, PET membrane; Corning Life Sciences) was coated with 10 µg/mL of fibronectin (Sigma-Aldrich), allowed to rest for 4 h at ambient temperature, rinsed with PBS, and left to dry overnight. The inserts were placed into 24-well plates containing 650 µL of starved (FBS-free) media supplemented with and without 40 ng/mL rCSF-1, depending on chemoattractant conditions. In parallel, cells were cultured for 24 h in starved media and then either labeled according to the respective protocol or left untreated. For azido-sugar metabolic labeling, cells were cultured in complete media containing the azido-sugar for 48 h, followed by replacement with starved media containing azido-sugar for 24 h. For each cell sample, 100 µL

containing 1×10^5 cells was added into the transwell insert and incubated for 12 h at 37 °C and 5% CO₂. Nonmigratory cells were removed with a Q-tip, and migratory cells at the bottom of the insert were fixed in 4% formaldehyde and stained with a 0.1% crystal violet solution in 25% methanol. Membranes were removed from the inset, mounted onto cover-glass, and visualized using a Zeiss Axio Observer Z1 with an Axio Cam 506 Color attachment. Using a 20x objective, cells were counted from three fields of view per membrane, with three membranes per condition (n = 9). Box and whisker plots were generated using OriginPro 2017, and statistical significance was determined using the student's t test (two tailed distribution and two sample unequal variance).

3.2.7. Coculture assays

MCF7, SKBR3, and MDA-MB-231 cells were plated on 24-well tissue culture plates at 1×10^5 cells per well and incubated overnight (~20 h). MDA-MB-231 cells were labeled with CellTracker Blue CMAC dye (Invitrogen) according to the manufacturer's protocol. RAW 264.7 cells were avidin-FITC labeled in suspension, and 1×10^5 cells were added to each cancer-cell containing well. Accounting for cancer cell growth, the ratio of cancer to macrophage cells was approximately 2:1. Time lapse microscopy was used to monitor cell behavior at 15 min intervals over 12 h using a Zeiss Spinning Disk Observer SD confocal microscope with excitation at 405 and 488 nm.

3.2.8. Generation of *in vivo* tumor models and macrophage biodistribution studies

Six to eight-week-old BALB/cAnNCrl mice (Charles River Laboratories) were orthotopically implanted with 5×10^4 4T1 murine breast cancer cells, similarly to previous

studies.³⁶ Briefly, mice were anesthetized with 400 mg/kg tribromoethanol, the ventral thoracic-inguinal region was shaved, and an incision was made to expose the fourth mammary fat pad. The veins leading to the fat pad were cauterized and the fat pad was removed using forceps. The 4T1 cells were injected into the fat pad cavity in 10 μ L of PBS using a 100 μ L Hamilton syringe. A total of 1 mg/kg of bupivacaine was administered to the surgical site, and the wound was closed using wound clips. Following closure, 1 mg/kg meloxicam was administered subcutaneously. Mice to be used for imaging were placed on an alfalfa-free diet. Once palpable tumors formed, 1×10^7 RAW 264.7 cells were labeled with avidin-DY680 using the suspension method described above. Cells were then suspended in 100 μ L of PBS and were injected into tumor-bearing mice intravenously through the tail vein. At 4 and 24 h following injection, mice were euthanized, and organs, blood, and tumors collected. Tissues were imaged using an *In Vivo* Imaging System (IVIS; PerkinElmer) available at UMass Amherst. All procedures involving the use of animals were conducted under a protocol approved by the Institutional Animal Care and Use Committee (IACUC) at UMass Amherst.

3.3. Results and discussion

3.3.1. Modification of macrophages to install fluorescent molecules

To determine whether macrophages (i.e., RAW 264.7 cells) are amenable to surface modifications, three different approaches were used (Figures 3.2 and 3.3A). In the first method, the cell surface is biotinylated by reacting exposed primary amines with sulfosuccinimidyl-6(biotinamido)hexanoate (Sulfo-NHS-LC-Biotin), prior to binding fluorescein isothiocyanate (FITC)-labeled avidin.⁴¹

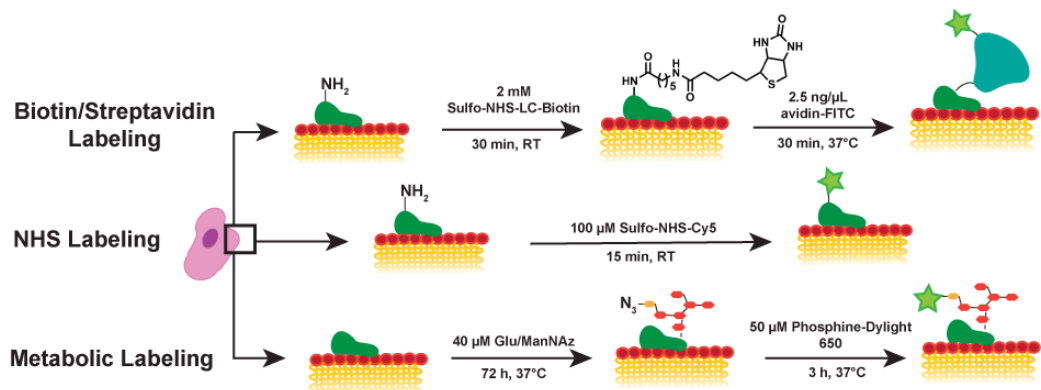


Figure 3.2. Detailed scheme of three cell surface modification methods including step-by-step reaction conditions.

Cellular labeling was confirmed by fluorescent confocal microscopy (Figure 3.3B). We also attached the dye moiety directly to the cells, forgoing the display of large avidin proteins on the cell surface, via N-hydroxysuccidimide (NHS)-dye conjugation. With sulfo-NHS-Cyanine5 (NHS-Cy5), we observed significant cellular modification (Figure 3.3C). As a third approach, we used metabolic labeling and “click” chemistry, which also utilizes small molecules, but modifies incorporated unnatural azido-glycans as opposed to amino acids.³⁸ Cells were metabolically labeled with azidoacetylmannosamine (ManNAz) or azidoacetylglucosamine (GlcNAz), and subsequent Staudinger ligation was performed using Phosphine-Dylight 650 (Phos-Dy680). Confocal microscopy images illustrate the extent of labeling (Figure 3.3D).

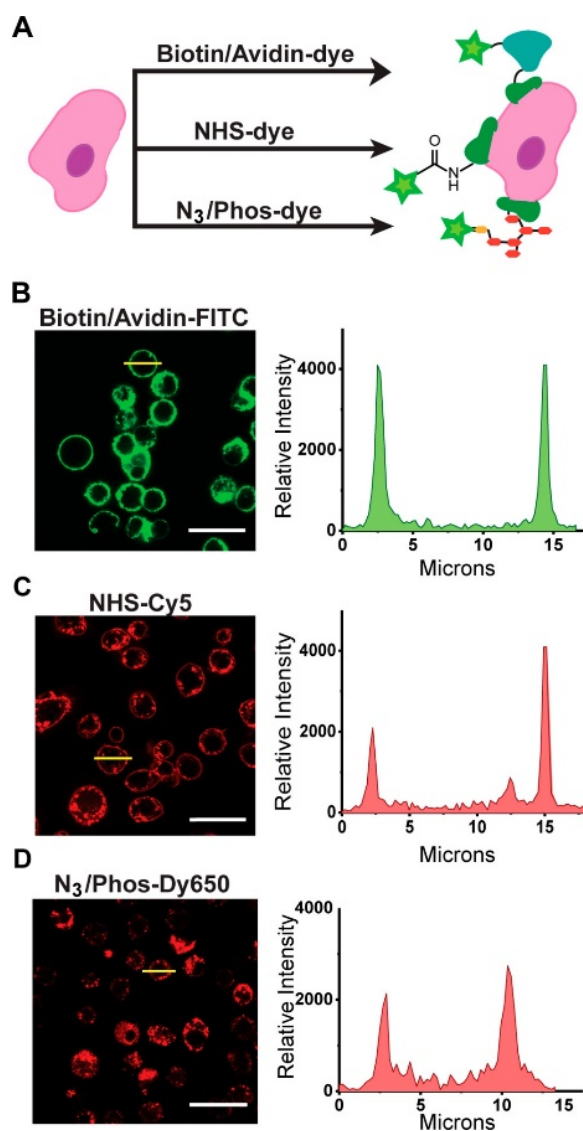


Figure 3.3. Approaches for chemical modification of macrophages. (A) Three methods used to modify the model macrophage cell line RAW 264.7 are an attachment of NHS-biotin followed by noncovalent interaction with fluorophore-conjugated avidin (Biotin/Avidin-dye), amide formation through direct linkage of NHS-fluorophores with cell surface lysines (NHS-dye), and bioorthogonal Staudinger ligation between phosphine conjugates and metabolically incorporated azido sugars (N₃/Phos-dye). Confocal microscopy images show suspended RAW 264.7 cells labeled with (B) avidin-FITC, (C) NHS-Cy5, and (D) phosphine-Dylight 650. Corresponding cellular dye distributions via fluorescence intensities are shown adjacent to the respective image. Modified sites are generally located at the membrane or endosomally throughout the cell (yellow line). Magnification = 60x, scale bar = 25 μ m.

All three conjugation approaches resulted in significant cellular modification with a majority of the dye intensities located at the cell membranes. As expected, fluorescence intensity decreases concomitantly with macrophage proliferation (doubling time is ~15 h; Figure 3.4) and the signal remains over several cell divisions. Following modifications, cells could be stored and were viable for up to 1 week without any manipulation, with the exception of metabolically installed ManNAz conjugates, which showed slightly diminished viabilities (data not shown). With the two-step strategies (biotin-avidin and metabolic labeling), we have found that the appendage of the fluorophores largely depends on the presence of the linker. For example, incorporation of avidin-FITC is not observed unless cells have been biotinylated (Figure 3.5A). Likewise, minimal uptake of Phos-Dy680 is detected in cells that have not incorporated the azido sugar (Figure 3.5B). Modifications did not affect macrophage polarization state (Figure 3.6), and cells largely retained their abilities to phagocytose entities (Figure 3.7). The employment of these three strategies is also useful for the modification of cells with other molecules; a wide array of NHS-, (strept)avidin-, and phosphine-linked molecules are commercially available or can be synthesized. Of particular interest for *in vivo* imaging applications is the installation of near-infrared dyes to facilitate tissue penetration. We have also found the surface functionalization methods to be versatile and amenable to use with other macrophage types, including J774.2 (murine monocyte macrophages) and bone marrow derived primary macrophages (Figure 3.5C).

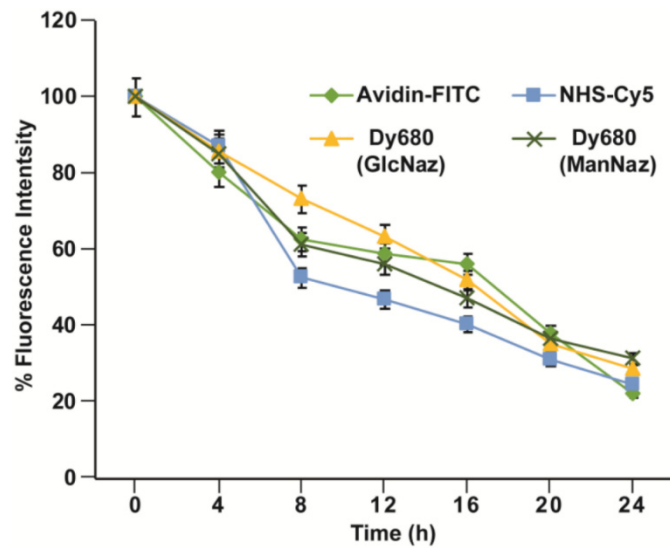


Figure 3.4. Cellular fluorescence over time. The results are shown as percentage difference in fluorescence from time = 0, which has been normalized to 100% for each modification type. Error is shown as standard deviation of the mean.

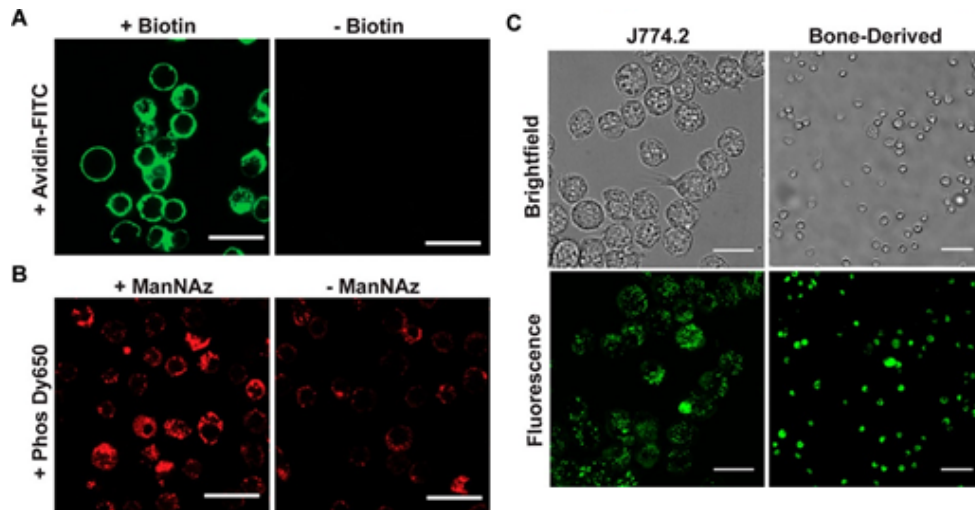


Figure 3.5. Specific cellular labeling in the presence of both linkers and dyes, which may be applied to different macrophage types. (A) Suspended cells are only labeled in the presence of both biotin and avidin; no fluorescence is observed where cells are incubated with only avidin. (B) Significant fluorescence is observed in suspended cells metabolically labeled with azidomannose followed by reaction with Dylight 650; in the absence of azidomannose, minimal fluorescence was seen. Magnification = 60x, scale bar = 25 μ m. (C) The biotin–avidin strategy is used to label J774.2 (monocyte-derived, magnification = 63x, scale bar = 20 μ m) and primary (harvested and differentiated from bone marrow, magnification = 20x, scale bar = 50 μ m) macrophages in suspension.

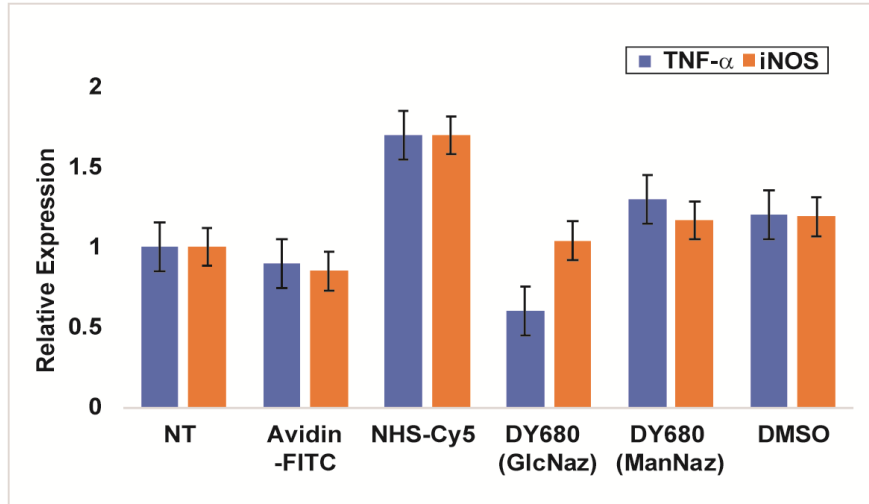


Figure 3.6. Macrophage polarization following chemical modification. Data for M1 markers (*Tnf- α* and *iNos*) are shown here. M2 markers (*Ym1* and *Arg1*) did not amplify in any of the samples shown. While NHS-Cy5 shows slightly increased levels of M1 markers, these are minimal compared to those accompanying M1 polarization. NT = Not Treated, and a DMSO control group is included to account for treatment of the metabolically incorporated azido-sugars. Error bars indicate standard deviation of the mean.

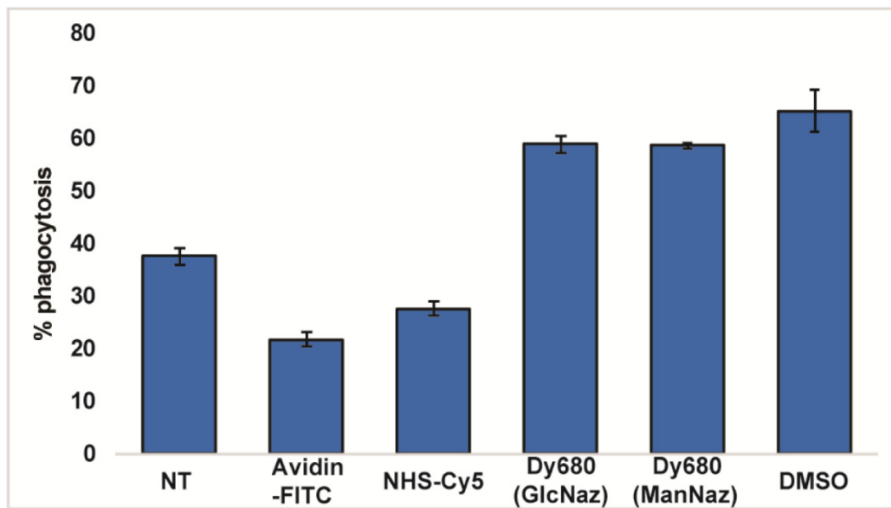


Figure 3.7. Macrophage phagocytosis following chemical modification. Biotin-streptavidin labeling and NHS coupling methods show reduced phagocytic efficacy. However, metabolic labeling methods had increased zymosan internalization possibly due to membrane permeabilization. Each group is the result of three separate measurements.

3.3.2. Macrophage migration and chemotaxis

Critical to the employment of functionalized macrophages as agents for the visualization of macrophage interactions with cancer cells, delivery of therapeutics to tumor sites, or localization of chemical probes to understand oncogenic microenvironments, is the retention of chemotactic properties. For this reason, it is important to assess motility following chemical modification. Because the biotin/avidin-dye modification results in the potential for steric hindrance on account of the resulting display of avidin proteins (monomer is approximately 16.5 kDa), the majority of studies described here were conducted using macrophages that were conjugated in this manner.

Wound healing/scratch assays were used to visualize cellular motility.⁴² A single “scratch” was generated through a monolayer of cells, and the ability of the cells to migrate and fill the scratch was tracked over time via fluorescence microscopy. We compared nonmodified cells with those appended with biotin/avidin-FITC (Figure 3.8A) and noted that the two were strikingly similar. Macrophage response to chemotactic signals was determined via Boyden chamber assay.⁴⁰ Here, labeled and non-labeled macrophages were compared in their abilities to migrate through a membrane in response to a chemoattractant (CSF-1 was used in all instances; Figure 3.8B). These experiments show that not only do cells survive chemical modification, but they continue to migrate toward a chemoattractant. Furthermore, even the presence of large avidin proteins on the cell surface does not hinder cellular sensing and trafficking abilities.

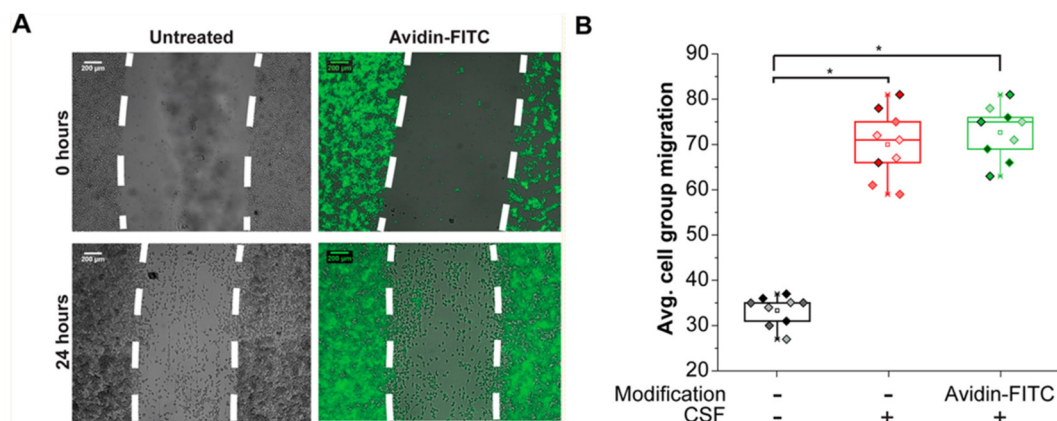


Figure 3.8. Motility capabilities retained by functionalized macrophages. (A) Assessment of adherent macrophage motility via wound healing assay. At time 0, a pipette tip-induced scratch was generated in both nonmodified and avidin-FITC labeled RAW 264.7 cells. Migration after 24 h was observed; both set behaved similarly. Dashed line indicates highest cell density border; scale bar is 200 μm . (B) Boyden chamber assay to determine migration changes following suspended modification. Modified cells migrate similarly to nontreated cells. Non-modified cells were tracked in starved media with and without the CSF chemoattractant and compared to Avidin-FITC modified cells exposed to CSF. Nine panels of cells were counted per treatment ($n = 9$, from three biological replicates, represented by differently colored diamonds). Boxes represent the interquartile range (25th to 75th percentile). The line bisecting the box represents the median. The small square in the center is the mean, and whiskers indicate the 5th and 95th percentiles. $*P \leq 0.0001$.

Having determined that the biotin/avidin-dye modification method has minimal effects on cellular chemotaxis, we evaluated the effects of other labeling strategies. Boyden chamber assays were used to determine the effects of direct NHS-dye incorporation and metabolic-Staudinger ligation methods (using both GlcNaz and ManNaz for azide incorporation) on migration toward CSF-1 chemoattractant (Figure 3.9). Similarly, to biotin/avidin, the use of these other strategies resulted in minimal change to migration ability in comparison with nonmodified cells exposed to CSF-1 in the positive control group. As a result, we conclude that each method assessed largely preserves the ability of macrophages to track and follow chemoattractant signals produced by cancer cells and may be amenable to use in further studies on macrophage-oncogenic interactions.

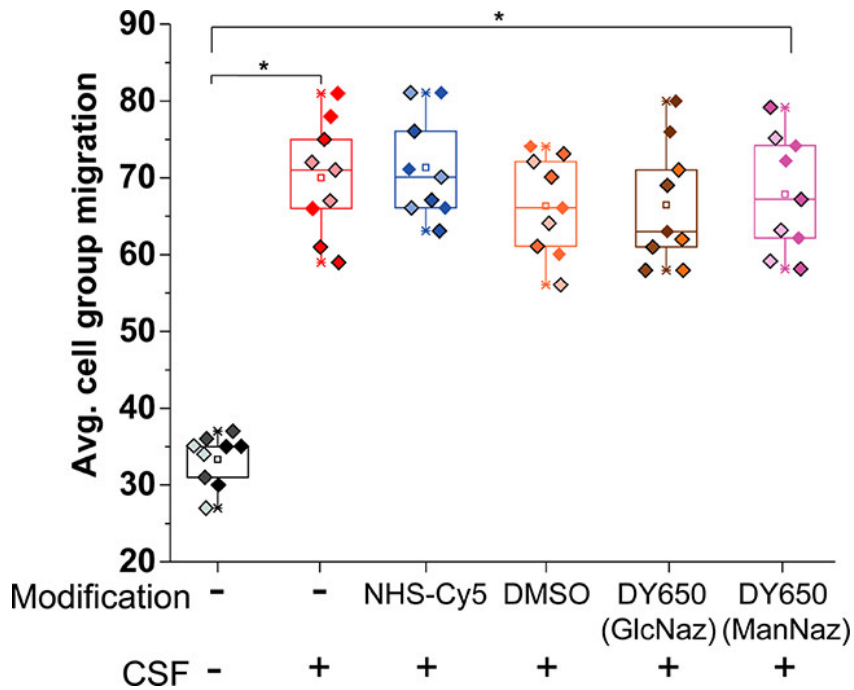


Figure 3.9. Similar behavior of modified suspended macrophages to one another and non-labeled cells exposed to CSF-1. Box and whisker plot of counted cell groups ($n = 9$ from three biological replicates, represented by differently colored diamonds) from Boyden chamber assay comparing migratory behaviors. Boxes represent the interquartile range (25th to 75th percentile). The line bisecting the box represents the median. The small square in the center is the mean, and whiskers indicate the 5th and 95th percentiles. We compare nonlabeled cells not exposed to and exposed to Colony Stimulating Factor-1 (CSF, controls), versus surface-labeled cells exposed to CSF (NHS-Cy5, cells metabolically labeled with N-azidoglucose (GlcNaz) or -mannose (ManNaz) conjugated to phos-DY650). As a control for the metabolically labeled cells, we have also included a DMSO-treated control. $*P \leq 0.0001$.

3.3.3. Macrophage association with *in vitro* models of breast cancer

After establishing that the migratory aptitude of macrophages is not altered upon modification, we investigated the association between these modified cell lines and cancer cells. Breast cancer is a heterogeneous disease generally classified into five subtypes based on genetic profile: luminal A (estrogen receptor (ER) positive, low grade), luminal B (ER positive, high grade), human epidermal growth factor receptor 2 (HER2) enriched, basal-

like (ER negative, HER2 negative, progesterone receptor (PR) negative; often referred to as triple negative), and claudin-low (triple negative with low expression of cell–cell junction proteins).⁴³ These disease types are not only associated with the presence and/or absence of cellular markers but with varying levels of aggression and patient outcomes. At different ends of the spectrum, luminal A is generally considered highly treatable and has high rates of survival, while triple negative types are extremely aggressive with few treatments available, resulting in far worse prognoses. Knowing that macrophages are strong contributors to cancer progression,^{5,10} that patients with higher levels of tumor associated macrophages have worse prognoses,³ and that CSF-1 both is a macrophage chemoattractant and has been correlated with breast cancer mortality,⁴⁴ we wished to determine whether particular cancer subtypes have an enhanced capability to recruit and interact with macrophages.

We present here the results from initial studies addressing the association of macrophages with cancer cells representing different subtypes and degrees of aggression, facilitated by chemically modified macrophages. While it has been observed that macrophage infiltration occurs to a lesser extent in luminal A versus other tumor subtypes,⁴⁵ interactions between cancer cells and macrophages have not been assessed. We utilize MCF7 (luminal A), SKBR3 (HER2+), and MDA-MB-231 (triple negative, claudin-low) cell lines in concert with RAW 264.7 macrophages at approximately a 2:1 ratio. Previous work has demonstrated the cross-species interaction of murine macrophages with human cancer cell lines.⁴⁶ Indeed, across multiple experiments the macrophages show the most vivid associations with the most aggressive cell line, MDA-MB-231 (Figure 3.10).

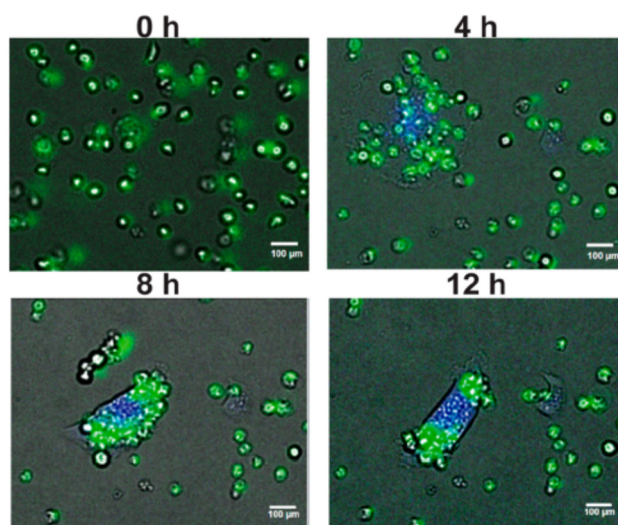


Figure 3.10. Modified macrophage homing and interaction with cancer cells. Time-lapse fluorescence microscopy images show migration and association of FITC-avidin labeled (in suspension) RAW 264.7 macrophages with MDA-MB-231 cancer cells at a 1:2 ratio across 0, 4, 8, and 12 h. Green = avidin-FITC macrophages; blue = MDA-MB-231 cells labeled with cell tracker dye. Scale bars indicate 100 µm.

Fluorescence microscopy was similarly used to evaluate macrophage interactions with MCF7 and SKBR3 cells. While macrophages associated with both of these breast cancer cell lines as well, the interactions were not nearly as dramatic. Whereas the macrophages appear to “pick up” and move the MDA-MB-231 cells, they seem to pull the MCF7 cells, which remain attached to the surface. The SKBR3 cells appear unperturbed by the macrophages, which hover in the vicinity and appear to make contact, but do not show any effect. Single-cell type experiments are provided for reference. Future work toward this end involves studying associations of macrophages with additional cell types and the use of three-dimensional cell culture tissue models.

3.3.4. Chemically modified macrophages show tumor homing capabilities in a mouse model of cancer

In vivo biodistribution studies of functionalized macrophages were performed to determine the applicability of our platform to studying the interactions between macrophages and tumors and metastases in mouse models of cancer. Because of the immune relevant nature of this work, it is critical to use animals with intact immune systems. For this reason, we used female BALB/c mice orthotopically implanted with isogenic 4T1 (mouse mammary carcinoma) cells;⁴⁷ RAW 264.7 macrophage cells also possess the same genetic background. 4T1 cells are highly tumorigenic and invasive. They have been widely used as a clinically relevant triple-negative breast cancer model and are considered to represent stage IV human breast cancer.⁴⁸ Once tumors were palpable, macrophage cells were modified using the biotin/avidin-dye method to append Dy680 to the cell surface. These cells were intravenously injected into the mice (n= 3) via tail veins. Because the mouse breed possesses auto-fluorescent hair, the removal of which can result in additional stress and inflammation and is not always effective in removing all signal, macrophage biodistribution was assessed *ex vivo* following euthanasia at 4 and 24 h following injection (Figure 3.11).

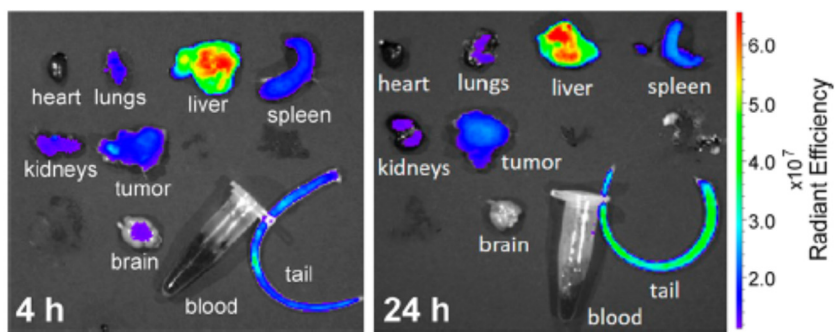


Figure 3.11. Macrophage biodistribution in an immune-competent mouse model of breast cancer. 4T1 cells (mouse mimic of stage IV human breast cancer) were orthotopically implanted into BALB/c mice. Macrophages were labeled via suspended methods with biotin/avidin-Dy680 immediately prior to intravenous injection via tail vein. Following euthanasia at 4 and 24 h after injection, fluorescent imaging of organs was performed *ex vivo* using IVIS-CT.

At the 4 h time-point, significant signal is observed in the liver, followed by the spleen, lungs, and tumor, with some signal in the brain. It is also noted that significant signal appears in the tail, which may be the result of macrophage accumulation near the site of injection due to the presence of a wound or inability to leave the tail vein. After 24 h, signal remains in the tumor, liver, and spleen. Considering that the macrophage surfaces are significantly modified with foreign entities (Figure 3.2), the accumulation of macrophages in the liver is not surprising. The hepatic route is a major pathway for elimination of a variety of drugs, nanoparticles, and other entities that are too large for renal (kidney) excretion. It is in fact encouraging that in general, macrophages that are not localized to the tumor are also not accumulating in other tissues but rather are likely being excreted. In the future, we will assess the biodistribution of macrophages modified with smaller functionalities. Also, in further work, we seek to use imaging modalities that will facilitate *in vivo* tracking of the macrophages (e.g., PET or MRI) and study their tracking to and accumulation at metastatic sites.

3.4. Conclusion

We have been able to demonstrate that macrophages can be functionalized via three different approaches, retaining viability and their inherent migratory and chemotactic properties *in vitro* and *in vivo*. While earlier work utilizing macrophages as delivery vehicles was constrained to the phagocytosis and release of nanoparticle-based agents, we have shown that surface modification is also feasible, and small molecules may be used. By using this strategy, we can now employ macrophage conjugates as delivery vehicles for *in vivo* imaging, therapeutic, and chemical-sensing agents for the diagnosis, treatment, and study of cancer. Furthermore, many groups are broadly interested in the chemical modification of cells toward a variety of applications-this work also serves to answer some fundamental questions regarding the biological effects of these alterations.

3.5 References

- (1) Grivennikov, S. I.; Greten, F. R.; Karin, M. Immunity, Inflammation, and Cancer. *Cell* **2010**, *140*, 883–899.
- (2) Qian, B.-Z.; Pollard, J. W. Macrophage Diversity Enhances Tumor Progression and Metastasis. *Cell* **2010**, *141*, 39–51.
- (3) Zhang, Y.; Cheng, S.; Zhang, M.; Zhen, L.; Pang, D.; Zhang, Q.; Li, Z. High-Infiltration of Tumor-Associated Macrophages Predicts Unfavorable Clinical Outcome for Node-Negative Breast Cancer. *PLoS ONE* **2013**, *8*, e76147.
- (4) Owen, J. L.; Mohamadzadeh, M. Macrophages and Chemokines as Mediators of Angiogenesis. *Front. Physiol.* **2013**, *4*.
- (5) Bonde, A.-K.; Tischler, V.; Kumar, S.; Soltermann, A.; Schwendener, R. A. Intratumoral Macrophages Contribute to Epithelial-Mesenchymal Transition in Solid Tumors. *BMC Cancer* **2012**, *12*, 35.
- (6) Condeelis, J.; Pollard, J. W. Macrophages: Obligate Partners for Tumor Cell Migration, Invasion, and Metastasis. *Cell* **2006**, *124*, 263–266.

- (7) Wyckoff, J. B.; Wang, Y.; Lin, E. Y.; Li, J.; Goswami, S.; Stanley, E. R.; Segall, J. E.; Pollard, J. W.; Condeelis, J. Direct Visualization of Macrophage-Assisted Tumor Cell Intravasation in Mammary Tumors. *Cancer Res.* **2007**, *67*, 2649–2656.
- (8) Mantovani, A.; Allavena, P. The Interaction of Anticancer Therapies with Tumor-Associated Macrophages. *J. Exp. Med.* **2015**, *212*, 435–445.
- (9) Su, S.; Liu, Q.; Chen, J.; Chen, J.; Chen, F.; He, C.; Huang, D.; Wu, W.; Lin, L.; Huang, W.; Zhang, J.; Cui, X.; Zheng, F.; Li, H.; Yao, H.; Su, F.; Song, E. A Positive Feedback Loop between Mesenchymal-like Cancer Cells and Macrophages Is Essential to Breast Cancer Metastasis. *Cancer Cell* **2014**, *25*, 605–620.
- (10) Chen, Q.; Zhang, X. H.-F.; Massagué, J. Macrophage Binding to Receptor VCAM-1 Transmits Survival Signals in Breast Cancer Cells That Invade the Lungs. *Cancer Cell* **2011**, *20*, 538–549.
- (11) Qian, B.; Deng, Y.; Im, J. H.; Muschel, R. J.; Zou, Y.; Li, J.; Lang, R. A.; Pollard, J. W. A Distinct Macrophage Population Mediates Metastatic Breast Cancer Cell Extravasation, Establishment and Growth. *PLoS ONE* **2009**, *4*, 6562.
- (12) Komohara, Y.; Jinushi, M.; Takeya, M. Clinical Significance of Macrophage Heterogeneity in Human Malignant Tumors. *Cancer Sci.* **2014**, *105*, 1–8.
- (13) Ries, C. H.; Cannarile, M. A.; Hoves, S.; Benz, J.; Wartha, K.; Runza, V.; Rey-Giraud, F.; Pradel, L. P.; Feuerhake, F.; Klamann, I.; Jones, T.; Jucknischke, U.; Scheiblich, S.; Kaluza, K.; Gorr, I. H.; Walz, A.; Abiraj, K.; Cassier, P. A.; Sica, A.; Gomez-Roca, C.; de Visser, K. E.; Italiano, A.; Le Tourneau, C.; Delord, J.-P.; Levitsky, H.; Blay, J.-Y.; Rüttinger, D. Targeting Tumor-Associated Macrophages with Anti-CSF-1R Antibody Reveals a Strategy for Cancer Therapy. *Cancer Cell* **2014**, *25*, 846–859.
- (14) Chaturvedi, P.; Gilkes, D. M.; Takano, N.; Semenza, G. L. Hypoxia-Inducible Factor-Dependent Signaling between Triple-Negative Breast Cancer Cells and Mesenchymal Stem Cells Promotes Macrophage Recruitment. *Proc. Natl. Acad. Sci. U.S. A.* **2014**, *111*, E2120-E2129.
- (15) Joshi, B. P.; Hardie, J.; Farkas, M. E. Harnessing Biology to Deliver Therapeutic and Imaging Entities via Cell-Based Methods. *Chem. Eur. J.* **2018**, *24*, 8717–8726.
- (16) Yu, W.; Chen, J.; Xiong, Y.; Pixley, F. J.; Yeung, Y.-G.; Stanley, E. R. Macrophage Proliferation Is Regulated through CSF-1 Receptor Tyrosines 544, 559, and 807. *J. Biol. Chem.* **2012**, *287*, 13694–13704.
- (17) Qian, B.-Z.; Li, J.; Zhang, H.; Kitamura, T.; Zhang, J.; Campion, L. R.; Kaiser, E. A.; Snyder, L. A.; Pollard, J. W. CCL2 Recruits Inflammatory Monocytes to Facilitate Breast-Tumour Metastasis. *Nature* **2011**, *475*, 222–225.
- (18) Brown, J. M.; Wilson, W. R. Exploiting Tumour Hypoxia in Cancer Treatment. *Nat. Rev. Cancer* **2004**, *4*, 437–447.

- (19) Choi, J.; Kim, H.-Y.; Ju, E. J.; Jung, J.; Park, J.; Chung, H.-K.; Lee, J. S.; Lee, J. S.; Park, H. J.; Song, S. Y.; Jeong, S.-Y.; Choi, E. K. Use of Macrophages to Deliver Therapeutic and Imaging Contrast Agents to Tumors. *Biomaterials* **2012**, *33*, 4195–4203.
- (20) Dou, H.; Destache, C. J.; Morehead, J. R.; Mosley, R. L.; Boska, M. D.; Kingsley, J.; Gorantla, S.; Poluektova, L.; Nelson, J. A.; Chaubal, M.; Werling, J.; Kipp, J.; Rabinow, B. E.; Gendelman, H. E. Development of a Macrophage-Based Nanoparticle Platform for Antiretroviral Drug Delivery. *Blood* **2006**, *108*, 2827–2835.
- (21) Li, Z.; Huang, H.; Tang, S.; Li, Y.; Yu, X.-F.; Wang, H.; Li, P.; Sun, Z.; Zhang, H.; Liu, C.; Chu, P. K. Small Gold Nanorods Laden Macrophages for Enhanced Tumor Coverage in Photothermal Therapy. *Biomaterials* **2016**, *74*, 144–154.
- (22) Feng, Q.; Liang, S.; Jia, H.; Stadlmayr, A.; Tang, L.; Lan, Z.; Zhang, D.; Xia, H.; Xu, X.; Jie, Z.; Su, L.; Li, X.; Li, X.; Li, J.; Xiao, L.; Huber-Schönauer, U.; Niederseer, D.; Xu, X.; Al-Aama, J. Y.; Yang, H.; Wang, J.; Kristiansen, K.; Arumugam, M.; Tilg, H.; Datz, C.; Wang, J. Gut Microbiome Development along the Colorectal Adenoma–Carcinoma Sequence. *Nat. Commun.* **2015**, *6*, 6528.
- (23) Choi, M.-R.; Bardhan, R.; Stanton-Maxey, K. J.; Badve, S.; Nakshatri, H.; Stantz, K. M.; Cao, N.; Halas, N. J.; Clare, S. E. Delivery of Nanoparticles to Brain Metastases of Breast Cancer Using a Cellular Trojan Horse. *Cancer Nano* **2012**, *3*, 47–54.
- (24) Choi, M.-R.; Stanton-Maxey, K. J.; Stanley, J. K.; Levin, C. S.; Bardhan, R.; Akin, D.; Badve, S.; Sturgis, J.; Robinson, J. P.; Bashir, R.; Halas, N. J.; Clare, S. E. A Cellular Trojan Horse for Delivery of Therapeutic Nanoparticles into Tumors. *Nano Lett.* **2007**, *7*, 3759–3765.
- (25) Weissleder, R.; Nahrendorf, M.; Pittet, M. J. Imaging Macrophages with Nanoparticles. *Nature Mater.* **2014**, *13*, 125–138.
- (26) Dass, C. R.; Choong, P. F. Targeting of Small Molecule Anticancer Drugs to the Tumour and Its Vasculature Using Cationic Liposomes: Lessons from Gene Therapy. *Cancer Cell. Int.* **2006**, *6*, 17.
- (27) Yang, M.; Reynoso, J.; Jiang, P.; Li, L.; Moossa, A. R.; Hoffman, R. M. Transgenic Nude Mouse with Ubiquitous Green Fluorescent Protein Expression as a Host for Human Tumors. *Cancer Res.* **2004**, *64*, 8651–8656.
- (28) Tran Cao, H. S.; Reynoso, J.; Yang, M.; Kimura, H.; Kaushal, S.; Snyder, C. S.; Hoffman, R. M.; Bouvet, M. Development of the Transgenic Cyan Fluorescent Protein (CFP)-Expressing Nude Mouse for “Technicolor” Cancer Imaging. *J. Cell. Biochem.* **2009**, *107*, 328–334.
- (29) Yang, M.; Reynoso, J.; Bouvet, M.; Hoffman, R. M. A Transgenic Red Fluorescent Protein-Expressing Nude Mouse for Color-Coded Imaging of the Tumor Microenvironment. *J. Cell. Biochem.* **2009**, *106*, 279–284.
- (30) Hoffman, R. M. The Multiple Uses of Fluorescent Proteins to Visualize Cancer in Vivo. *Nat. Rev. Cancer* **2005**, *5*, 796–806.

- (31) Suetsugu, A.; Katz, M.; Fleming, J.; Truty, M.; Thomas, R.; Saji, S.; Moriwaki, H.; Bouvet, M.; Hoffman, R. M. Non-Invasive Fluorescent-Protein Imaging of Orthotopic Pancreatic-Cancer-Patient Tumorgraft Progression in Nude Mice. *Anticancer Res.* **2012**, *32*, 3063–3068.
- (32) Yang, M.; Li, L.; Jiang, P.; Moossa, A. R.; Penman, S.; Hoffman, R. M. Dual-Color Fluorescence Imaging Distinguishes Tumor Cells from Induced Host Angiogenic Vessels and Stromal Cells. *Proc. Natl. Acad. Sci. U. S. A.* **2003**, *100*, 14259–14262.
- (33) Hoffman, R. M.; Yang, M. Color-Coded Fluorescence Imaging of Tumor-Host Interactions. *Nat. Protoc.* **2006**, *1*, 928–935.
- (34) Kellam, B.; De Bank, P. A.; Shakesheff, K. M. Chemical Modification of Mammalian Cell Surfaces. *Chem. Soc. Rev.* **2003**, *32*, 327.
- (35) Wilson, J. T.; Krishnamurthy, V. R.; Cui, W.; Qu, Z.; Chaikof, E. L. Noncovalent Cell Surface Engineering with Cationic Graft Copolymers. *J. Am. Chem. Soc.* **2009**, *131*, 18228–18229.
- (36) Cheng, H.; Kastrup, C. J.; Ramanathan, R.; Siegwart, D. J.; Ma, M.; Bogatyrev, S. R.; Xu, Q.; Whitehead, K. A.; Langer, R.; Anderson, D. G. Nanoparticulate Cellular Patches for Cell-Mediated Tumor-tropic Delivery. *ACS Nano* **2010**, *4*, 625–631.
- (37) Koniev, O.; Wagner, A. Developments and Recent Advancements in the Field of Endogenous Amino Acid Selective Bond Forming Reactions for Bioconjugation. *Chem. Soc. Rev.* **2015**, *44*, 5495–5551.
- (38) Laughlin, S. T.; Bertozzi, C. R. Metabolic Labeling of Glycans with Azido Sugars and Subsequent Glycan-Profilng and Visualization via Staudinger Ligation. *Nat. Protoc.* **2007**, *2*, 2930–2944.
- (39) Weischenfeldt, J.; Porse, B. Bone Marrow-Derived Macrophages (BMM): Isolation and Applications. *Cold Spring Harb. Protoc.* **2008**, *2008*, 5080.
- (40) Livnah, O.; Bayer, E. A.; Wilchek, M.; Sussman, J. L. Three-Dimensional Structures of Avidin and the Avidin-Biotin Complex. *Proc. Natl. Acad. Sci. U. S. A.* **1993**, *90*, 5076–5080.
- (41) Rodriguez, L. G.; Wu, X.; Guan, J.-L. Wound-Healing Assay. *Cell Migr.* **2004**, *294*, 23–30.
- (42) Chen, H.-C. Boyden Chamber Assay. *Cell Migr.* **2004**, *294*, 15–22.
- (43) The Cancer Genome Atlas Network. Comprehensive Molecular Portraits of Human Breast Tumours. *Nature* **2012**, *490*, 61–70.
- (44) Richardsen, E.; Uglehus, R. D.; Johnsen, S. H.; Busund, L.-T. Macrophage-Colony Stimulating Factor (CSF1) Predicts Breast Cancer Progression and Mortality. *Anticancer Res.* **2015**, 865–874.

- (45) Gwak, J. M.; Jang, M. H.; Kim, D. I.; Seo, A. N.; Park, S. Y. Prognostic Value of Tumor-Associated Macrophages According to Histologic Locations and Hormone Receptor Status in Breast Cancer. *PLoS ONE* **2015**, *10*, 0125728.
- (46) Sousa, S.; Brion, R.; Lintunen, M.; Kronqvist, P.; Sandholm, J.; Mönkkönen, J.; Kellokumpu-Lehtinen, P.-L.; Lauttia, S.; Tynninen, O.; Joensuu, H.; Heymann, D.; Määttä, J. A. Human Breast Cancer Cells Educate Macrophages toward the M2 Activation Status. *Breast Cancer Res.* **2015**, *17*, 101.
- (47) Pulaski, B. A.; Ostrand-Rosenberg, S. Mouse 4T1 Breast Tumor Model. *Curr. Protoc. Immunol.* **2000**, *39*, 20.
- (48) Gregório, A. C.; Fonseca, N. A.; Moura, V.; Lacerda, M.; Figueiredo, P.; Simões, S.; Dias, S.; Moreira, J. N. Inoculated Cell Density as a Determinant Factor of the Growth Dynamics and Metastatic Efficiency of a Breast Cancer Murine Model. *PLoS ONE* **2016**, *11*, 0165817.

CHAPTER 4

MODIFICATION OF PRIMARY AND IMMORTALIZED MACROPHAGES AND STEM CELLS VIA BIOTIN-STREPTAVIDIN ASSOCIATION

4.1. Introduction

The use of modified T cell infusions as cancer immunotherapies in patients has demonstrated the potential of cell-based agents.¹ Multiple cell types have been used and/or studied in tracking inflammatory micro-environments *in vivo* via optical imaging²⁻⁴ as well as for generating biological entities at targeted locations via therapeutic gene delivery.⁵⁻⁷ Additionally, they have been studied for use in cell replacement therapy to fortify metabolic disorders like diabetes,^{8,9} in tandem with nanoparticle/drug delivery,¹⁰ and regenerative medicine applications.¹¹⁻¹³ Cells have shown distinct advantages over other vehicle systems and implants in terms of biocompatibility, extended circulatory lifetimes, and specificity.^{10,12} Cell-based delivery vehicles respond to chemotactic markers and cytokines present in disease microenvironments, leading to a greater propensity to accumulate in the desired tissues. In particular, wounds, inflamed tissues, infected sites, and tumors are known to secrete chemo-attractants like colony stimulating factor (CSF-1) and chemokines like C-X-C motif ligand 1 (CXCL1), resulting in their recruitment of macrophages,¹⁴ and mesenchymal stem cells (MSCs).^{4,15,16} These can include hypoxic and ischemic areas of wounded tissues and tumor sites,¹⁷ as well as sites of bacterial infection pertaining to acute pneumonia,¹⁸ chronic implant infections,¹⁹ and urinary tract infections.²⁰ In contrast, most small molecule drugs and macromolecular delivery vehicles (e.g., nanoparticles and liposomes) rely on passive accumulation and the enhanced

permeability and retention (EPR) effect.²¹ Thus, cells have emerged as attractive candidates for next generation theragnostics. In particular, macrophages and MSCs have been widely used in tissue repair applications^{7,8,10,22} and as delivery vehicles. In the latter case, phagocytic loading strategies have typically been used to encapsulate drugs and nanoparticles.^{23,24} However, to harness the therapeutic potential of cells in various applications cell surface modification is desired.^{9,25} Similarly, facile surface engineering of therapeutic cells is crucial in other theragnostic applications involving labeling, tethering, or sensing.^{26,27}

One strategy often employed to modify cell surface is non-covalent engineering of the cell surface. Non-covalent cell surface bioconjugation methods based on physisorption can be of various types like electrostatic layer-by-layer surface deposition²⁸⁻³¹ or hydrophobic lipid insertion³²⁻³⁴ into the cell membrane. The electrostatic nanofabrication of multilayered films for cell transplants or tissue engineering applications has been utilized.²⁹ Surface adsorption mediated via electrostatic adsorption of poly(L-lysine)-graft-poly(ethylene glycol) (PLL-g-PEG) grafts terminally functionalized with biotin, hydrazide, and azide moieties to selectively conjugate to streptavidin, aldehyde, and cyclooctyne-labeled probes, respectively, on cell surfaces have been studied in the remodeling of cells for biomedical and biotechnological applications.²⁸ However, for clinical purposes, systemically injected cells must withstand shear stress exerted by vascular drag while in circulation.³⁵ Thus, ensuring robust and uniform labeling of the surface still remains a challenge. To overcome these issues, while harnessing the disease tissue specific recruiting ability of cellular vehicles, researchers have engineered cell surfaces via covalent conjugations.

Unlike non-covalent surface labeling, covalent conjugations at the cell surface can enable attachment of various entities and provide a stable linkage. Metabolic labeling incorporating non-natural glycans and other clickable functional groups like azides,³⁶ thiols,³⁷ and methacryloyl groups³⁸ for bio-orthogonal reactions³⁹ was an approach pioneered by Bertozzi and followed by many others.^{40,41} These methods have been applied in various applications like attaching tracking entities such as fluorophores or affinity tags at the cell surface to visualize and quantitatively monitor changes of sialylation during tumor progression⁴² or to display uncommon functional groups like ketones which could then be covalently ligated to molecules having complementary reactive handles like hydrazide for the selective chemical engineering of cell surfaces.⁴³ Apart from metabolic engineering, other non-genetic membrane engineering methods like enzymatic “sortagging” have been used to conjugate antibodies onto naturally exposed N-terminal glycine residues of surface proteins.⁴⁴

The cell membrane is a dynamic layer comprised of lipids, proteins, and carbohydrates, presenting a variety of available chemical handles for attachment. While the lipid bilayer is often used for non-covalent electrostatic depositions and hydrophobic insertions, surface proteins and glycans are often taken advantage of to achieve covalent surface modifications. Unlike metabolic incorporation of non-natural sugars or enzymatic modification of proteins, chemical modifications at the cell surface may be used to manipulate proteins or glycans endogenous to the cell surface.^{10,45} Surface biomolecules with exposed chemical groups such as amines^{46,47} or thiols⁴⁸ on surface proteins and generation of carbonyl groups like aldehydes⁴⁹ and ketones,^{50,51} on surface glycans. These moieties present excellent handles to modify the cell membrane and have been explored

for the attachment of different tracker fluorophores,^{46,52} N-hydroxysuccinimide-DNA (NHS–DNA) conjugates,⁵³ nanoparticles,^{48,51,54} and drug-nanoparticle hybrids.⁴⁹

Live-cell surface engineering can be particularly challenging as the cell membrane is incredibly delicate. Any method for cell surface modification must be performed at or around physiological temperature, pH, ionic strength, and osmolality to maintain minimal alterations to the native biological environment of the cells. A commonly used strategy for the covalent modification of exposed lysine side chains is the amide bond formation with an N-hydroxysuccinimide (NHS) ester.^{46,47,53} This has been used for the attachment of biotin for the association of the avidin protein.^{46,47} This has been shown to form a robust attachment on the cell surface that remains intact in sufficient concentrations for several days even as cells proliferate.⁵²

While these different covalent surface modifications have been attempted in various cell types independently, a parallel comparison of functionalizations under the same conditions in different types of cells commonly used as vehicles is lacking. Hence, we sought to compare macrophages with stem cells, and also utilized primary versions of each. Here, we attached NHS-biotin to exposed lysine residues on cell surfaces and facilitated associations with avidin-FITC on RAW 264.7 (immortalized macrophages), bone marrow derived macrophages (BMDMs), hTERT (immortalized) stem cells, and primary stem cells (Figure 4.1). While RAW 264.7⁵³ and hTERT-MS⁵⁴ cells are standard model macrophage and stem cell lines, respectively, primary bone marrow derived macrophages (BMDMs) and primary mesenchymal stem cells (MSCs) are translationally more relevant in clinical studies of cell-based therapies. Thus, we tested the surface modification strategy on model immortalized and primary macrophages and stem cells, in

parallel. As immortalized cell lines offer multiple passages and growth to perform optimization studies and primary cells are more representative of developed therapeutic strategies while being more difficult to obtain. After initial validation of proof-of-concept surface labeling and assessment on immortalized cells, we extended the same studies to their primary counterparts. By using this approach, we obtained robust covalent chemical modification of the cell surfaces.

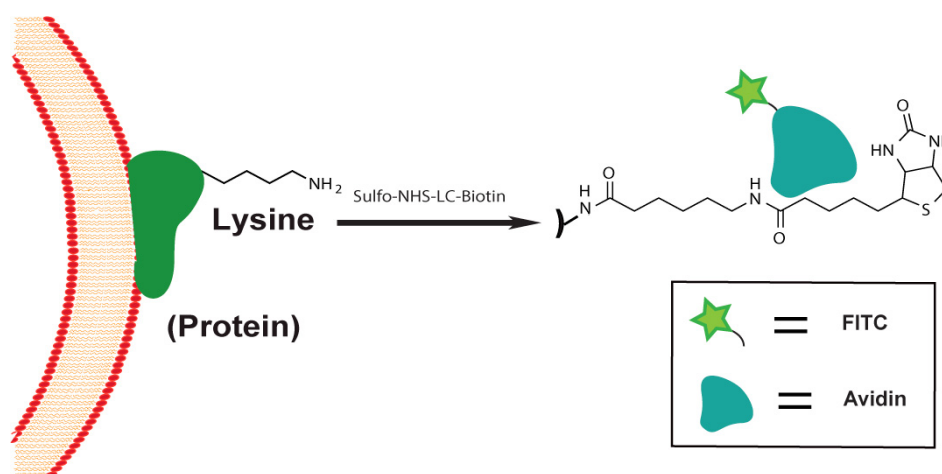


Figure 4.1. Overview of approach used for modification of cells. The conjugation of NHS-esters with free amines is used for the attachment of biotin, which is subsequently allowed to associate with avidin-fluorophore.

While there have been some studies¹⁰ on covalent cell surface modification for theragnostic applications including some from our own lab,⁵² previous studies lacked rigorous quantification. With the help of surface fluorophore quenching experiments, we tracked the surface modification over time. We assessed the retention of fluorescein complexes on cell surfaces for up to 48 h, looking at the cellular images qualitatively via confocal microscopy and quantitatively using a fluorescent plate reader. Thereafter, we compared NHS-lysine conjugation chemistry in terms of cellular characteristics such as

viability and migration post modification across all four cell types. This work sets the stage for further use of surface-modified cells as potential carriers for diagnostic tools as well as delivery agents for therapeutics and molecular probes to study the disease microenvironments both qualitatively and quantitatively. In summary, these studies to optimize and compare chemical reactions on live cell surfaces will benefit their use as next generation delivery vehicles for cellular therapies.

4.2. Materials & Methods

4.2.1. Materials

Sulfo-NHS-LC-biotin (referred to as NHS-biotin) and all other reagents were purchased from Thermo-Fisher Scientific except where otherwise noted.

4.2.2. Cell culture

RAW 264.7 cells were obtained from the American Tissue Culture Collection (ATCC), human telomerase reverse transcriptase-immortalized mesenchymal stem cells (hTERT MSCs) and MDA-MB-231 cells were obtained from Prof. Shelly Peyton (Chemical Engineering, UMass Amherst), and L929 cells were obtained from obtained from Prof. Barbara Osborne (Veterinary and Animal Sciences, UMass Amherst). Primary macrophages and stem cells were isolated and differentiated from bone marrow of BALB/c mice, described below. All cells were maintained in a humidified 5% CO₂ atmosphere at 37 °C. Cells were sub-cultured approximately once every 3-4 days and only cells between passages 7 and 20 were used for all experiments. RAW 264.7, BMDMs, MDA-MB-231, and L929 cells were cultured in high glucose Dulbecco's Modified Eagle Medium

(DMEM, Gibco) supplemented with 10% fetal bovine serum (FBS, Corning), 1% L-Glutamine (200 mM, L-Glut, Gibco) and 1% antibiotics (100 µg/ml penicillin and 100 µg/ml streptomycin, P/S, Gibco), referred to herein as complete DMEM. hTERT MSCs and primary stem cells were cultured in Minimum Essential Media (MEM)-alpha (Gibco) supplemented with 10% FBS and 1% P/S, referred to as complete MEM-alpha. For detachment from culture flasks/dishes, 0.25% trypsin-EDTA was used with RAW 264.7 cells, and 0.05% trypsin-EDTA was used with hMSCs and primary stem cells. BMDMs were physically dislodged using a cell scraper while in complete DMEM media.

4.2.3. Generation of conditioned media

Cells were cultured and passaged at least once before being used to generate conditioned media. The procedure used to generate conditioned media follows a previously established protocol,⁵⁵ and was used for both L929 and MDA-MB-231 cells. Briefly, cells were cultured in T175 flasks with complete DMEM until they became > 90% confluent. At that point, media was replaced with complete DMEM media and cells were cultured for an additional 7 days. On day 7, the media was collected and filtered through a 0.45 µm syringe filter and stored at -20 °C. For experiments described here, L929 conditioned media was used within the first six months, and MDA-MB-231 conditioned media was used within one month.

4.2.4. Isolation of progenitor cells and differentiation into primary macrophages and stem cells

Isolation of progenitor cells, and differentiation into primary macrophages was performed following a previously established procedure.⁵⁶ Bones were collected from femurs and tibiae from BALB/c mice and put into 0.6 mL micro-centrifuge tubes containing a small hole at the bottom (perforated prior to use with an 18G needle). Each 0.6 mL micro-centrifuge tube (containing one femur and one tibia) was inserted into a 1.5 mL micro-centrifuge tube and centrifuged for 30 seconds at 10,000 rpm. The 0.6 mL tube with marrow-less bones was then discarded and the pelleted bone marrow (in the 1.5 mL-tube) was re-suspended in 500 μ L of media containing 70% complete DMEM and 30% L929-conditioned media, together referred to as differentiation media. The contents of each 1.5 mL tube were then transferred to a T175 tissue culture flask, mixed with 12 mL of differentiation media, and incubated for 3 days, after which the media was replaced with 12 mL of fresh differentiation media for an additional 4 days. Following differentiation, media was replaced with complete DMEM, and the cells were incubated until needed for experiments (for a maximum of 3 weeks). For differentiation of primary mesenchymal stem cells (MSCs), once the pelleted marrow was obtained, it was re-suspended in 500 μ L of complete MEM-alpha. The contents of each 1.5mL tube were then transferred to a T175 tissue culture flask, mixed with 12 mL of complete MEM-alpha, and incubated overnight to allow cells to adhere. 24 h later, the media was replaced with 12 mL of fresh complete MEM-alpha and the cells were then incubated until confluent (2-3 weeks). To ensure homogeneity, MSCs were passaged at least three times (allowing the cells to become confluent between each passage).

4.2.5. NHS-biotin/avidin-FITC modification of cells

For confocal microscopy experiments involving all cell types, 5×10^4 cells in 250 μL of the corresponding complete media were plated in borosilicate glass bottom 8-well chamber slides (Nunc Lab-Tek). For viability experiments, 1×10^5 cells in 500 μL of corresponding media were added to 24-well plates (Costar). Prior to labeling, the cells were maintained overnight in a humidified 5% CO_2 atmosphere at 37 $^\circ\text{C}$. The following day, cells were modified while adhered to the respective surfaces. First, culture medium was removed, and cells were washed with 500 μL of phosphate-buffered saline (PBS, Gibco). Cells were then incubated in 250 μL and 500 μL of 0.5 mM sulfo-NHS-LC-biotin in PBS in 8-well chambers and 24-well plates respectively for 30 min at ambient temperature and then washed once with 250 μL and 500 μL PBS respectively. Then, 0.05 mg/mL avidin-FITC in 250 μL PBS for 8-well chambers and 500 μL PBS for 24-well plates were added to the cells, which were then incubated for 30 min at ambient temperature. This was followed by an additional two washes with PBS (250 & 500 μL each). Finally, 250 & 500 μL each of the phenol red-free version of the corresponding complete growth media was added and the cells were used for further experiments. For Boyden chamber migration assays, cells were modified while in suspension. 1×10^6 cells were detached from flasks and washed with 5 mL PBS twice were modified while suspended in 15 mL conical tubes in 5 mL of the corresponding labeling reagents in PBS (all concentrations and incubation times consistent with adherent labelling described above). Between steps, cells were pelleted via centrifugation at 1500 rpm for 5 minutes. The pellets were washed with 5 mL PBS before each individual treatment.

4.2.6. Confocal microscopy of modified cells

Cell images were acquired using a Nikon Point Scanning C2+ confocal microscope with excitation at 488 nm at 0 h and 24 h time points following modification in borosilicate glass bottom 8-well chamber slides. Between time-points, the cells were incubated at 37 °C under a humidified atmosphere containing 5% CO₂. Fluorescent and merged cell images were analyzed with Nikon NIS-Elements and FIJI (Image J) software.⁵⁷

4.2.7. Assessment of changes in surface fluorescence over time

5×10^4 cells were plated in borosilicate glass bottom 8-well chamber slides (Nunc Lab-Tek) in three different wells and labeled with sulfo-NHS-LC-biotin/avidin-FITC as described in *Section 4.2.5*, above. Surface modified cells were imaged with confocal microscope as described in *Section 4.2.6*. Of the three wells modified using the same method at the same time, the first well was imaged at 0 h. Immediately after imaging, the cells in the first well were quenched with 0.4% Trypan Blue and imaged again. The cells in the other two wells were incubated at 37 °C and 5% CO₂ and imaged at 24 h and 48 h, respectively, without quenching followed by quenching with Trypan Blue. To quantify the cell surface retention of fluorescence over time the following method was employed: using the selection tool in the ImageJ software, three different areas of approximately 300 x 300 pixels consisting of around 10 cells imaged at 60 X magnification per area for cells and 10 x 10 pixels for nearby areas with no cells were selected as background. Thus, a total of approximately 30 cells were used for each set of analysis. The integrated fluorescence intensity for the selected cells was determined by Image J at the indicated time points,

averaged across all cells, and background intensity subtracted. Thus, the corrected total cell fluorescence (CTCF) was calculated as:

$$\text{CTCF} = \text{Integrated Density} - (\text{Area of selected cell} \times \text{Mean background fluorescence}).$$

Since Trypan Blue is impermeable to living cells, the fluorescence quenched by it at a given time for a selected area of cells amounts to the amount of fluorescence retained by living cells at the surface. The FITC labelled cells were imaged before and after quenching with Trypan Blue at time intervals of 0, 24 and 48 h. Then, the corresponding corrected total cell fluorescence (CTCF) was calculated using Image J. The fluorescence retained at the surface was calculated as CTCF of cells quenched with Trypan Blue (fluorescence retained at the surface of cells in the selected are at that time point) divided by CTCF of non-quenched cells (total fluorescence of cells in the selected are at that time point before quenching the surface fluorescence) multiplied by 100. The percentage change in surface fluorescence over time was then plotted.

4.2.8. Viability studies

Cells were labeled as described above in a 24 well plate at a density of 1×10^5 cells per well. 48 hours after modification, viability was determined using Alamar Blue reagent (Thermo Fisher Scientific) according to the manufacturer's instructions. Briefly, 10% Alamar Blue reagent and 90 % phenol red-free complete media was added to the cells and the plate was incubated for an hour. Then the fluorescence absorption was measured at 540/590 nm using BioTek Gen5 software in SpectraMax microplate reader.

4.2.9. Chemotaxis assays

Boyden chamber cell migration assays were performed using trans-well inserts (8 μm pore, 6.5 mm, PET membrane, Corning) based on a previously established protocol.⁶⁶ Prior to the experiment, cells were cultured in DMEM- or MEM-alpha generated similarly to the “complete” versions with the exception that 1% FBS was used (referred to as starved media) for 24 h, after which they were modified using the methods described above. Inserts were placed into 24-well plates containing 650 μL of the respective starved media, which was supplemented with 40 ng/mL rCSF-1 (R&D Systems) for RAW 264.7 and BMDM cells and MDA-MB-231 conditioned media for hMSCs and primary MSCs; no rCSF-1 supplements were added for non-chemoattractant controls for macrophages and regular (non-conditioned) MEM-alpha medium for stem cells. 1×10^5 modified cells in 100 μL of corresponding complete media were added to each insert and incubated for 12 h at 37 °C, 5% CO₂. Non-migratory cells were removed with a Q-tip, and migratory cells at the bottom of the insert were fixed in 4% formaldehyde (Pierce 16% with a 4x dilution in PBS) and stained with 0.1% crystal violet (MilliporeSigma) in 25% methanol and 75% Milli-Q water. Membranes were removed from the insert, mounted onto cover glass slips and imaged using a Zeiss Axio Cam 506 Color attachment (20X) to image crystal violet-stained membranes in the brightfield. Cells were counted from three fields of view per membrane, with three membranes per condition (n = 9) using a Nikon inverted TE2000-S light microscope. Box and whisker plots were generated using OriginPro 2017 (Origin lab).

4.3. Results and discussion

4.3.1. Cell surface engineering with NHS-biotin chemistry

Cell surface modifications were performed on immortalized and primary macrophages, RAW 264.7 and BMDM, respectively, and immortalized and primary stem cells, hTERT and Primary MSC, respectively. We used NHS-ester modification of accessible amines. Biotin moieties were installed via use of NHS-biotin, which were immediately associated with avidin-FITC, resulting in the display of a substantially large (66-67 kDa) protein on cell surfaces. In each case, significant amounts of fluorophore were observed on the cells, with the RAW 264.7 cells appearing to have the highest levels of internalization (Figure 4.2).

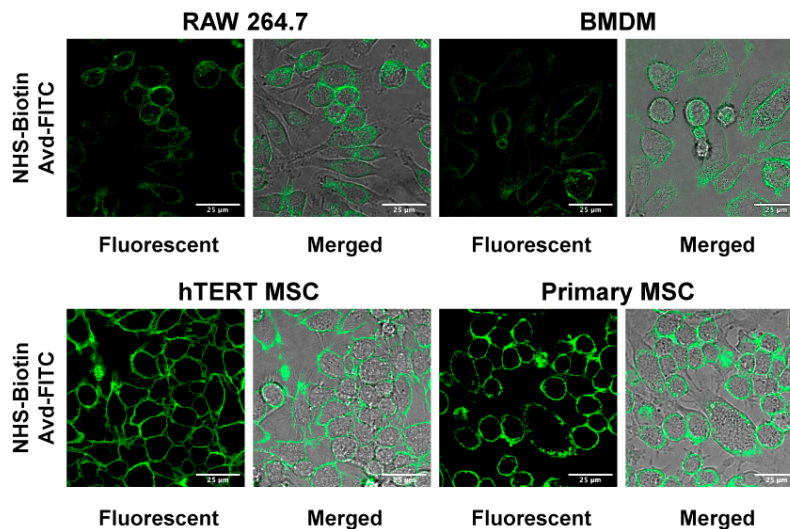


Figure 4.2. Comparison of attachments to different cell types using biotin-avidin association. Cells are labelled in the presence of NHS-biotin/avidin -FITC. Immortalized and primary cells of macrophages (right) and stem cells (left) were labelled. Magnification = 60x, scale bar = 25 µm.

Appropriate control experiments were also performed, relevant to each stage of the modifications to confirm that specific labeling was achieved in RAW 264.7 cells (Figure

4.3). For conditions involving NHS-biotin/avidin associations, no-NHS-biotin controls were used. No fluorescence was observed where cells were incubated with only avidin, indicating the absence of non-specific interactions.

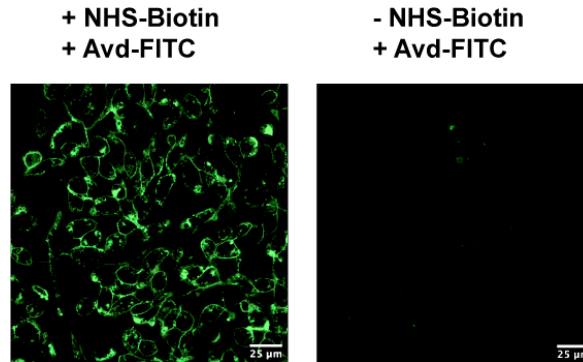


Figure 4.3. Control experiments for cell modifications. Conditions were validated by labelling in the presence or lack of biotin-NHS. Without treatment of biotin-NHS, no labelling was observed (right). RAW 264.7 cells were used for these experiments.

Prior to arriving at the conditions used, we performed optimization studies with 5×10^4 cells and cell viability using 1×10^5 cells. For NHS-biotin/avidin-FITC associations, we found that treatment 0.5 mM NHS-biotin followed by 0.05 mg/mL avidin-FITC yielded the best results. Treatments performed with lower concentrations of avidin-FITC in the range 0.01-0.025 mg/mL resulted in inconsistent surface labeling while higher concentrations of avidin-FITC in the range of 0.1-0.25 mg/mL resulted in increased internalization.

4.3.2. Tracking retention of cell-surface fluorescence over time

The stability of initial covalent conjugation at the cell surface is affected by kinetic and thermodynamic factors apart from concentration of bio-conjugating reagents used.

However, the retention of a molecule on the cell surface over time can be affected by various cellular characteristics such as the phenotype of the modified cell (whether it is a phagocyte or not), doubling times, and whether the cell is primary or immortalized. After confirming labelling, we assessed the retention of fluorescein complexes on cell surfaces over time for up to 48 h. Trypan Blue has been used in literature to quench extracellular green fluorophores in phagocytosis assays.⁵⁸ Cells labelled with avidin-FITC were imaged before and after quenching with Trypan Blue at 0, 24 and, 48 h of initial labeling (Figure 4.4). For quantification of the cell surface fluorescence change over time, the fluorescence intensity of the cells plated in the same well was compared before and after quenching with 0.4% Trypan Blue (Figure 4.5). The details of the experimental methods used are described in *Section 4.2.7*. For all four cell types, almost 50% of the fluorophore appears to be internalized after 24 h, with additional internalization after 48 h (25-30% retained). We observed that the mesenchymal stem cells were slightly better than the phagocytic macrophages in terms of retention of the NHS-biotin/avid-FITC complexes. In the future, this assay should be repeated with additional biological replicates and more cells analyzed.

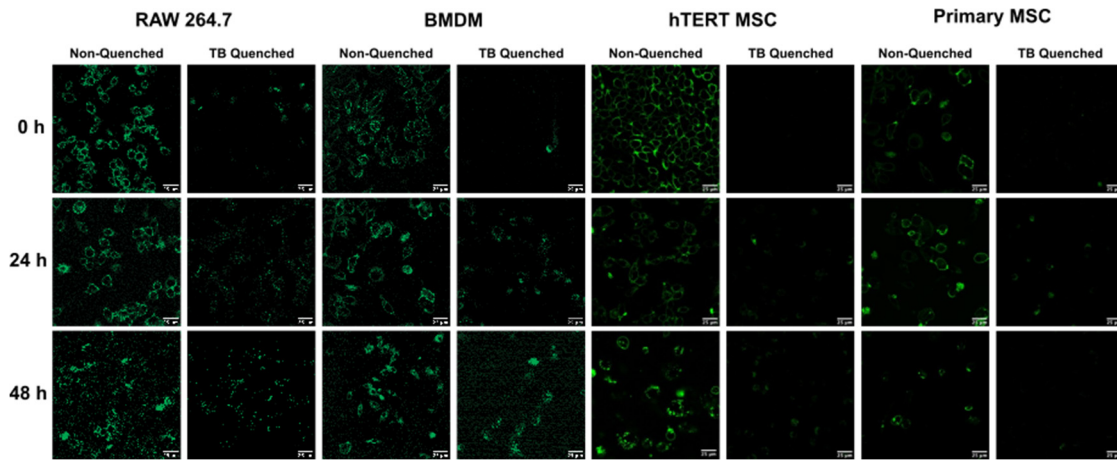


Figure 4.4. Representative quenching images for (left to right) RAW 264.7 cells, BMDMs, hTERT MSCs, and primary MSCs after modification with NHS-biotin/avidin-FITC. Each pair of images per cell type includes (left) non-quenched and (right) quenched examples. Magnification = 60x, scale bar = 25 μ m. Quenching was performed 0, 24, or 48 hours after modification. TB = trypan blue.

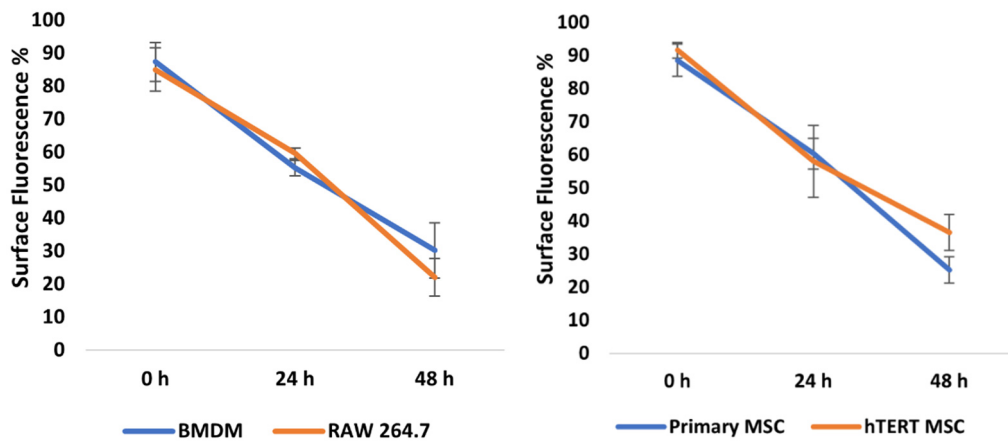


Figure 4.5. Surface fluorescence over time in BMDM, RAW 264.7 cells, Primary MSC, and hTERT MSC after modification with NHS-biotin/avidin-FITC.

4.3.3. Viability studies

For posited applications of surface-modified cells, it is critical that they maintain their viability following conjugations. Hence, we assessed their viability using the Alamar Blue reagent (Figure 4.6). We observed that the mild modification strategies did not impact cellular viability for up to 48 h after labeling. The NHS-biotin/avidin-FITC modification resulted in greater than 90% cell viability for both immortalized and primary macrophages and stem cells.

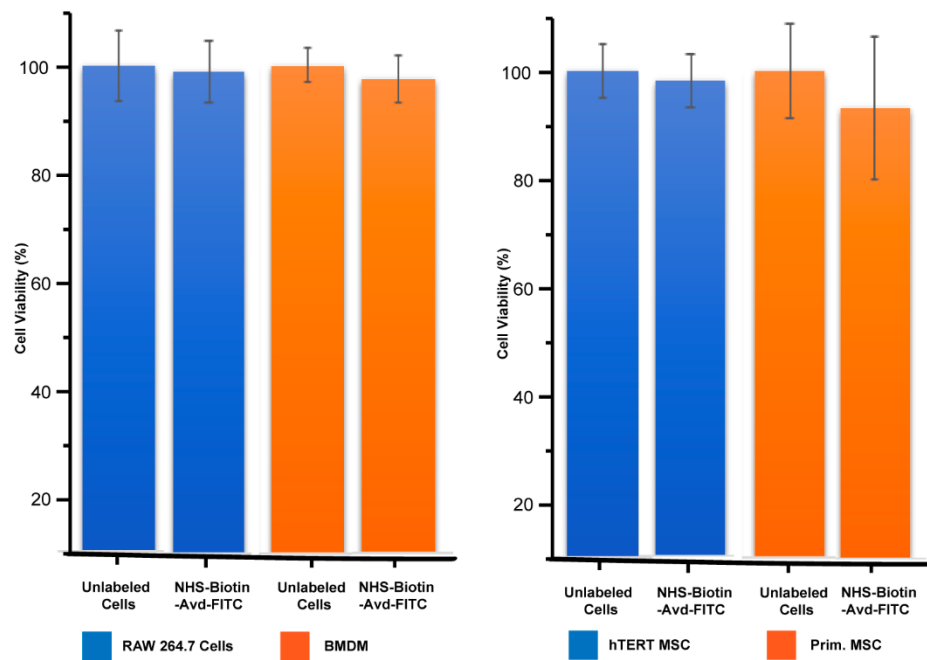


Figure 4.6. Viability of cells 48 h post-modification macrophages (left) and mesenchymal stem cells (right). Cell viability was performed via Alamar Blue assay. No significant difference in viability is found via comparison with unlabeled cells. Bars indicate the average values across three biological replicates. Error is represented as standard deviation of the mean.

4.3.4. Motility studies

Since migration and chemotaxis are pivotal attributes of macrophages and stem cells that make them ideal vehicles, we sought to confirm that cell motility and chemosensing were not impacted by modifications. To this end, we performed Boyden chamber cell migration assays (Figure 4.7) to quantitatively measure modified cells' response to chemoattractant. Following exposure and migration, cells that passed through the membrane were counted. Box and whisker plots comparing the migratory behavior of labelled versus unlabeled cells in response to the chemoattractant MCSF-1 for macrophages and MDA-MB-231 conditioned media for the stem cells. The number of cells that migrated toward chemoattractant was at least three-fold higher compared to controls without any chemoattractant (Figure 4.7). It is interesting to note that overall, macrophages migrated to greater extents than stem cells. This is consistent with existing literature, which suggests that large number of macrophages are recruited to the tumor site, in some cases comprising up to 50% of the tumor mass.⁵⁹ While recruitment of stem cells to MDA-MB-231 breast cancer tumor xenografts⁶⁰ and other cancers (e.g., glioma) are reported, this is usually in range of only 5 to 10%.⁶¹

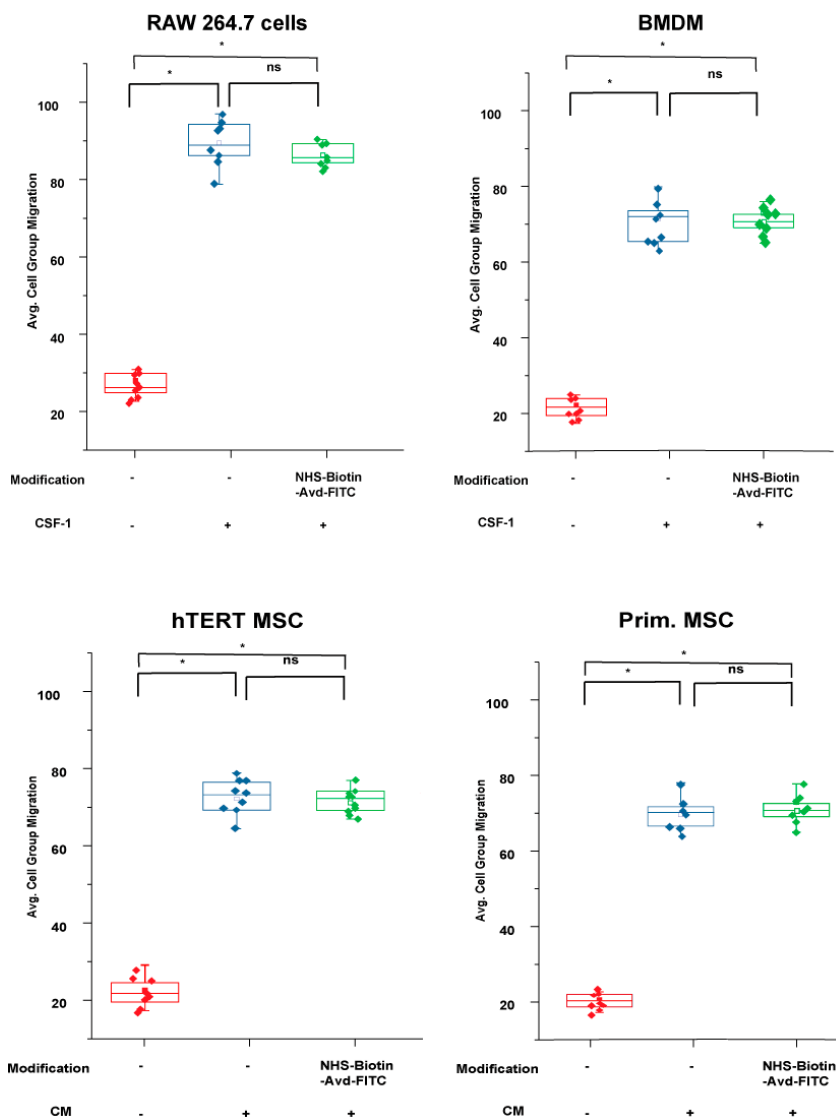


Figure 4.7. Migration and chemotaxis of modified and control cells. Boyden chamber experiments were carried out using colony stimulating factor 1 (CSF-1) chemoattractant for macrophages and MDA-MB-231 conditioned media (CM) for stem cells. Immortalized and primary macrophages (above) and stem cells (below) were labelled before being introduced to chemoattractant opposite a membrane (8 μm pore size); controls included no modification and no chemoattractant. Following migration, cells were stained, and membranes were fixed to glass slides for imaging and counting. The line bisecting the box represents the median. Squares in the center represent the mean while whiskers indicate the 5th and 95th percentiles. Statistical significance is determined using the student's t test (two-tailed distribution and two sample unequal variance). * $P \leq 0.000$.

4.4. Conclusion and future directions

There is an array of applications that exterior-modified cells could advance, including imaging, diagnostics, and drug delivery. Given that macrophage and stem cells possess innate biocompatibility and migratory capabilities, the retention of these characteristics post-modification is critical. Hence, we performed covalent bioconjugations at the cell surfaces to modify immortalized model macrophages and stem cells (RAW 264.7 cells and hTERT MSCs, respectively), and also their primary counterparts (BMDMs and primary MSCs). In the work presented here, we demonstrated that the use of bio-compatible, cell-surface modifications involving NHS reactions with accessible amines result in substantial display of cargo and do not impact cellular characteristics vital to their use. For those applications that require the payload to remain on the cell exterior or to do so for a longer extent of time, the use of additional linkers/retention moieties may be feasible if larger (e.g., protein-based) agents cannot be used to prevent uptake. In future work, the attachment of different types of cargo (e.g., antibodies, peptides, small molecules with varying charges, or nucleic acids) should also be evaluated, both as linkers and payloads. Further, since the environment, model, and application where surface-engineered cells are used may also play a role in their efficacy and behavior, it is advisable to evaluate multiple iterations of these tools (e.g., cell type or modification strategy/extent) in the relevant context prior to settling on a single approach.

4.5. References

- (1) Miliotou, A. N.; Papadopoulou, L. C. CAR T-Cell Therapy: A New Era in Cancer Immunotherapy. *Curr. Pharm. Biotechnol.* **2018**, *19*, 5–18.
- (2) Eisenblätter, M.; Ehrchen, J.; Varga, G.; Sunderkötter, C.; Heindel, W.; Roth, J.; Bremer, C.; Wall, A. In Vivo Optical Imaging of Cellular Inflammatory Response in Granuloma Formation Using Fluorescence-Labeled Macrophages. *J. Nucl. Med.* **2009**, *50*, 1676–1682.
- (3) Simon, G. H.; Daldrup-Link, H. E.; Kau, J.; Metz, S.; Schlegel, J.; Piontek, G.; Saborowski, O.; Demos, S.; Duyster, J.; Pichler, B. J. Optical Imaging of Experimental Arthritis Using Allogeneic Leukocytes Labeled with a Near-Infrared Fluorescent Probe. *Eur. J. Nucl. Med. Mol. Imaging* **2006**, *33*, 998–1006.
- (4) Kidd, S.; Spaeth, E.; Dembinski, J. L.; Dietrich, M.; Watson, K.; Klopp, A.; Battula, V. L.; Weil, M.; Andreeff, M.; Marini, F. C. Direct Evidence of Mesenchymal Stem Cell Tropism for Tumor and Wounding Microenvironments Using In Vivo Bioluminescent Imaging. *Stem Cells* **2009**, *27*, 2614–2623.
- (5) He, W.; Qiang, M.; Ma, W.; Valente, A. J.; Quinones, M. P.; Wang, W.; Reddick, R. L.; Xiao, Q.; Ahuja, S. S.; Clark, R. A.; Freeman, G. L.; Li, S. Development of a Synthetic Promoter for Macrophage Gene Therapy. *Hum. Gene Ther.* **2006**, *17*, 949–959.
- (6) Yan, F.; Li, X.; Li, N.; Zhang, R.; Wang, Q.; Ru, Y.; Hao, X.; Ni, J.; Wang, H.; Wu, G. Immunoproapoptotic Molecule ScFv-Fdt-TBid Modified Mesenchymal Stem Cells for Prostate Cancer Dual-Targeted Therapy. *Cancer Lett.* **2017**, *402*, 32–42.
- (7) Lai, Q.-G.; Yuan, K.-F.; Xu, X.; Li, D.; Li, G.-J.; Wei, F.-L.; Yang, Z.-J.; Luo, S.-L.; Tang, X.-P.; Li, S. Transcription Factor Osterix Modified Bone Marrow Mesenchymal Stem Cells Enhance Callus Formation during Distraction Osteogenesis. *Oral Surg. Oral Med. Oral Pathol. Oral Radiol. and Endodontol.* **2011**, *111*, 412–419.
- (8) Xie, Q.-P.; Huang, H.; Xu, B.; Dong, X.; Gao, S.-L.; Zhang, B.; Wu, Y.-L. Human Bone Marrow Mesenchymal Stem Cells Differentiate into Insulin-Producing Cells upon Microenvironmental Manipulation in Vitro. *Differen.* **2009**, *77*, 483–491.
- (9) Lee, D. Y.; Park, S. J.; Nam, J. H.; Byun, Y. A New Strategy Toward Improving Immunoprotection in Cell Therapy for Diabetes Mellitus: Long-Functioning PEGylated Islets *In Vivo*. *Tissue Eng.* **2006**, *12*, 615–623.
- (10) Joshi, B. P.; Hardie, J.; Farkas, M. E. Harnessing Biology to Deliver Therapeutic and Imaging Entities via Cell-Based Methods. *Chem. Eur. J.* **2018**, *24*, 8717–8726.
- (11) Rajabzadeh, N.; Fathi, E.; Farahzadi, R. Stem Cell-Based Regenerative Medicine. *Stem Cell Investig.* **2019**, *6*, 19.
- (12) Porada, C. D.; Almeida-Porada, G. Mesenchymal Stem Cells as Therapeutics and Vehicles for Gene and Drug Delivery. *Adv. Drug Deliv. Rev.* **2010**, *62*, 1156–1166.

- (13) Park, J. S.; Suryaprakash, S.; Lao, Y.-H.; Leong, K. W. Engineering Mesenchymal Stem Cells for Regenerative Medicine and Drug Delivery. *Methods* **2015**, *84*, 3–16.
- (14) Miyake, M.; Lawton, A.; Goodison, S.; Urquidi, V.; Gomes, G. E.; Zhang, G.; Ross, S.; Kim, J.; Rosser, C.J. Chemokine (CXC) ligand 1 (CXCL1) protein expression is increased in aggressive bladder cancers. *BMC Cancer*. **2013**, *13*, 1-7.
- (15) Porada, C.; Zanjani, E.; Almeida-Porada, G. Adult Mesenchymal Stem Cells: A Pluripotent Population with Multiple Applications. *Curr. Stem Cell Res. Ther.* **2006**, *1*, 365–369.
- (16) Motaln, H.; Schichor, C.; Lah, T. T. Human Mesenchymal Stem Cells and Their Use in Cell-Based Therapies. *Cancer* **2010**, *116*, 2519–2530.
- (17) Murdoch, C.; Giannoudis, A.; Lewis, C. E. Mechanisms Regulating the Recruitment of Macrophages into Hypoxic Areas of Tumors and Other Ischemic Tissues. *Blood* **2004**, *104*, 2224–2234.
- (18) Gupta, N.; Krasnodembskaya, A.; Kapetanaki, M.; Mouded, M.; Tan, X.; Serikov, V.; Matthay, M. A. Mesenchymal Stem Cells Enhance Survival and Bacterial Clearance in Murine *Escherichia Coli* Pneumonia. *Thorax* **2012**, *67*, 533–539.
- (19) Johnson, V.; Webb, T.; Norman, A.; Coy, J.; Kurihara, J.; Regan, D.; Dow, S. Activated Mesenchymal Stem Cells Interact with Antibiotics and Host Innate Immune Responses to Control Chronic Bacterial Infections. *Sci. Rep.* **2017**, *7*, 9575.
- (20) Schiwon, M.; Weisheit, C.; Franken, L.; Gutweiler, S.; Dixit, A.; Meyer-Schwesinger, C.; Pohl, J.-M.; Maurice, N. J.; Thiebes, S.; Lorenz, K.; Quast, T.; Fuhrmann, M.; Baumgarten, G.; Lohse, M. J.; Opdenakker, G.; Bernhagen, J.; Bucala, R.; Panzer, U.; Kolanus, W.; Gröne, H.-J.; Garbi, N.; Kastenmüller, W.; Knolle, P. A.; Kurts, C.; Engel, D. R. Crosstalk between Sentinel and Helper Macrophages Permits Neutrophil Migration into Infected Uroepithelium. *Cell* **2014**, *156*, 456–468.
- (21) Maeda, H. Macromolecular Therapeutics in Cancer Treatment: The EPR Effect and Beyond. *J Control Release* **2012**, *164*, 138–144.
- (22) Spiller, K. L.; Koh, T. J. Macrophage-Based Therapeutic Strategies in Regenerative Medicine. *Adv. Drug Deliv. Rev* **2017**, *122*, 74–83.
- (23) Choi, M.-R.; Stanton-Maxey, K. J.; Stanley, J. K.; Levin, C. S.; Bardhan, R.; Akin, D.; Badve, S.; Sturgis, J.; Robinson, J. P.; Bashir, R.; Halas, N. J.; Clare, S. E. A Cellular Trojan Horse for Delivery of Therapeutic Nanoparticles into Tumors. *Nano Lett.* **2007**, *7*, 3759–3765.
- (24) Das, R.; Hardie, J.; Joshi, B. P.; Zhang, X.; Gupta, A.; Luther, D. C.; Fedeli, S.; Farkas, M. E.; Rotello, V. M. Macrophage-Encapsulated Bioorthogonal Nanozymes for Targeting Cancer Cells. *JACS Au* **2022**, *2*, 1679–1685.
- (25) Sugimoto, S.; Iwasaki, Y. Surface Modification of Macrophages with Nucleic Acid Aptamers for Enhancing the Immune Response against Tumor Cells. *Bioconjug. Chem.* **2018**, *29*, 4160–4167.

- (26) Park, J.; Andrade, B.; Seo, Y.; Kim, M.-J.; Zimmerman, S. C.; Kong, H. Engineering the Surface of Therapeutic “Living” Cells. *Chem. Rev.* **2018**, *118*, 1664–1690.
- (27) Abbina, S.; Siren, E. M. J.; Moon, H.; Kizhakkedathu, J. N. Surface Engineering for Cell-Based Therapies: Techniques for Manipulating Mammalian Cell Surfaces. *ACS Biomater. Sci. Eng.* **2018**, *4*, 3658–3677.
- (28) Wilson, J. T.; Krishnamurthy, V. R.; Cui, W.; Qu, Z.; Chaikof, E. L. Noncovalent Cell Surface Engineering with Cationic Graft Copolymers. *J. Am. Chem. Soc.* **2009**, *131* (51), 18228–18229.
- (29) Oliveira, M. B.; Hatami, J.; Mano, J. F. Coating Strategies Using Layer-by-Layer Deposition for Cell Encapsulation. *Chem. Asian J.* **2016**, *11*, 1753–1764.
- (30) Germain, M.; Balaguer, P.; Nicolas, J.-C.; Lopez, F.; Esteve, J.-P.; Sukhorukov, G. B.; Winterhalter, M.; Richard-Foy, H.; Fournier, D. Protection of Mammalian Cell Used in Biosensors by Coating with a Polyelectrolyte Shell. *Biosens. Bioelectron.* **2006**, *21*, 1566–1573.
- (31) Doshi, N.; Swiston, A. J.; Gilbert, J. B.; Alcaraz, M. L.; Cohen, R. E.; Rubner, M. F.; Mitragotri, S. Cell-Based Drug Delivery Devices Using Phagocytosis-Resistant Backpacks. *Adv. Mater.* **2011**, *23*, H105–H109.
- (32) Rabuka, D.; Forstner, M. B.; Groves, J. T.; Bertozzi, C. R. Noncovalent Cell Surface Engineering: Incorporation of Bioactive Synthetic Glycopolymers into Cellular Membranes. *J. Am. Chem. Soc.* **2008**, *130*, 5947–5953.
- (33) Teramura, Y.; Kaneda, Y.; Totani, T.; Iwata, H. Behavior of Synthetic Polymers Immobilized on a Cell Membrane. *Biomaterials* **2008**, *29*, 1345–1355.
- (34) Lin, M.; Chen, Y.; Zhao, S.; Tang, R.; Nie, Z.; Xing, H. A Biomimetic Approach for Spatially Controlled Cell Membrane Engineering Using Fusogenic Spherical Nucleic Acid. *Angew. Chem. Intl. Ed.* **2022**, *61*, 1-9.
- (35) Huang, N. F.; Li, S. Mesenchymal Stem Cells for Vascular Regeneration. *Regen. Med.* **2008**, *3*, 877–892.
- (36) Shi, P.; Ju, E.; Yan, Z.; Gao, N.; Wang, J.; Hou, J.; Zhang, Y.; Ren, J.; Qu, X. Spatiotemporal Control of Cell–Cell Reversible Interactions Using Molecular Engineering. *Nat. Commun.* **2016**, *7*, 13088.
- (37) Sampathkumar, S.-G.; Li, A. V.; Jones, M. B.; Sun, Z.; Yarema, K. J. Metabolic Installation of Thiols into Sialic Acid Modulates Adhesion and Stem Cell Biology. *Nat. Chem. Biol.* **2006**, *2*, 149–152.
- (38) Iwasaki, Y.; Ota, T. Efficient Biotinylation of Methacryloyl-Functionalized Nonadherent Cells for Formation of Cell Microarrays. *Chem. Commun.* **2011**, *47*, 10329.
- (39) Hong, V.; Steinmetz, N. F.; Manchester, M.; Finn, M. G. Labeling Live Cells by Copper-Catalyzed Alkyne–Azide Click Chemistry. *Bioconj. Chem.* **2010**, *21*, 1912–1916.

- (40) Saxon, E.; Bertozzi, C. R. Cell Surface Engineering by a Modified Staudinger Reaction. *Science* **2000**, *287*, 2007–2010.
- (41) Xie, R.; Hong, S.; Feng, L.; Rong, J.; Chen, X. Cell-Selective Metabolic Glycan Labeling Based on Ligand-Targeted Liposomes. *J. Am. Chem. Soc.* **2012**, *134*, 9914–9917.
- (42) Du, J.; Hong, S.; Dong, L.; Cheng, B.; Lin, L.; Zhao, B.; Chen, Y.-G.; Chen, X. Dynamic Sialylation in Transforming Growth Factor- β (TGF- β)-Induced Epithelial to Mesenchymal Transition. *J. Biol. Chem.* **2015**, *290*, 12000–12013.
- (43) Mahal, L. K.; Yarema, K. J.; Bertozzi, C. R. Engineering Chemical Reactivity on Cell Surfaces Through Oligosaccharide Biosynthesis. *Science* **1997**, *276*, 1125–1128.
- (44) Csizmar, C. M.; Petersburg, J. R.; Wagner, C. R. Programming Cell-Cell Interactions through Non-Genetic Membrane Engineering. *Cell Chem. Biol.* **2018**, *25*, 931–940.
- (45) Karp, J.; Zhao, W. *Micro- and Nanoengineering of the Cell Surface*; William Andrew **2014**, *3*, 44–58.
- (46) Sarkar, D.; Vemula, P. K.; Teo, G. S. L.; Spelke, D.; Karnik, R.; Wee, L. Y.; Karp, J. M. Chemical Engineering of Mesenchymal Stem Cells to Induce a Cell Rolling Response. *Bioconj. Chem.* **2008**, *19*, 2105–2109.
- (47) Sarkar, D.; Spencer, J. A.; Phillips, J. A.; Zhao, W.; Schafer, S.; Spelke, D. P.; Mortensen, L. J.; Ruiz, J. P.; Vemula, P. K.; Sridharan, R.; Kumar, S.; Karnik, R.; Lin, C. P.; Karp, J. M. Engineered Cell Homing. *Blood* **2011**, *118*, 184–191.
- (48) Stephan, M. T.; Moon, J. J.; Um, S. H.; Bershteyn, A.; Irvine, D. J. Therapeutic Cell Engineering with Surface-Conjugated Synthetic Nanoparticles. *Nat. Med.* **2010**, *16*, 1035–1041.
- (49) Mooney, R.; Weng, Y.; Garcia, E.; Bhojane, S.; Smith-Powell, L.; Kim, S. U.; Annala, A. J.; Aboody, K. S.; Berlin, J. M. Conjugation of PH-Responsive Nanoparticles to Neural Stem Cells Improves Intratumoral Therapy. *J Control Release* **2014**, *191*, 82–89.
- (50) De Bank, P. A.; Kellam, B.; Kendall, D. A.; Shakesheff, K. M. Surface Engineering of Living Myoblasts via Selective Periodate Oxidation. *Biotechnol. Bioeng.* **2003**, *81*, 800–808.
- (51) Holden, C. A.; Yuan, Q.; Yeudall, W. A.; Lebman, D. A.; Yang, H. Surface Engineering of Macrophages with Nanoparticles to Generate a Cell-Nanoparticle Hybrid Vehicle for Hypoxia-Targeted Drug Delivery. *Int. J. Nanomed.* **2010**, *5*, 25–36.
- (52) Joshi, B. P.; Hardie, J.; Mingroni, M. A.; Farkas, M. E. Surface-Modified Macrophages Facilitate Tracking of Breast Cancer-Immune Interactions. *ACS Chem. Biol.* **2018**, *13*, 2339–2346.
- (53) Taciak, B.; Białasek, M.; Braniewska, A.; Sas, Z.; Sawicka, P.; Kiraga, Ł.; Rygiel, T.; Król, M. Evaluation of Phenotypic and Functional Stability of RAW 264.7 Cell Line through Serial Passages. *PLoS ONE* **2018**, *13*, 1–13.

- (54) Hamada, H.; Kobune, M.; Nakamura, K.; Kawano, Y.; Kato, K.; Honmou, O.; Houkin, K.; Matsunaga, T.; Niitsu, Y. Mesenchymal Stem Cells (MSC) as Therapeutic Cytoreagents for Gene Therapy. *Cancer Sci.* **2005**, *96*, 149–156.
- (55) de Brito Monteiro, L.; Davanzo, G. G.; de Aguiar, C. F.; Corrêa da Silva, F.; Andrade, J. R. de; Campos Codo, A.; Silva Pereira, J. A. da; Freitas, L. P. de; Moraes-Vieira, P. M. M-CSF- and L929-Derived Macrophages Present Distinct Metabolic Profiles with Similar Inflammatory Outcomes. *Immunobiology* **2020**, *225*, 151935.
- (56) Weischenfeldt, J.; Porse, B. Bone Marrow-Derived Macrophages (BMM): Isolation and Applications. *Cold Spring Harb. Protoc.* **2008**, *2008* (12).
- (57) Hartig, S. M. Basic Image Analysis and Manipulation in ImageJ. *Curr. Protoc. Mol. Biol.* **2013**, *102* (1).
- (58) Chen, H.-C. Boyden Chamber Assay. In *Cell Migration*; Humana Press: New Jersey, **2004**, *294*, 015–022.
- (59) Zhang, Y.; Cheng, S.; Zhang, M.; Zhen, L.; Pang, D.; Zhang, Q.; Li, Z. High-Infiltration of Tumor-Associated Macrophages Predicts Unfavorable Clinical Outcome for Node-Negative Breast Cancer. *PLoS ONE* **2013**, *8*, 1-8.
- (60) Kalimuthu, S.; Zhu, L.; Oh, J. M.; Gangadaran, P.; Lee, H. W.; Baek, S. hwan; Rajendran, R. L.; Gopal, A.; Jeong, S. Y.; Lee, S.-W.; Lee, J.; Ahn, B.-C. Migration of Mesenchymal Stem Cells to Tumor Xenograft Models and *in Vitro* Drug Delivery by Doxorubicin. *Int. J. Med. Sci.* **2018**, *15*, 1051–1061.
- (61) Shahar, T.; Rozovski, U.; Hess, K. R.; Hossain, A.; Gumin, J.; Gao, F.; Fuller, G. N.; Goodman, L.; Sulman, E. P.; Lang, F. F. Percentage of Mesenchymal Stem Cells in High-Grade Glioma Tumor Samples Correlates with Patient Survival. *Neurooncol.* **2017**, *19*, 660-668.

CHAPTER 5

CONCLUSION AND FUTURE DIRECTIONS

On account of their recruitment to sites of disease and amenable biodistribution properties, cells have great promise as imaging and chemotherapeutic delivery vehicles. While most applications utilizing cell-based agents involve phagocytosis of the payload, in this thesis, I have conducted studies to demonstrate feasibility of alternative approaches. As part of a collaboration, I showed that macrophages can be loaded with nanozymes, which then convert pro-drugs to active molecules at the site of macrophage accumulation, without affecting the cells' behavior. Much of this work focused on using covalent chemical modifications to append small molecules and proteins at the surfaces of cells, and evaluation of resulting biological effects. I used biocompatible methods to perform reactions with both native and installed chemical functionalities present on cells, including proteins and glycans. I conducted facile surface modifications of immortalized, model macrophages. Having established that cells were not detrimentally affected, I used them as agents for assessment of interactions between immune and cancer cells *in vitro*, and accumulation in tumors *in vivo*. I then expanded the surface protein engineering to both primary and immortalized macrophages and stem cells. I assessed the extents of each modification and their properties, including retention on cell surfaces and effects on cells, including viability and chemotactic migration.

With increasing research and development in the fields of cellular therapies and cell-based vehicles, the numbers of feasible applications for modified cells will continue to expand. This platform has the potential to improve efficacy and reduce undesirable effects of existing therapies and can also lead to new generations of therapeutics and

imaging agents. Following the initial work on surface modification of cells presented in this thesis, the next stages of applying the strategy can be pursued.

First, surface retention must be considered and optimized depending on the cargo and application. For example, this is important in the attachment of chemical sensors for studying disease environments. A strategy is to develop chemical moieties that possess sufficient negative charge to prolong the presence of the conjugates at the exterior. In the instance of drug delivery, cargo release from the carrier is critical. Use of a stimuli-responsive linkage between therapeutics and carrier cells can provide an additional layer of specificity. By using moieties that are labile under conditions present in targeted microenvironments, release can only occur in tissues where cells accumulate that also meet the linkers' requirements. This can also decrease the risk of off-target effects. Towards this end, further development, design, and optimization of responsive linkers is also needed. Some examples include those that are labile to endogenous stimuli, including pH or enzyme presence (e.g., matrix metalloproteinases (MMPs) or cathepsins), and also exogenous stimuli like light, temperature, ultrasound waves, or magnetic fields. Taken together, the use of suitable moieties with prolonged surface retention capabilities and microenvironment stimuli responsive linkers can go a long way in designing more efficient drug carriers.

By using chemistry to enhance biology, next generation targeted, controlled release vehicles can be developed that are capable of delivering a variety of therapeutics to combat cancer and other diseases. In addition, the surface functionalized cellular vehicles can be used as diagnostics and tools, including in imaging, tracking of cell therapies, and study of conditions present in disease environments. In summary, this work has shown the

feasibility of using cells as carriers via new strategies, pushing beyond typical phagocytic loading of payload. via approaches. While anticipated applications include imaging and therapeutic delivery, it is likely that this research will also enable uses of chemically modified cells in other scientific areas, including materials and engineering.

APPENDIX

CHALLENGES OF BIOCONJUGATION OF AMINES TO OXIDIZED CELL SURFACE SIALIC ACID RESIDUES

A.1. Introduction

A commonly used strategy for the covalent modification of exposed lysine side chains is amide bond formation using an N-hydroxysuccinimide (NHS) ester.¹ This has been shown to form a robust attachment on the cell surface that remains intact in sufficient concentrations for several days even as cells proliferate.² In our own experiments we used NHS-biotin for the attachment of biotin for the association of the avidin protein (*Chapter 3* and *Chapter 4*). However, not all handles on the cell surface are reactive enough to attach cargo covalently without prior modification. One example of this is sialic acid, which is ubiquitously present at terminal glycans on mammalian cell surfaces.³ While sialic acid is not reactive on its own, an aldehyde can be introduced via mild oxidation of the triol unit of the glycan. This approach has previously been shown to modify cells while retaining cell morphology, and has been used to conjugate polymers with amine handles to deliver chemotherapeutics using cell–nanoparticle hybrid vehicles.⁴

While these covalent surface modifications have been attempted in different cell types separately with cargos of various sizes, a parallel comparison of functionalization type and cargo size is lacking. We conducted such comparative studies by covalently linking the mildly oxidized sialic acid residues on the cell surface with the small molecule fluorescein hexylamine (NH₂-FL) or biotin-hexylamine/avidin-fluorescein isothiocyanate (NH₂-Biotin/Avd-FITC), performing evaluations side by side (Figure A.1). Sialic acid

residues on surface glycans of four different cell types, immortalized and primary macrophages, RAW 264.7 and bone marrow-derived macrophages (BMDM), respectively, and immortalized and primary stem cells, hTERT and primary mesenchymal stem cells (MSC), respectively were covalently modified.

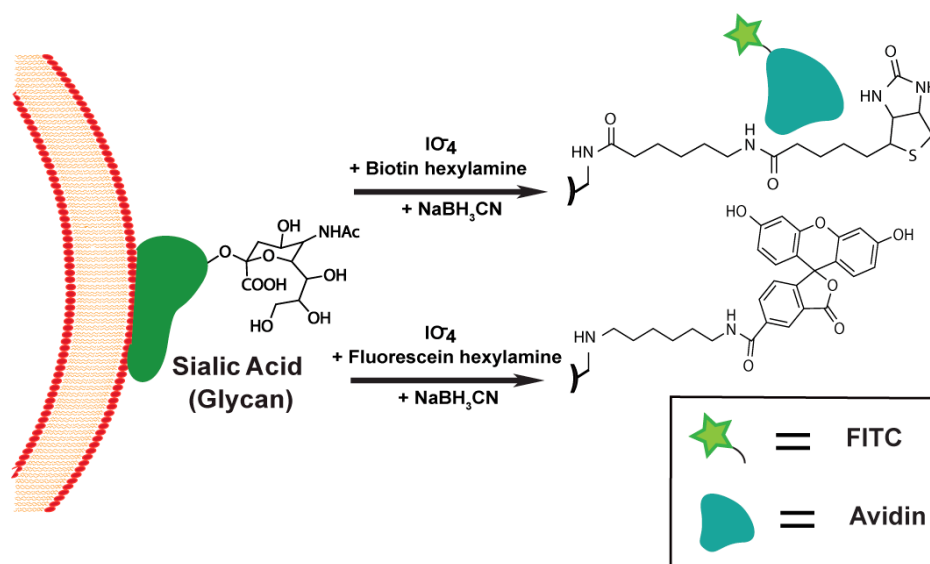


Figure A.1. Comparison of fluorescein hexylamine ($\text{NH}_2\text{-FL}$) and biotin-hexylamine/avidin-fluorescein isothiocyanate ($\text{NH}_2\text{-biotin/avd-FITC}$) bioconjugations at cell-surface glycans.

For these reactions to occur, the sialic acid must be mildly oxidized with periodate to convert the triol moiety into an aldehyde, which can be reacted with amines at mild conditions to form an imine.³ To give more stable linkages, the imine should be converted to an amide via reductive amination. Thus, mild periodate pre-treated terminal sialic acid aldehydes were conjugated to amines to generate Schiff's bases which in turn were further reduced to stable amides using cyanoborohydride.⁴ By these methods, we obtained covalent chemical modifications of cell surfaces (Figure A.2). We then compared the modifications using small molecule vs. biotin-avidin complex in terms of efficiency of surface labeling, retention over time, and cellular viability. Unlike the robust modification

of cell surface exposed amines via N-hydroxysuccinimide, biotin/avidin-fluorescein isothiocyanate (NHS-biotin/avid-FITC) described in *Chapters 3* and *4*, the modifications of mildly oxidized exposed cell surface sialic acid residues via NH₂-biotin/avid-FITC or NH₂-FL methods are not very efficient or reproducible. We have described the issues with these modification methods in detail in the results and discussion section below.

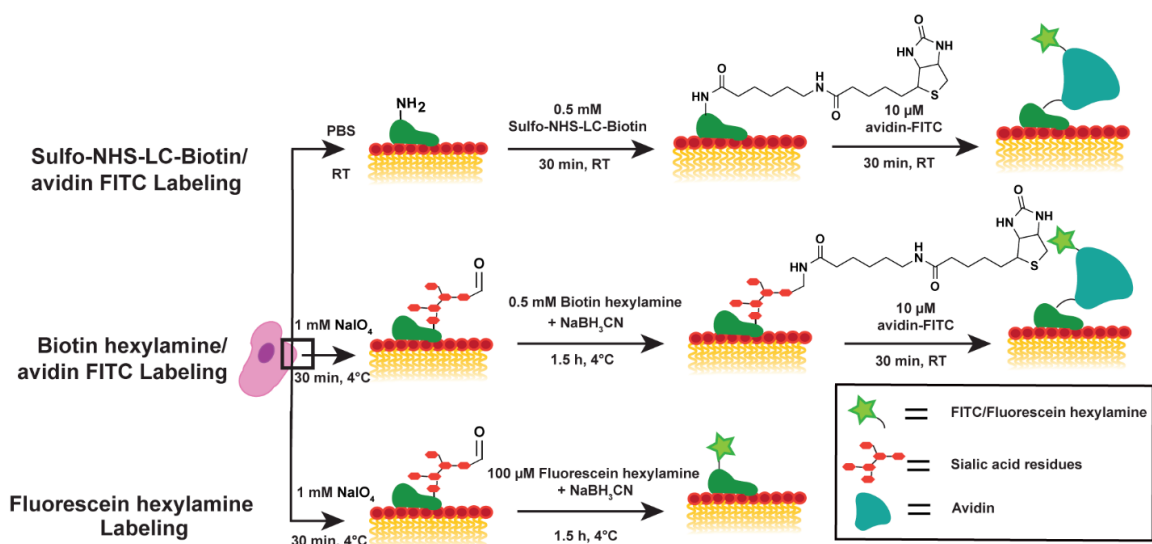


Figure A.2. Detailed scheme comparing cell surface lysine and glycan modification methods including reaction conditions.

A.2. Materials and methods

All reagents were purchased from Thermo-Fisher Scientific except where otherwise noted. Sodium periodate was obtained from Sigma-Aldrich, sodium cyanoborohydride from Acros Organics, fluorescein hexylamine (referred to as NH₂-FL) from Biotium, fluorescein (FITC) conjugated avidin from Invitrogen Pierce, and D-biotin from Alfa Aesar. The synthesis of and characterization data for biotin hexylamine (referred to as NH₂-Biotin) is provided in *Section A.2.1*, below.

A.2.1. Synthesis and characterization of biotin hexylamine

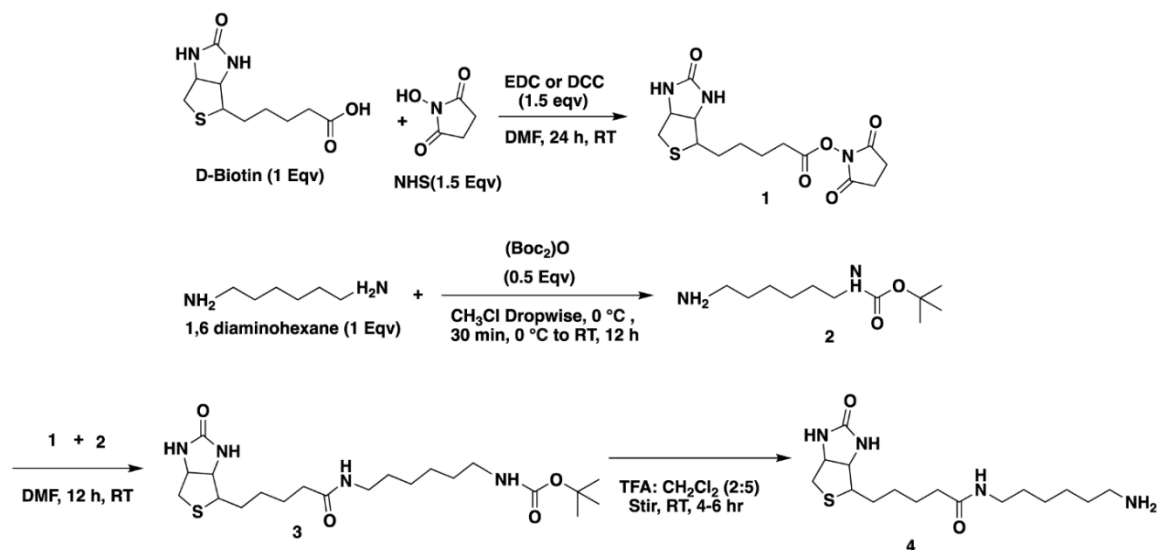


Figure A.3. Synthesis of biotin hexylamine from D-biotin.

All chemical reagents and solvents for synthesis were purchased from commercial sources (Thermo Fischer, Alfa Aesar, and Sigma-Aldrich Chemical) and were used without further purification. ^1H NMR spectra were recorded on an Ascend 400 MHz (Bruker) at room temperature. Mass spectra were recorded using ESI-MS (Bruker MicrOTOF ESI-TOF Mass Spectrometer).

[1]: A mixture of biotin (1.0 g, 4.09 mmol), N-hydroxysuccinimide (753 mg, 6.54 mmol), and EDC (1.02 g, 5.32 mmol) was dissolved in DMF (40 mL) and stirred for 24 h at room temperature under ambient atmosphere.⁵ The solution was poured onto crushed ice and the solid obtained was filtered, washed with ice-cold water and dried to give N-hydroxysuccinimido biotin (**1**). ~ 90% Yield. ^1H NMR (DMSO- d_6 , 400 MHz): δ 6.40 (brs, 1H), 6.34 (brs, 1H), 4.30-4.26 (m, 1H), 4.16-4.12 (m, 1H), 2.84-2.76 (m, 6H), 2.67-2.62 (m, 2H), 2.58 (d, 1H), 1.66 -1.57 (m, 3H), 1.52-1.36 (m, 3H).

[2]: 450 mL (Boc)₂O was added dropwise to solution of 1,6-diaminohexane in CH₃Cl at 0 °C (ice bath) over 30 min. The mixture was stirred overnight at room temperature under ambient atmosphere, washed with sodium bicarbonate and brine, and extracted in 10% MeOH-CH₃Cl mixture. The extract was evaporated, followed by wash with brine and 10% MeOH-CH₃Cl. This was repeated in instances when the product **2** was paste-like, until a viscous colorless liquid was obtained. Furthermore **2** was used within a month of synthesis due to issues with stability. ~ 50% Yield. ¹H NMR (400 MHz) (CDCl₃) δ: 4.54 (s, 1H, CONH), 3.11 (t, 2H, CH₂NH), 2.68 (t, 2H, CH₂NH₂), 1.40–1.50 (s, 9H, CH₃; m, 4H, CH₂), 1.25–1.37 (m, 4H, CH₂).

[3]: A mixture of N-hydroxysuccinimido biotin (**1**, 500 mg, 1.46 mmol) and N-boc-1,6-diaminohexane (**2**, 411 mL, 1.90 mmol) in DMF (20 mL) was stirred for 18 h at room temperature, under ambient atmosphere. The reaction mixture was poured onto crushed ice, the solid was collected by vacuum filtration, washed with ice-cold water, and dried to give N-Biotinyl-N-Boc-1,6-hexanediamine (**3**). ~ 90% Yield. ¹H NMR (DMSO-d₆, 400 MHz): δ 7.71 (brt, 1H), 6.73 (brt, 1H), 6.39 (s, 1H), 6.33 (s, 1H), 4.29-4.26 (m, 1H), 4.11-4.09 (m, 1H), 3.09-3.04 (m, 1H), 3.01 (q, 2H), 2.88-2.77 (m, 3H), 2.57 (d, 1H), 2.03 (t, 2H), 1.62-1.20 (m, 23H).

[Biotin hexylamine, 4]: **3** (100 mg, 0.3 mmol) was dissolved in a mixture of CH₂Cl₂ (1 mL) and CF₃COOH (0.4 mL) and stirred at room temperature for 4 h under ambient atmosphere. Washed with 20% w/v NaOH, extracted in CH₂Cl₂. The solvents were evaporated to dryness to give pure **4**. Washing with 20% w/v NaOH, and extraction in CH₂Cl₂ was repeated in instances when the product **4** was paste-like, until a white powder was obtained. ~ 50% Yield. ¹H NMR (DMSO-d₆, 400 MHz): δ 7.75 (t, 1H), 7.63 (brs, 2H),

6.41 (brs, 2H), 4.30-4.27 (m, 1H), 4.12-4.09 (m, 1H), 3.09-3.04 (m, 1H), 3.02 (q, 2H), 2.82-2.71 (m, 3H), 2.57 (d,1H), 2.04 (t, 2H), 1.63-1.22 (m, 14H). Mass: Calculated= 342, Found=343 [M+1].

A.2.2. NH₂-FL (fluorescein hexylamine) modification of cells

Macrophages and stem cells (5×10^4 cells) were plated in borosilicate glass bottom 8-well chambers slides (Nunc Lab-Tek) in 0.25 mL corresponding media for high-magnification microscopy and confocal image analysis or 1×10^5 cells in 24-well plates (Costar) in 500 μ L corresponding media for all other adherently labelled experiments such as quenching and viability. Prior to adherent labeling the cells were maintained overnight in a humidified 5% CO₂ atmosphere at 37 °C. Culture medium was removed, and cells were rinsed with 500 μ L of phosphate-buffered saline (PBS). Cells were then incubated in 500 μ L of 1 mM NaIO₄ in PBS (sterile filtered) for 30 min at 4 °C and then washed once with PBS (500 μ L per wash). Cells were then incubated in 250 μ L of 0.1 mM of fluorescein hexylamine (NH₂-FL, Biotium) in PBS with 0.1% DMSO (sterile filtered) for 90 minutes at 4 °C. Treatment solution was removed, and cells were washed once with PBS (500 μ L). Cells were then treated with 250 μ L of 0.1 mM NaCNBH₃ in PBS (sterile filtered) for 60 minutes at 4 °C then washed twice with PBS (500 μ L per wash). Following the second PBS wash, 250 μ L corresponding media (phenol red-free) was added, and cells were used for further experiments.

A.2.3. NH₂-biotin/avidin-FITC modification of cells

For confocal microscopy 5×10^4 cells in 8-well chambers and 250 μ L PBS and corresponding reagents in PBS were used, while for quenching and viability experiments 1×10^5 cells in 24-well plates and 500 μ L PBS and corresponding reagents in PBS were used. All cells were prepared as described above and incubated overnight prior to modification. Culture medium was removed, and cells were washed with 250 μ L and 500 μ L PBS. 1 mM NaIO₄ in 250 μ L and 500 μ L PBS in PBS (sterile filtered) was added to the cells, which were then incubated for 30 min at 4 °C. Following, cells were washed once with PBS (250 or 500 μ L), and then 250 μ L or 500 μ L of 0.5 mM biotin hexylamine in PBS with 0.1% DMSO (sterile filtered) was added and cells were incubated for 90 minutes at 4 °C. The solution was removed, and cells were washed once with PBS (250 and 500 μ L). Then the cells were treated with 250 μ L or 500 μ L of 1 mM NaCNBH₃ in PBS (sterile filtered) for 60 minutes at 4 °C, and washed twice with PBS (500 μ L per wash). Cells were then incubated in 250 μ L or 500 μ L of 0.05 mg/mL avidin-FITC in PBS for 30 min at ambient temperature and washed twice with PBS (250 or 500 μ L per wash). Following the second PBS wash, the 250 or 500 μ L of phenol red-free version of the corresponding complete media was added, and cells were used for further experiments.

A.2.4. NHS-Biotin/Avd-FITC modification of cells

The detailed description of this type of modification is described in *Chapter 4*.

A.2.5. Confocal microscopy of modified cells

Cell images were acquired using a Nikon Point Scanning C2+ confocal microscope with excitation at 488 nm at 0 h and 24 h time points following modification in borosilicate glass bottom 8-well chamber slides. Between time-points, the cells were incubated at 37 °C under a humidified atmosphere containing 5% CO₂. Fluorescent and merged cell images were analyzed with Nikon NIS-Elements and FIJI (Image J) software.

A.2.6. Assessment of changes in surface fluorescence over time

5×10^4 cells were plated in borosilicate glass bottom 8-well chamber slides (Nunc Lab-Tek) in two different wells and labeled with Fluorescein hexylamine (NH₂-FL), Biotin hexylamine/Avidin-FITC (NH₂-Biotin/Avd-FITC), as described in *Section 4.2.2* and *4.2.3* above. Surface modified cells were imaged with confocal microscope as described in *Section 4.2.5* above. Out of three wells modified by same method at the same time the first well was imaged at 0 h. Immediately after imaging the cells in the first well were quenched with 0.4% Trypan Blue and imaged again. The cells in the other two wells were incubated at 37 °C and 5% CO₂ and imaged again at 24 h and 48 h without quenching followed by quenching with Trypan Blue. To quantify the cell surface retention of fluorescence over time the following method was employed: using the selection tool in the ImageJ software, three different areas of approximately 300 x 300 pixels consisting of approximately 10 cells imaged at 60X magnification per area for cells and 10 x 10 pixels for nearby areas with no cells were selected as background. Thus, a total of approximately 30 cells were used for each set of analyses. The integrated fluorescence intensity for the selected cells was determined by Image J at the indicated time points, averaged across all cells, and

background intensity subtracted. Thus, the corrected total cell fluorescence (CTCF) was calculated as:

$$\text{CTCF} = \text{Integrated Density} - (\text{Area of selected cell} \times \text{Mean background fluorescence}).$$

Since Trypan Blue is impermeable to living cells, the fluorescence quenched by it at a given time on a selected area of cells amounts to the amount of fluorescence retained by living cell at the surface. The Fluorescein/FITC labelled cells were imaged before and after quenching with Trypan Blue at time intervals 0, 24, and 48 h. Then, the corresponding corrected total cell fluorescence (CTCF) was calculated using Image J. The fluorescence retained at the surface was calculated as CTCF of cells quenched with Trypan Blue (fluorescence retained at the surface of cells in the selected are at that time point) divided by CTCF of non-quenched cells (total fluorescence of cells in the selected are at that time point before quenching the surface fluorescence) multiplied by 100. The percentage change in surface fluorescence over time for each labeling method was then plotted.

A.3. Results and discussion

A.3.1. Cell surface engineering with NH₂-sialic acid chemistry

After covalently modifying the cell surface of four cell types using described in *Sections 4.2.2. - 4.2.4*, we acquired fluorescent and brightfield-merged images with a confocal microscope (Figure A.4).

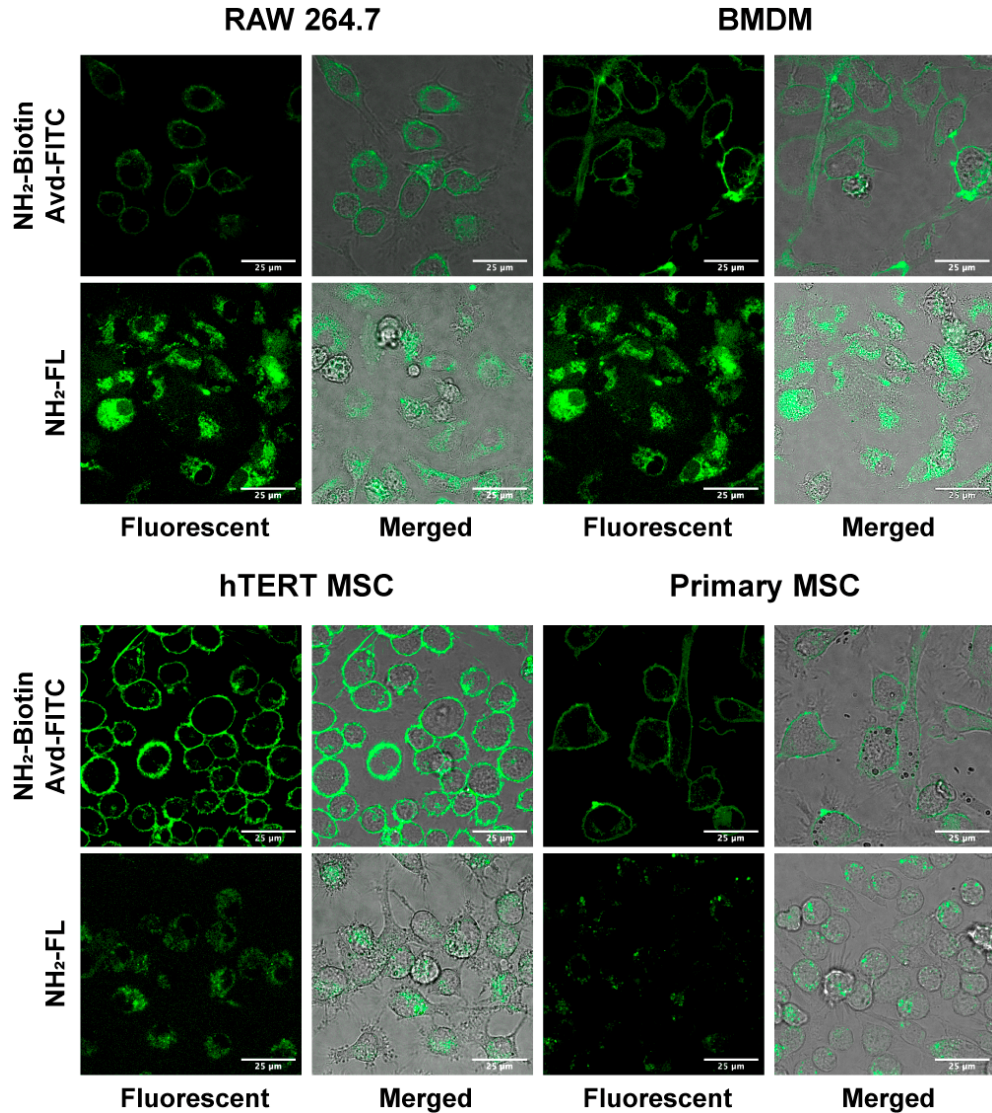


Figure A.4. Comparison of attachment methods for sialic acid modifications. Cells are labelled in the presence of NH₂-biotin/avidin-FITC and NH₂-FL. Immortalized and primary cells of macrophages (top) and stem cells (bottom) were labelled. All images taken at 0 hours. Magnification = 60x, scale bar = 25 μm.

Appropriate control experiments were also performed, relevant to each step of the modifications to confirm that specific labeling was achieved in RAW 264.7 cells (Figure A.5). For conditions involving NH₂-Biotin/avidin associations, little to no fluorescence was observed when no-NH₂-Biotin controls were used. However, fluorescence inside the

cells was observed where cells were incubated with only NH₂-Fluorescein, making it hard to distinguish the surface labeling from the internalized fluorescence (Figures A.4 & A.5).

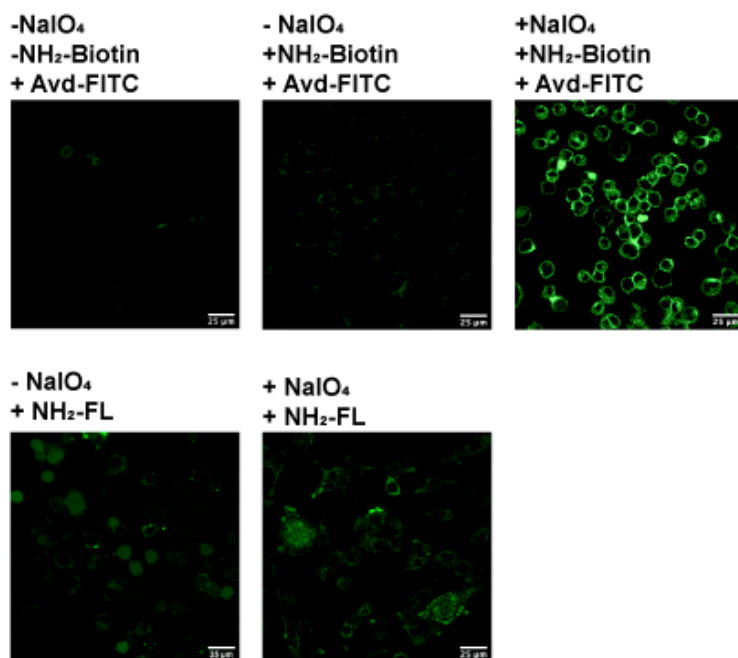


Figure A.5. Control experiments for amine modifications of sialic acids. Conditions were validated by labelling in the presence or absence of NaIO₄ followed by presence or absence of NH₂-fluorescein and NH₂-biotin/avd-FITC. Without treatment of NaIO₄, no labelling was observed (left, above). Some fluorescence was seen on the cells (left, below) due to rapid internalization of fluorescein hexylamine (NH₂-FL). RAW 264.7 cells were used for these experiments.

Prior to arriving at the conditions used, we performed optimization studies with 5×10^4 cells and cell viability using 1×10^5 cells. For sialic acid oxidations, previous reports used a 0.1 mM final concentration of cold ($\sim 4^\circ\text{C}$) NaIO₄ in 100 μL of PBS (pH 7.4) followed by an equal concentrations (0.1 mM) of NaBH₃CN with 1.2×10^4 cells.⁴ Elsewhere, 1 to 2 mM cold NaIO₄ has been used.³ In our own optimizations, we found that a 1 mM final concentration of cold NaIO₄ in 250 μL or 500 μL of PBS (pH 7.4) with equivalent concentrations of NaBH₃CN and NH₂-biotin (0.5 mM) or NH₂-FL (0.1 mM)

used with 5×10^4 and 1×10^5 cells, respectively yielded optimal modifications. Periodate treatments using lower than 1 mM final concentrations resulted in inconsistent extents of cell labeling, while higher concentrations (10 mM) affected the viability of the cells. For the amines, NH₂-FL had optimal labelling when treated at 0.1 mM for direct attachment while 0.5 mM was found to be optimal for NH₂-biotin. For direct glycoengineering of cell surfaces with fluorescein hexylamine, the concentrations that worked best were 1 mM of periodate to activate the sialic acid to the aldehyde. However, during this optimization we saw that any concentration of periodate permeabilized the cell surface leading to internalization of NH₂-FL.

The NH₂-fluorescein and NH₂-biotin/avidin-FITC labelled cells were imaged at time intervals 0 and 24 h (Figure A.6) The images of NHS-biotin/avidin-FITC are included as well for comparison of surface protein vs glycan modifications. However, the bioconjugation of biotin hexylamine and fluorescein hexylamine to cell mildly oxidized sialic acid residues on cell surface were not consistent (Figure A.7). When the conjugation partly worked, FITC or fluorescein hexylamine rapidly entered the cells making it difficult to differentiate what is on the surface and what is inside of the cells. Further, more recently, we have found our successful modifications to be un-reproducible. This is partly due to use of periodate salt during the oxidation steps which permeabilize the surface and partly due to slow and reversible nature of imine formation by conjugation of sialic acid aldehydes and amines. The imine formation can take about an hour with addition of cyanoborohydride to reduce the unstable imine to stable amide taking another half hour the whole conjugation can take up to 90 minutes whereas the fluorophores can enter the cell within 10 minutes.

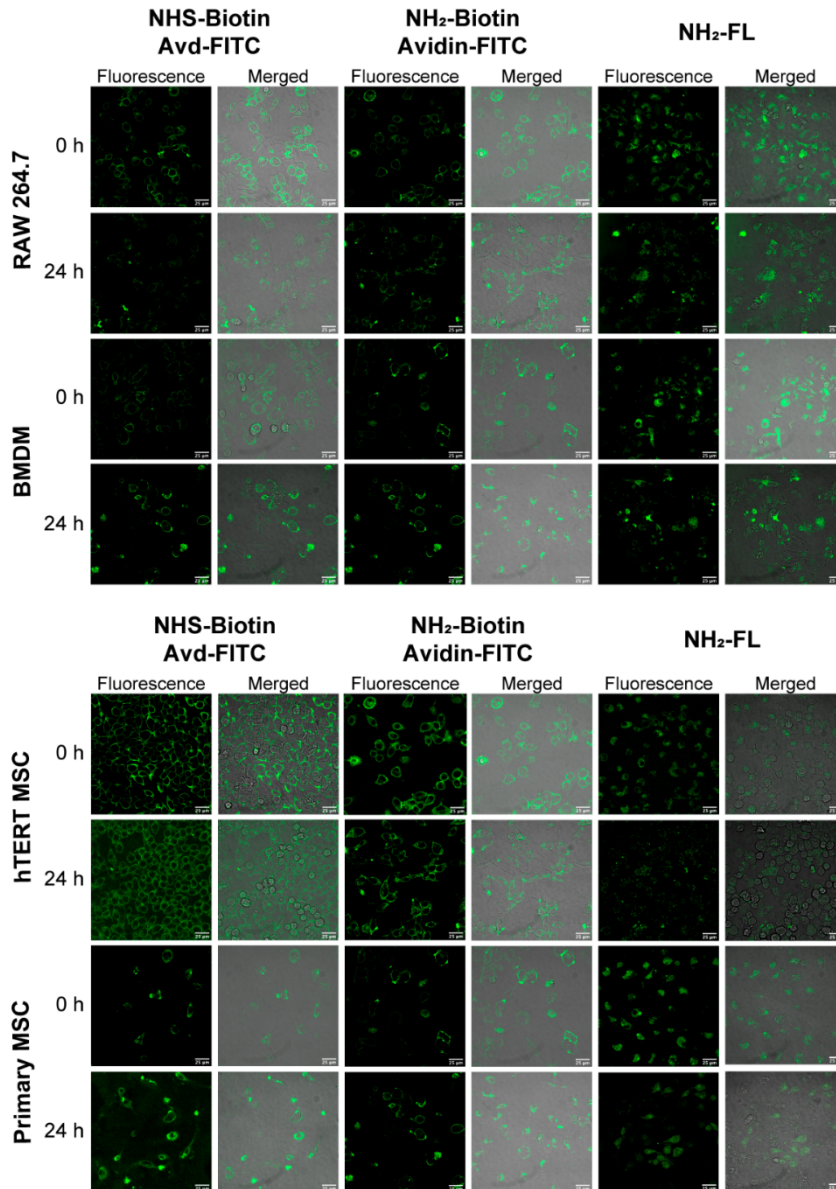


Figure A.6. Representative images of all modification types in all cell lines. Brightfield and fluorescent images of RAW 264.7 cells and BMDMs (above), hTERT MSCs, and Primary SCs (below) modified with either NHS-Biotin/Avd-FITC, NH₂-Biotin/Avd-FITC, or NH₂-FL. Images were taken at 0 and 24 hours after modification. Magnification = 60x, scale bar = 25 μm. Images of NHS-Biotin/ Avd-FITC are included as well for comparison of surface protein versus glycan modifications.

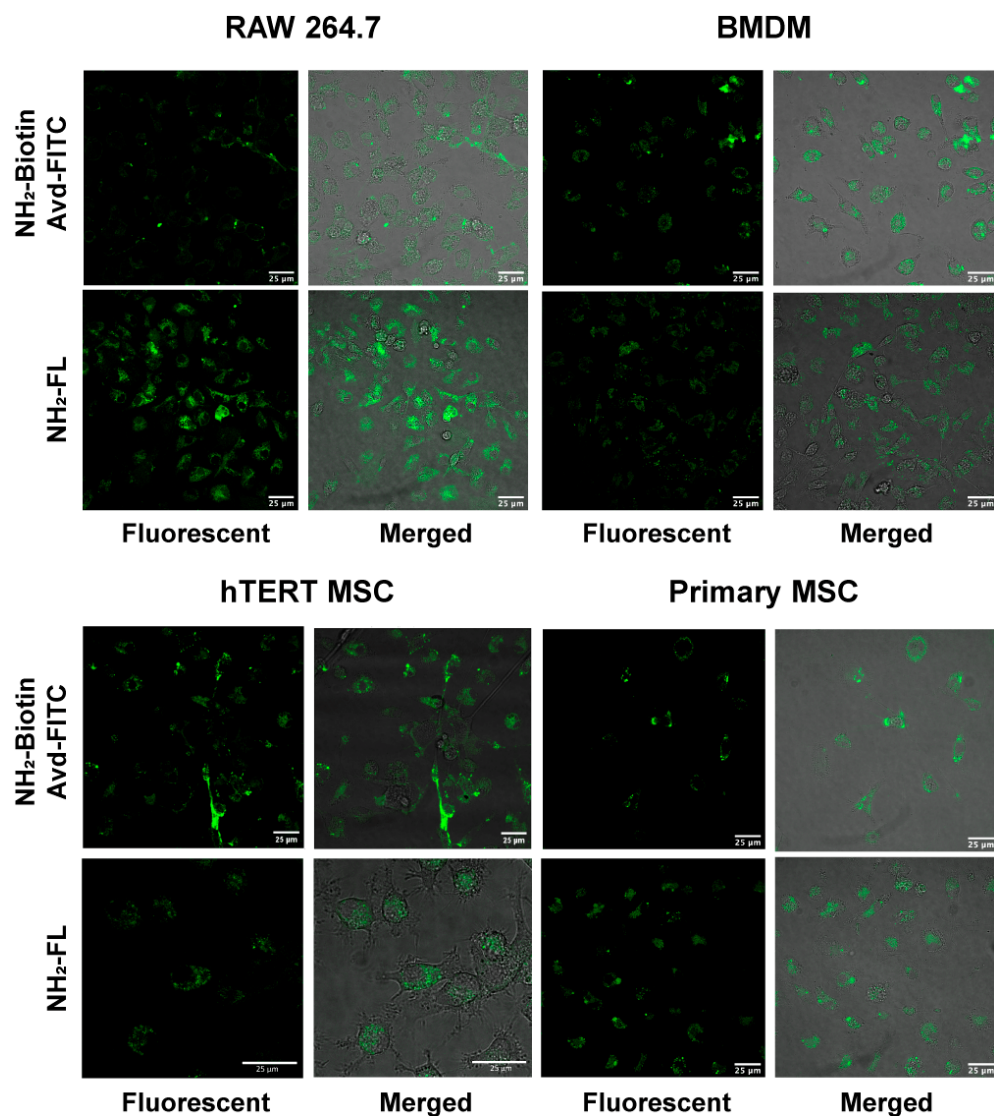


Figure A.7. Examples of unsuccessful bioconjugations using NH₂-biotin/avidin-FITC and NH₂-FL. Following oxidations, cells were labelled in the presence of NH₂-biotin/Avid-FITC or NH₂-FL. Immortalized and primary cells of macrophages (top) and stem cells (bottom) were labelled. All images taken at 0 hours. Internalization is seen even at 0 h. The surface modification is not always consistent (compare with Figure A.4). Magnification = 60x, scale bar = 25 μ m.

A.3.2. Tracking retention of cell-surface fluorescence and internalization over time

The stability of initial covalent conjugation at the cell surface is affected by kinetic and thermodynamic factors apart from concentration of bio-conjugating reagents used. However, the retention of a molecule on the cell surface over time can be affected by various cellular characteristics such as the phenotype of the modified cell (whether it is a phagocyte or not), doubling times, and whether the cell is primary or immortalized. After confirming the labelling mechanisms of the above methods, we assessed the retention of fluorescein complexes on cell surfaces over time for up to 48 h. We looked at the confocal images of non-quenched fluorescent and Trypan Blue quenched images of macrophages (RAW 264.7 and BMDM) and stem cells (hTERT MSC and primary MSC) surface engineered via NH₂-biotin/avd-FITC, or NH₂-FL at 0, 24, and 48 h (Figure A.8).

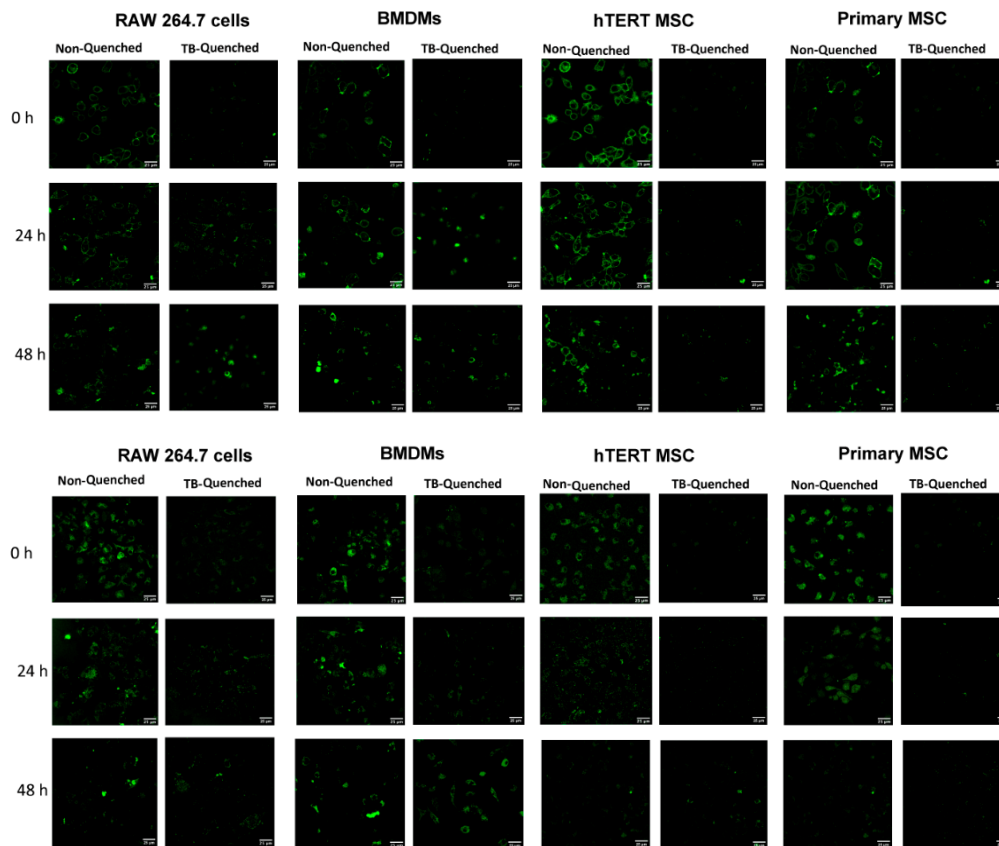


Figure A.8. Representative quenching images for (left to right) RAW 264.7 cells, BMDMs, hTERT MSCs, and primary MSCs after modification with NH₂-Biotin/Avd-FITC (above) and NH₂-FL (below). Each pair of images per cell type includes (left) non-quenched and (right) quenched examples. Magnification = 60x, scale bar = 25 μm. Quenching was performed 0, 24, or 48 hours after modification. TB = trypan blue.

We observed that in the case of direct conjugation to surface glycans via NH₂-FL, even at time 0 h, the cells had 10-15% more internalization compared to NHS or NH₂-Biotin/Avd-FITC complexes, which retained about 90% of fluorophores on the surface just after initial modification (Figure A.9). This implies that small molecules without sufficient negative charge and/or bulk are likely to be internalized even before they react with biomolecules having exposed reactive handles on the cell surface. This can be further rationalized by the kinetics of the sialic acid oxidation, as the imine formation takes more than an hour whereas internalization can occur within minutes.

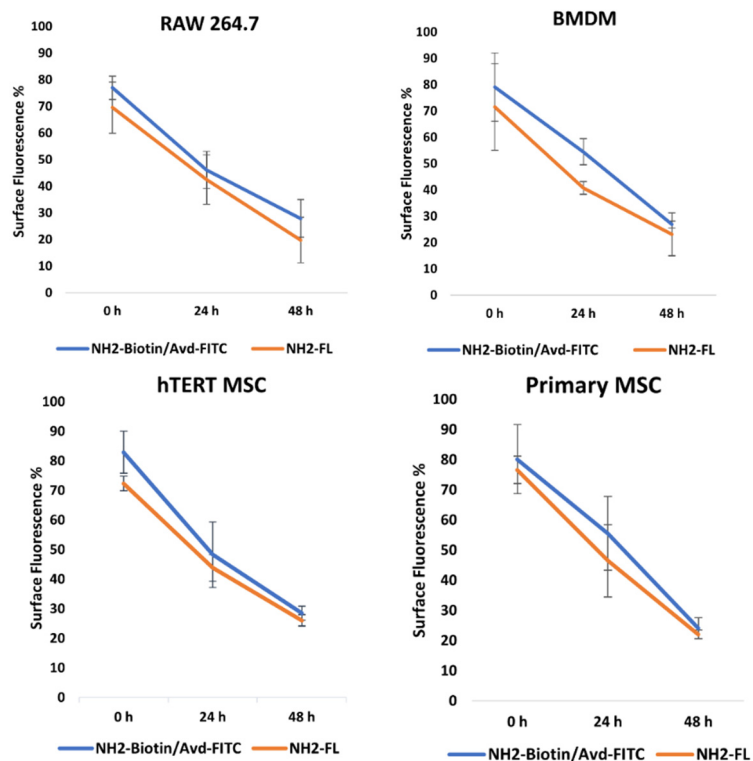


Figure A.9. Surface fluorescence over time in RAW 264.7 (top left), BMDM (top right), hTERT MSC, and Primary MSC (bottom right) after modification with NH₂-biotin/avd-FITC (blue), and NH₂-FL (orange). Surface fluorescence was based on the drop in signal following quenching with Trypan Blue.

With this combination of treatments, the viabilities of immortalized RAW 264.7 and hTERT MSC cells were not affected. The primary cells were not always consistent in this regard, and at times showed slight reduction of viability following modification (Figure A.10).

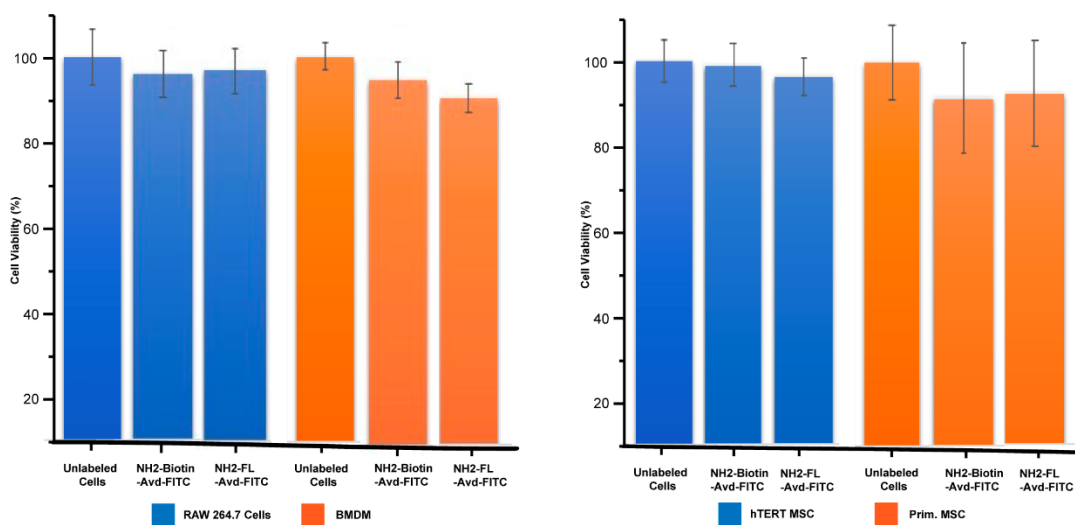


Figure A.10. Viability of cells 48 h post-modification following sialic acid modifications with amines. Cell viability was performed via Alamar Blue assay. Some difference in viability is found while comparing immortalized with their primary counterparts. Bars indicate the average values across three biological replicates. Error is represented as standard deviation of the mean.

A.3.3. Inconsistency in bioconjugation of amine-handles to sialic acid residues

Unlike robust conjugation of NHS-biotin handles to exposed lysine residues of cell surface proteins, the conjugation of amine handles to surface glycans is too complicated to apply to living cells. Several dynamic variables in multi-step conjugation make the results hard to reproduce.

In many experiments with bioconjugation of amine handles to cell surface glycans we found that amine labeling with both biotin hexylamine and fluorescein hexylamine were not consistent. Even when the conjugation worked, the direct fluorescein hexylamine always entered the cells, making it difficult to differentiate what is on the surface and what is inside of the cells. This is partly due to rapid internalization of the conjugates by cells. This internalization is enhanced by the first step in bio-conjugation, which is the mild

oxidation of surface sialic acid residues to sialic acid aldehydes using periodate. This step makes the cell even more permeable (Figure A.2). For mild oxidation, periodate treatments using lower than 1 mM final concentrations resulted in inconsistent labeling, while higher concentrations (10 mM) affected the viability of the cells. 1 mM final concentrations periodate oxidation leads to formation of sialic acid aldehyde.

The transient intermediate imine is reversible and susceptible to hydrolysis in aqueous solutions used in the reactions. To prevent the hydrolysis, reducing agent sodium cyanoborohydride to reduce Schiff bases to stable secondary amine linkages has to be used. We found that mild oxidation of cell surface by 1 mM final concentration of cold NaIO_4 in of PBS (pH 7.4) followed by concentrations of NaBH_3CN equal to NH_2 -biotin (0.5 mM) or NH_2 -FL (0.1 mM), respectively yielded optimal modifications.

We used 500 μM cyanoborohydride to convert the unstable imine to stable amide bond (Figure A.2). Periodate treatments using lower than 1 mM final concentrations resulted in inconsistent extents of cell labeling, while higher concentrations of 10 mM affected the viability of the cells. The existing literature has extensive debates and discussion on the optimization of sialic acid modification using amine handles. They also speak of the potential role of pH. It is claimed that a pH range of 8-10 helps the reduction of amine without impacting viability of RAW 264.7 cells.^{3,4} However, in our observation, that was not always the case with other cells, particularly the primary cells. It was difficult to determine whether the fluorescein was on the surface or within cells (Figure A.6, A.7, A.8). This is partly due to rapid internalization of the conjugates by cells as opposed to the slow conjugation reaction of sialic acid aldehyde and amine to form the imine intermediate. Unlike with the robust NHS-biotin modification, in the conjugation of amine handles to

surface glycans, we observed some inconsistencies in labeling, enhanced internalization of fluorophore, and diminished viability.

A.4. Conclusion and future directions

Owing to the above-mentioned complications researchers have moved away from using amine and started to use hydrazone and other linkers.⁶ The oxidation to an aldehyde followed by reaction with an amine to form an unstable intermediate imine that requires immediate reduction to an amine is too aggressive for cells. Additionally, this reaction is reversible in aqueous environments.

This can also be seen in the commercially available surface glycan labeling probes. Lately most of the published work includes use of aminooxy (as aminooxy-biotin) or hydrazide (as biotin-LC-hydrazide) rather than biotin-LC-amine.⁶ Moving forward, labeling of cell surface glycan with aminooxy-biotin or biotin-LC-hydrazide rather than biotin-LC-amine or amino-fluorescein derivatives like fluorescein hexylamine seems more feasible and viable. A parallel comparison of all sialic acid-based aldehydes reacting with handles including amines, aminooxys, and hydrazides with same conditions and cell types would benefit the field. Also, before proceeding to surface glycan labeling, a careful review of the conditions, catalysts, and buffers, as well as cytocompatibility of the reagents to be used is recommended.

A.5. References

(1) Sarkar, D.; Vemula, P. K.; Teo, G. S. L.; Spelke, D.; Karnik, R.; Wee, L. Y.; Karp, J. M. Chemical Engineering of Mesenchymal Stem Cells to Induce a Cell Rolling Response. *Bioconj. Chem.* **2008**, *19*, 2105–2109.

- (2) Sarkar, D.; Spencer, J. A.; Phillips, J. A.; Zhao, W.; Schafer, S.; Spelke, D. P.; Mortensen, L. J.; Ruiz, J. P.; Vemula, P. K.; Sridharan, R.; Kumar, S.; Karnik, R.; Lin, C. P.; Karp, J. M. Engineered Cell Homing. *Blood* **2011**, *118*, e184–e191.
- (3) De Bank, P. A.; Kellam, B.; Kendall, D. A.; Shakesheff, K. M. Surface Engineering of Living Myoblasts via Selective Periodate Oxidation. *Biotechnol. Bioeng.* **2003**, *81* (7), 800–808.
- (4) Holden, C. A.; Yuan, Q.; Yeudall, W. A.; Lebman, D. A.; Yang, H. Surface Engineering of Macrophages with Nanoparticles to Generate a Cell-Nanoparticle Hybrid Vehicle for Hypoxia-Targeted Drug Delivery. *Int. J. Nanomed.* **2010**, *5*, 25–36.
- (5) Wang, T. P.; Hwang, Y. J.; Chen, Y. H. Versatile Phosphoramidation Reactions for Nucleic Acid Conjugations with Peptides, Proteins, Chromophores, and Biotin Derivatives. *Bioconj. Chem.* **2010**, *21*, 1642-1655.
- (6) Kölmel, D. K.; Kool, E. T. Oximes and hydrazones in bioconjugation: mechanism and catalysis. *Chem. Rev.* **2017**, *117*, 10358-10376.

BIBLIOGRAPHY

Abbina, S.; Siren, E. M. J.; Moon, H.; Kizhakkedathu, J. N. Surface Engineering for Cell-Based Therapies: Techniques for Manipulating Mammalian Cell Surfaces. *ACS Biomater. Sci. Eng.* **2018**, *4*, 3658–3677.

Aboody, K. S.; Najbauer, J.; Metz, M. Z.; D'Apuzzo, M.; Gutova, M.; Annala, A. J.; Synold, T. W.; Couture, L. A.; Blanchard, S.; Moats, R. A.; Garcia, E.; Aramburo, S.; Valenzuela, V. V.; Frank, R. T.; Barish, M. E.; Brown, C. E.; Kim, S. U.; Badie, B.; Portnow, J. Neural Stem Cell-Mediated Enzyme/Prodrug Therapy for Glioma: Preclinical Studies. *Sci. Transl. Med.* **2013**, *5*, 184.

Albanese, A.; Tang, P. S.; Chan, W. C. W. The Effect of Nanoparticle Size, Shape, and Surface Chemistry on Biological Systems. *Annu. Rev. Biomed. Eng.* **2012**, *14*, 1–16.

Allen, T. M.; Cullis, P. R. Liposomal Drug Delivery Systems: From Concept to Clinical Applications. *Adv. Drug Deliv. Rev.* **2013**, *65*, 36–48.

Anselmo, A. C.; Gilbert, J. B.; Kumar, S.; Gupta, V.; Cohen, R. E.; Rubner, M. F.; Mitragotri, S. Monocyte-Mediated Delivery of Polymeric Backpacks to Inflamed Tissues: A Generalized Strategy to Deliver Drugs to Treat Inflammation. *J. Control. Release* **2015**, *199*, 29–36.

Anselmo, A. C.; Gupta, V.; Zern, B. J.; Pan, D.; Zakrewsky, M.; Muzykantov, V.; Mitragotri, S. Delivering Nanoparticles to Lungs While Avoiding Liver and Spleen through Adsorption on Red Blood Cells. *ACS Nano* **2013**, *7*, 11129–11137.

Anselmo, A. C.; Mitragotri, S. Cell-Mediated Delivery of Nanoparticles: Taking Advantage of Circulatory Cells to Target Nanoparticles. *J. Control. Release* **2014**, *190*, 531–541.

Ashley, G. W.; Henise, J.; Reid, R.; Santi, D. V. Hydrogel Drug Delivery System with Predictable and Tunable Drug Release and Degradation Rates. *Proc. Natl. Acad. Sci. U. S. A.* **2013**, *110*, 2318–2323.

Baek, S.-K.; Makkouk, A. R.; Krasieva, T.; Sun, C.-H.; Madsen, S. J.; Hirschberg, H. Photothermal Treatment of Glioma; an in Vitro Study of Macrophage-Mediated Delivery of Gold Nanoshells. *J. Neurooncol.* **2011**, *104*, 439–448.

Bai, Y.; Chen, J.; Zimmerman, S. C. Designed Transition Metal Catalysts for Intracellular Organic Synthesis. *Chem. Soc. Rev.* **2018**, *47*, 1811–182.

Baron, S.; Poast, J.; Rizzo, D.; McFarland, E.; Kieff, E. Electroporation of Antibodies, DNA, and Other Macromolecules into Cells: A Highly Efficient Method. *J. Immunol. Methods* **2000**, *242*, 115–126.

Batrakova, E. V.; Gendelman, H. E.; Kabanov, A. V. Cell-Mediated Drug Delivery. *Expert Opin. Drug Deliv.* **2011**, *8*, 415–433.

Bianco, P.; Robey, P. G. Stem Cells in Tissue Engineering. *Nature* **2001**, *414*, 118–121.

- Björnheden, T.; Levin, M.; Evaldsson, M.; Wiklund, O. Evidence of Hypoxic Areas Within the Arterial Wall In Vivo. *Arterioscl. Thromb. Vasc. Biol.*, **1999**, *19*, 870–876.
- Blackman, M. L.; Royzen, M.; Fox, J. M. Tetrazine Ligation: Fast Bioconjugation Based on Inverse-Electron-Demand Diels–Alder Reactivity. *J. Am. Chem. Soc.* **2008**, *130*, 13518–13519.
- Bonde, A.-K.; Tischler, V.; Kumar, S.; Soltermann, A.; Schwendener, R. A. Intratumoral Macrophages Contribute to Epithelial-Mesenchymal Transition in Solid Tumors. *BMC Cancer* **2012**, *12*, 35.
- Bottaro, D. P.; Liotta, L. A. Out of Air Is Not out of Action. *Nature* **2003**, *423*, 593–595.
- Brannon-Peppas, L.; Blanchette, J. O. Nanoparticle and Targeted Systems for Cancer Therapy. *Adv. Drug Deliv. Rev.* **2004**, *56*, 1649–1659.
- Brown, J. M. Exploiting the Hypoxic Cancer Cell: Mechanisms and Therapeutic Strategies. *Mol. Med. Today* **2000**, *6*, 157–162.
- Brown, J. M.; Giaccia, A. J. The Unique Physiology of Solid Tumors: Opportunities (and Problems) for Cancer Therapy. *Cancer Res.* **1998**, *58*, 1408–1416.
- Brown, J. M.; Wilson, W. R. Exploiting Tumour Hypoxia in Cancer Treatment. *Nat. Rev. Cancer* **2004**, *4*, 437–447.
- Burke, J.; Hunter, M.; Kolhe, R.; Isales, C.; Hamrick, M.; Fulzele, S. Therapeutic Potential of Mesenchymal Stem Cell Based Therapy for Osteoarthritis. *Clin. Transl. Med.* **2016**, *5*, 1-8.
- Byrne, J. D.; Betancourt, T.; Brannon-Peppas, L. Active Targeting Schemes for Nanoparticle Systems in Cancer Therapeutics. *Adv. Drug Deliv. Rev.* **2008**, *60*, 1615–1626.
- Cai, Y.; Xi, Y.; Cao, Z.; Xiang, G.; Ni, Q.; Zhang, R.; Chang, J.; Du, X.; Yang, A.; Yan, B.; Zhao, J. Dual Targeting and Enhanced Cytotoxicity to HER2-Overexpressing Tumors by Immunoapoptin-Armored Mesenchymal Stem Cells. *Cancer Lett.* **2016**, *381*, 104–112.
- Cao, P.; Mooney, R.; Tirughana, R.; Abidi, W.; Aramburo, S.; Flores, L.; Gilchrist, M.; Nwokafor, U.; Haber, T.; Tiet, P.; Annala, A. J.; Han, E.; Dellinger, T.; Aboody, K. S.; Berlin, J. M. Intraperitoneal Administration of Neural Stem Cell–Nanoparticle Conjugates Targets Chemotherapy to Ovarian Tumors. *Bioconjug. Chem.* **2017**, *28*, 1767–1776.
- Cao-milan, R.; Gopalakrishnan, S.; He, L. D.; Huang, R.; Wang, L.; Castellanos, L.; Luther, D. C.; Landis, R. F.; Makabenta, J. M. V; Li, C. -H.; Zhang, X.; Scaletti, F.; Vachet, R. W.; Rotello, V. M. Thermally Gated Bio-Orthogonal Nanozymes with Supramolecularly Confined Porphyrin Catalysts for Antimicrobial Uses Thermally Gated Bio-Orthogonal Nanozymes with Supramolecularly Confined Porphyrin Catalysts for Antimicrobial Uses. *Chem.* **2020**, *6*, 1–12.

- Cao-Milán, R.; He, L. D.; Shorkey, S.; Tonga, G. Y.; Wang, L.-S.; Zhang, X.; Uddin, I.; Das, R.; Sulak, M.; Rotello, V. M. Modulating the Catalytic Activity of Enzyme-like Nanoparticles through Their Surface Functionalization. *Mol. Syst. Des. Eng.* **2017**, *2*, 624–628.
- Chamberlain, G.; Fox, J.; Ashton, B.; Middleton, J. Concise Review: Mesenchymal Stem Cells: Their Phenotype, Differentiation Capacity, Immunological Features, and Potential for Homing. *Stem Cells* **2007**, *25*, 2739–2749.
- Chambers, E.; Mitragotri, S. Long Circulating Nanoparticles via Adhesion on Red Blood Cells: Mechanism and Extended Circulation. *Exp. Biol. Med.* **2007**, *232*, 958–966.
- Chambers, E.; Mitragotri, S. Prolonged Circulation of Large Polymeric Nanoparticles by Non-Covalent Adsorption on Erythrocytes. *J. Control. Release* **2004**, *100*, 111–119.
- Champion, J. A.; Mitragotri, S. Role of Target Geometry in Phagocytosis. *Proc. Natl. Acad. Sci. U. S. A.* **2006**, *103*, 4930–4934.
- Champion, J. A.; Walker, A.; Mitragotri, S. Role of Particle Size in Phagocytosis of Polymeric Microspheres. *Pharm. Res.* **2008**, *25*, 1815–1821.
- Chaturvedi, P.; Gilkes, D. M.; Takano, N.; Semenza, G. L. Hypoxia-Inducible Factor-Dependent Signaling between Triple-Negative Breast Cancer Cells and Mesenchymal Stem Cells Promotes Macrophage Recruitment. *Proc. Natl. Acad. Sci. U.S. A.* **2014**, *111*, E2120-E2129.
- Chen, H.-C. Boyden Chamber Assay. In *Cell Migration*; Humana Press: New Jersey, **2004**, *294*, 015–022.
- Chen, H.-C. Boyden Chamber Assay. *Cell Migr.* **2004**, *294*, 015–022.
- Chen, Q.; Zhang, X. H.-F.; Massagué, J. Macrophage Binding to Receptor VCAM-1 Transmits Survival Signals in Breast Cancer Cells That Invade the Lungs. *Cancer Cell* **2011**, *20*, 538–549.
- Chen, Y.; Xiang, L.-X.; Shao, J.-Z.; Pan, R.-L.; Wang, Y.-X.; Dong, X.-J.; Zhang, G.-R. Recruitment of Endogenous Bone Marrow Mesenchymal Stem Cells towards Injured Liver. *J. Cell. Mol. Med.* **2009**, *14*, 1494–1508.
- Cheng, H.; Kastrup, C. J.; Ramanathan, R.; Siegwart, D. J.; Ma, M.; Bogatyrev, S. R.; Xu, Q.; Whitehead, K. A.; Langer, R.; Anderson, D. G. Nanoparticulate Cellular Patches for Cell-Mediated Tumortropic Delivery. *ACS Nano* **2010**, *4*, 625–631.
- Chhour, P.; Naha, P. C.; O’Neill, S. M.; Litt, H. I.; Reilly, M. P.; Ferrari, V. A.; Cormode, D. P. Labeling Monocytes with Gold Nanoparticles to Track Their Recruitment in Atherosclerosis with Computed Tomography. *Biomaterials* **2016**, *87*, 93–103.
- Choi, J.; Kim, H.-Y.; Ju, E. J.; Jung, J.; Park, J.; Chung, H.-K.; Lee, J. S.; Lee, J. S.; Park, H. J.; Song, S. Y.; Jeong, S.-Y.; Choi, E. K. Use of Macrophages to Deliver Therapeutic and Imaging Contrast Agents to Tumors. *Biomaterials* **2012**, *33*, 4195–4203.

- Choi, M.-R.; Bardhan, R.; Stanton-Maxey, K. J.; Badve, S.; Nakshatri, H.; Stantz, K. M.; Cao, N.; Halas, N. J.; Clare, S. E. Delivery of Nanoparticles to Brain Metastases of Breast Cancer Using a Cellular Trojan Horse. *Cancer Nano* **2012**, *3*, 47–54.
- Choi, M.-R.; Stanton-Maxey, K. J.; Stanley, J. K.; Levin, C. S.; Bardhan, R.; Akin, D.; Badve, S.; Sturgis, J.; Robinson, J. P.; Bashir, R.; Halas, N. J.; Clare, S. E. A Cellular Trojan Horse for Delivery of Therapeutic Nanoparticles into Tumors. *Nano Lett.* **2007**, *7*, 3759–3765.
- Cohen, S. S.; Flaks, J. G.; Barner, H. D.; Loeb, M. R.; Lichtenstein, J. The mode of action of 5-fluorouracil and its derivatives. *Proc. Natl. Acad. Sci. U. S. A.* **1958**, *44*, 1004–1012.
- Condeelis, J.; Pollard, J. W. Macrophages: Obligate Partners for Tumor Cell Migration, Invasion, and Metastasis. *Cell* **2006**, *124*, 263–266.
- Csizmar, C. M.; Petersburg, J. R.; Wagner, C. R. Programming Cell-Cell Interactions through Non-Genetic Membrane Engineering. *Cell Chem. Biol.* **2018**, *25*, 931–940.
- Dai, Q.; Wilhelm, S.; Ding, D.; Syed, A. M.; Sindhvani, S.; Zhang, Y.; Chen, Y. Y.; Macmillan, P.; Chan, W. C. W. Quantifying the Ligand-Coated Nanoparticle Delivery to Cancer Cells in Solid Tumors. *ACS Nano* **2018**, *12*, 8423–8435.
- Danhier, F.; Feron, O.; Pr at, V. To Exploit the Tumor Microenvironment: Passive and Active Tumor Targeting of Nanocarriers for Anti-Cancer Drug Delivery. *J. Control. Release* **2010**, *148*, 135–146.
- Das, R.; Hardie, J.; Joshi, B. P.; Zhang, X.; Gupta, A.; Luther, D. C.; Fedeli, S.; Farkas, M. E.; Rotello, V. M. Macrophage-Encapsulated Bioorthogonal Nanozymes for Targeting Cancer Cells. *JACS Au* **2022**, *2*, 1679–1685.
- Das, R.; Landis, R. F.; Tonga, G. Y.; Cao-Mil an, R.; Luther, D. C.; Rotello, V. M. Control of Intra-versus Extracellular Bioorthogonal Catalysis Using Surface-Engineered Nanozymes. *ACS Nano* **2018**, *13*, 229–235.
- Dass, C. R.; Choong, P. F. Targeting of Small Molecule Anticancer Drugs to the Tumour and Its Vasculature Using Cationic Liposomes: Lessons from Gene Therapy. *Cancer Cell. Int.* **2006**, *6*, 17.
- De Bank, P. A.; Kellam, B.; Kendall, D. A.; Shakesheff, K. M. Surface Engineering of Living Myoblasts via Selective Periodate Oxidation. *Biotechnol. Bioeng.* **2003**, *81* (7), 800–808.
- De Brito Monteiro, L.; Davanzo, G. G.; de Aguiar, C. F.; Corr ea da Silva, F.; Andrade, J. R. de; Campos Codo, A.; Silva Pereira, J. A. da; Freitas, L. P. de; Moraes-Vieira, P. M. M-CSF- and L929-Derived Macrophages Present Distinct Metabolic Profiles with Similar Inflammatory Outcomes. *Immunobiology* **2020**, *225*, 151935.
- De Jong, W. H.; Borm, P. J. A. Drug Delivery and Nanoparticles: Applications and Hazards. *Int. J. Nanomed.* **2008**, *3*, 133-149.

- Denmeade, S. R.; Mhaka, A. M.; Rosen, D. M.; Brennen, W. N.; Dalrymple, S.; Dach, I.; Olesen, C.; Gurel, B.; Demarzo, A. M.; Wilding, G.; Carducci, M. A.; Dionne, C. A.; Møller, J. V.; Nissen, P.; Christensen, S. B.; Isaacs, J. T. Engineering a Prostate-Specific Membrane Antigen – Activated Tumor Endothelial Cell Prodrug for Cancer Therapy. *Sci. Transl. Med.* **2012**, *4*, 140ra86.
- Devaraj, N. K.; Weissleder, R.; Hilderbrand, S. A. Tetrazine-Based Cycloadditions: Application to Pretargeted Live Cell Imaging. *Bioconjug. Chem.* **2008**, *19*, 2297–2299.
- Doshi, N.; Swiston, A. J.; Gilbert, J. B.; Alcaraz, M. L.; Cohen, R. E.; Rubner, M. F.; Mitragotri, S. Cell-Based Drug Delivery Devices Using Phagocytosis-Resistant Backpacks. *Adv. Mater.* **2011**, *23*, H105–H109.
- Dou, H.; Destache, C. J.; Morehead, J. R.; Mosley, R. L.; Boska, M. D.; Kingsley, J.; Gorantla, S.; Poluektova, L.; Nelson, J. A.; Chaubal, M.; Werling, J.; Kipp, J.; Rabinow, B. E.; Gendelman, H. E. Development of a Macrophage-Based Nanoparticle Platform for Antiretroviral Drug Delivery. *Blood* **2006**, *108*, 2827–2835.
- Du, J.; Hong, S.; Dong, L.; Cheng, B.; Lin, L.; Zhao, B.; Chen, Y.-G.; Chen, X. Dynamic Sialylation in Transforming Growth Factor- β (TGF- β)-Induced Epithelial to Mesenchymal Transition. *J. Biol. Chem.* **2015**, *290*, 12000–12013.
- Du, Z.; Liu, C.; Song, H.; Scott, P.; Liu, Z.; Ren, J.; Qu, X. Neutrophil-Membrane-Directed Bioorthogonal Synthesis of Inflammation-Targeting Chiral Drugs. *Chem* **2020**, *6*, 2060–2072.
- Duran, N. E.; Hommes, D. W. Stem Cell-Based Therapies in Inflammatory Bowel Disease: Promises and Pitfalls. *Therap. Adv. Gastroenterol.* **2016**, *9*, 533–547.
- Eisenblätter, M.; Ehrchen, J.; Varga, G.; Sunderkötter, C.; Heindel, W.; Roth, J.; Bremer, C.; Wall, A. In Vivo Optical Imaging of Cellular Inflammatory Response in Granuloma Formation Using Fluorescence-Labeled Macrophages. *J. Nucl. Med.* **2009**, *50*, 1676–1682.
- Eisenblätter, M.; Ehrchen, J.; Varga, G.; Sunderkötter, C.; Heindel, W.; Roth, J.; Bremer, C.; Wall, A. In Vivo Optical Imaging of Cellular Inflammatory Response in Granuloma Formation Using Fluorescence-Labeled Macrophages. *J. Nucl. Med.* **2009**, *50*, 1676–1682.
- Eming, S. A.; Krieg, T.; Davidson, J. M. Inflammation in Wound Repair: Molecular and Cellular Mechanisms. *J. Invest. Dermatol.* **2007**, *127*, 514–525.
- Encabo-Berzosa, M. M.; Gimeno, M.; Lujan, L.; Sancho-Albero, M.; Gomez, L.; Sebastian, V.; Quintanilla, M.; Arruebo, M.; Santamaria, J.; Martin-Duque, P. Selective Delivery of Photothermal Nanoparticles to Tumors Using Mesenchymal Stem Cells as Trojan Horses. *RSC Adv.* **2016**, *6*, 58723–58732.
- Favretto, M. E.; Cluitmans, J. C. A.; Bosman, G. J. C. G. M.; Brock, R. Human Erythrocytes as Drug Carriers: Loading Efficiency and Side Effects of Hypotonic Dialysis,

Chlorpromazine Treatment and Fusion with Liposomes. *J. Control. Release* **2013**, *170*, 343–351.

Feng, Q.; Liang, S.; Jia, H.; Stadlmayr, A.; Tang, L.; Lan, Z.; Zhang, D.; Xia, H.; Xu, X.; Jie, Z.; Su, L.; Li, X.; Li, X.; Li, J.; Xiao, L.; Huber-Schönauer, U.; Niederseer, D.; Xu, X.; Al-Aama, J. Y.; Yang, H.; Wang, J.; Kristiansen, K.; Arumugam, M.; Tilg, H.; Datz, C.; Wang, J. Gut Microbiome Development along the Colorectal Adenoma–Carcinoma Sequence. *Nat. Commun.* **2015**, *6*, 6528.

Frank, R. T.; Edmiston, M.; Kendall, S. E.; Najbauer, J.; Cheung, C.-W.; Kassa, T.; Metz, M. Z.; Kim, S. U.; Glackin, C. A.; Wu, A. M.; Yazaki, P. J.; Aboody, K. S. Neural Stem Cells as a Novel Platform for Tumor-Specific Delivery of Therapeutic Antibodies. *PLoS ONE* **2009**, *4*, e8314.

Fu, J.; Wang, D.; Mei, D.; Zhang, H.; Wang, Z.; He, B.; Dai, W.; Zhang, H.; Wang, X.; Zhang, Q. Macrophage Mediated Biomimetic Delivery System for the Treatment of Lung Metastasis of Breast Cancer. *J. Control. Release* **2015**, *204*, 11–19.

Ganta, S.; Devalapally, H.; Shahiwala, A.; Amiji, M. A Review of Stimuli-Responsive Nanocarriers for Drug and Gene Delivery. *J. Control. Release* **2008**, *126*, 187–204.

Gao, M.; Hu, A.; Sun, X.; Wang, C.; Dong, Z.; Feng, L.; Liu, Z. Photosensitizer Decorated Red Blood Cells as an Ultrasensitive Light-Responsive Drug Delivery System. *ACS Appl. Mater. Interfaces* **2017**, *9*, 5855–5863.

Garzon, R.; Marcucci, G.; Croce, C. M. Targeting MicroRNAs in Cancer: Rationale, Strategies and Challenges. *Nat. Rev. Drug Discov.* **2010**, *9*, 775–789.

Germain, M.; Balaguer, P.; Nicolas, J.-C.; Lopez, F.; Esteve, J.-P.; Sukhorukov, G. B.; Winterhalter, M.; Richard-Foy, H.; Fournier, D. Protection of Mammalian Cell Used in Biosensors by Coating with a Polyelectrolyte Shell. *Biosens. Bioelectron.* **2006**, *21*, 1566–1573.

Ghosh, P.; Han, G.; De, M.; Kim, C. K.; Rotello, V. M. Gold Nanoparticles in Delivery Applications. *Adv. Drug Deliv. Rev.* **2008**, *60*, 1307–1315.

Ginhoux, F.; Guilliams, M.; Naik, S. H. Editorial: Dendritic Cell and Macrophage Nomenclature and Classification. *Front. Immunol.* **2016**, *7*, 168.

Gregório, A. C.; Fonseca, N. A.; Moura, V.; Lacerda, M.; Figueiredo, P.; Simões, S.; Dias, S.; Moreira, J. N. Inoculated Cell Density as a Determinant Factor of the Growth Dynamics and Metastatic Efficiency of a Breast Cancer Murine Model. *PLoS ONE* **2016**, *11*, 0165817.

Gribova, V.; Auzely-Velty, R.; Picart, C. Polyelectrolyte Multilayer Assemblies on Materials Surfaces: From Cell Adhesion to Tissue Engineering. *Chem. Mater.* **2012**, *24*, 854–869.

Griffiths, L.; Binley, K.; Iqbal, S.; Kan, O.; Maxwell, P.; Ratcliffe, P.; Lewis, C.; Harris, A.; Kingsman, S.; Naylor, S. The Macrophage – a Novel System to Deliver Gene Therapy to Pathological Hypoxia. *Gene Ther.* **2000**, *7*, 255–262.

- Grivennikov, S. I.; Greten, F. R.; Karin, M. Immunity, Inflammation, and Cancer. *Cell* **2010**, *140*, 883–899.
- Guan, J.; Chen, J. Mesenchymal Stem Cells in the Tumor Microenvironment. *Biomed. Rep.* **2013**, *1*, 517–521.
- Gupta, A.; Das, R.; Yesilbag Tonga, G.; Mizuhara, T.; Rotello, V. M. Charge-Switchable Nanozymes for Bioorthogonal Imaging of Biofilm-Associated Infections. *ACS Nano* **2018**, *12*, 89–94.
- Gupta, N.; Krasnodembskaya, A.; Kapetanaki, M.; Mouded, M.; Tan, X.; Serikov, V.; Matthay, M. A. Mesenchymal Stem Cells Enhance Survival and Bacterial Clearance in Murine *Escherichia Coli* Pneumonia. *Thorax* **2012**, *67*, 533–539.
- Gwak, J. M.; Jang, M. H.; Kim, D. I.; Seo, A. N.; Park, S. Y. Prognostic Value of Tumor-Associated Macrophages According to Histologic Locations and Hormone Receptor Status in Breast Cancer. *PLoS ONE* **2015**, *10*, 0125728.
- Haber, T.; Baruch, L.; Machluf, M. Ultrasound-Mediated Mesenchymal Stem Cells Transfection as a Targeted Cancer Therapy Platform. *Sci. Rep.* **2017**, *7*, 42046.
- Hamada, H.; Kobune, M.; Nakamura, K.; Kawano, Y.; Kato, K.; Honmou, O.; Houkin, K.; Matsunaga, T.; Niitsu, Y. Mesenchymal Stem Cells (MSC) as Therapeutic Cytoreagents for Gene Therapy. *Cancer Sci.* **2005**, *96*, 149–156.
- Han, J.; Zhen, J.; Du Nguyen, V.; Go, G.; Choi, Y.; Ko, S. Y.; Park, J.-O.; Park, S. Hybrid-Actuating Macrophage-Based Microrobots for Active Cancer Therapy. *Sci. Rep.* **2016**, *6*, 28717.
- Hartig, S. M. Basic Image Analysis and Manipulation in ImageJ. *Curr. Protoc. Mol. Biol.* **2013**, *102* (1).
- He, W.; Qiang, M.; Ma, W.; Valente, A. J.; Quinones, M. P.; Wang, W.; Reddick, R. L.; Xiao, Q.; Ahuja, S. S.; Clark, R. A.; Freeman, G. L.; Li, S. Development of a Synthetic Promoter for Macrophage Gene Therapy. *Hum. Gene Ther.* **2006**, *17*, 949–959.
- Heine, D.; Müller, R.; Brüsselbach, S. Cell Surface Display of a Lysosomal Enzyme for Extracellular Gene-Directed Enzyme Prodrug Therapy. *Gene Ther.* **2001**, *8*, 1005–1010.
- Hoffman, J. F. On Red Blood Cells, Hemolysis and Resealed Ghosts. In The Use of Resealed Erythrocytes as Carriers and Bioreactors. *Adv. Exp. Med. Biol.* **1992**, *326*, 1–15.
- Hoffman, R. M. The Multiple Uses of Fluorescent Proteins to Visualize Cancer in Vivo. *Nat. Rev. Cancer* **2005**, *5*, 796–806.
- Hoffman, R. M.; Yang, M. Color-Coded Fluorescence Imaging of Tumor-Host Interactions. *Nat. Protoc.* **2006**, *1*, 928–935.
- Holden, C. A.; Yuan, Q.; Yeudall, W. A.; Lebman, D. A.; Yang, H. Surface Engineering of Macrophages with Nanoparticles to Generate a Cell-Nanoparticle Hybrid Vehicle for Hypoxia-Targeted Drug Delivery. *Int. J. Nanomed.* **2010**, *5*, 25–36.

- Hong, V.; Steinmetz, N. F.; Manchester, M.; Finn, M. G. Labeling Live Cells by Copper-Catalyzed Alkyne–Azide Click Chemistry. *Bioconj. Chem.* **2010**, *21*, 1912–1916.
- Huai, Y.; Hossen, M. N.; Wilhelm, S.; Bhattacharya, R.; Mukherjee, P. Nanoparticle Interactions with the Tumor Microenvironment. *Bioconjug. Chem.* **2019**, *30*, 2247–2263.
- Huang, N. F.; Li, S. Mesenchymal Stem Cells for Vascular Regeneration. *Regen. Med.* **2008**, *3*, 877–892.
- Huang, R.; Li, C.; Cao-milan, R.; He, L. D.; Makabenta, J. M.; Zhang, X.; Yu, E.; Rotello, V. M. Polymer-Based Bioorthogonal Nanocatalysts for the Treatment of Bacterial Biofilms. *J. Am. Chem. Soc.* **2020**, *142*, 10723–10729.
- Huang, W.-C.; Chiang, W.-H.; Cheng, Y.-H.; Lin, W.-C.; Yu, C.-F.; Yen, C.-Y.; Yeh, C.-K.; Chern, C.-S.; Chiang, C.-S.; Chiu, H.-C. Tumortropic Monocyte-Mediated Delivery of Echogenic Polymer Bubbles and Therapeutic Vesicles for Chemotherapy of Tumor Hypoxia. *Biomaterials* **2015**, *71*, 71–83.
- Huang, W.-C.; Shen, M.-Y.; Chen, H.-H.; Lin, S.-C.; Chiang, W.-H.; Wu, P.-H.; Chang, C.-W.; Chiang, C.-S.; Chiu, H.-C. Monocytic Delivery of Therapeutic Oxygen Bubbles for Dual-Modality Treatment of Tumor Hypoxia. *J. Control. Release* **2015**, *220*, 738–750.
- Huang, Y.; Ren, J.; Qu, X. Nanozymes: Classification, Catalytic Mechanisms, Activity Regulation, and Applications. *Chem. Rev.* **2019**, *119*, 4357–4412.
- Hughes, R. M.; Marvin, C. M.; Rodgers, Z. L.; Ding, S.; Oien, N. P.; Smith, W. J.; Lawrence, D. S. Phototriggered Secretion of Membrane Compartmentalized Bioactive Agents. *Angew. Chem. Int. Ed.* **2016**, *55*, 16080–16083.
- Hunault-Berger, M.; Leguay, T.; Huguet, F.; Leprêtre, S.; Deconinck, E.; Ojeda-Urbe, M.; Bonmati, C.; Escoffre-Barbe, M.; Bories, P.; Himmerlin, C.; Chevallerier, P.; Rousselot, P.; Reman, O.; Boulland, M.-L.; Lissandre, S.; Turlure, P.; Bouscary, D.; Sanhes, L.; Legrand, O.; Lafage-Pochitaloff, M.; Béné, M. C.; Liens, D.; Godfrin, Y.; Ifrah, N.; Dombret, H.; Group for Research on Adult Acute Lymphoblastic Leukemia (GRAALL). A Phase 2 Study of L-Asparaginase Encapsulated in Erythrocytes in Elderly Patients with Philadelphia Chromosome Negative Acute Lymphoblastic Leukemia: The GRASPALL/GRAALL-SA2-2008 Study: L-Asparaginase within Erythrocytes in Elderly ALL Patients. *Am. J. Hematol.* **2015**, *90*, 811–818.
- Ihler, G. M.; Glew, R. H.; Schnure, F. W. Enzyme Loading of Erythrocytes. *Proc. Natl. Acad. Sci. U. S. A.* **1973**, *70*, 2663–2666.
- Iwasaki, Y.; Ota, T. Efficient Biotinylation of Methacryloyl-Functionalized Nonadherent Cells for Formation of Cell Microarrays. *Chem. Commun.* **2011**, *47*, 10329.
- Jeong, Y.; Tonga, G. Y.; Duncan, B.; Yan, B.; Das, R.; Sahub, C.; Rotello, V. M. Solubilization of Hydrophobic Catalysts Using Nanoparticle Hosts. *Small* **2018**, *14*, 1702198.

- Jewett, J. C.; Sletten, E. M.; Bertozzi, C. R. Rapid Cu-Free Click Chemistry with Readily Synthesized Biarylazacyclooctynones. *J. Am. Chem. Soc.* **2010**, *132*, 3688–3690.
- Jiang, Y.; Huo, S.; Mizuhara, T.; Das, R.; Lee, Y.; Hou, S.; Moyano, D. F.; Duncan, B.; Liang, X.; Rotello, V. M. The Interplay of Size and Surface Functionality on the Cellular Uptake of Sub-10 Nm Gold Nanoparticles. *ACS Nano* **2015**, *9*, 9986–9993.
- Johnson, V.; Webb, T.; Norman, A.; Coy, J.; Kurihara, J.; Regan, D.; Dow, S. Activated Mesenchymal Stem Cells Interact with Antibiotics and Host Innate Immune Responses to Control Chronic Bacterial Infections. *Sci. Rep.* **2017**, *7*, 9575.
- Joshi, B. P.; Hardie, J.; Farkas, M. E. Harnessing Biology to Deliver Therapeutic and Imaging Entities via Cell-Based Methods. *Chem. Eur. J.* **2018**, *24*, 8717–8726.
- Joshi, B. P.; Hardie, J.; Mingroni, M. A.; Farkas, M. E. Surface-Modified Macrophages Facilitate Tracking of Breast Cancer-Immune Interactions. *ACS Chem. Biol.* **2018**, *13*, 2339–2346.
- Kaczorowski, A.; Hammer, K.; Liu, L.; Villhauer, S.; Nwaeburu, C.; Fan, P.; Zhao, Z.; Gladkikh, J.; Groß, W.; Nettelbeck, D. M.; Herr, I. Delivery of Improved Oncolytic Adenoviruses by Mesenchymal Stromal Cells for Elimination of Tumorigenic Pancreatic Cancer Cells. *Oncotarget* **2016**, *7*, 9046–9059.
- Kalimuthu, S.; Zhu, L.; Oh, J. M.; Gangadaran, P.; Lee, H. W.; Baek, S. hwan; Rajendran, R. L.; Gopal, A.; Jeong, S. Y.; Lee, S.-W.; Lee, J.; Ahn, B.-C. Migration of Mesenchymal Stem Cells to Tumor Xenograft Models and *in Vitro* Drug Delivery by Doxorubicin. *Int. J. Med. Sci.* **2018**, *15*, 1051–1061.
- Kang, S.; Lee, H. W.; Jeon, Y. H.; Singh, T. D.; Choi, Y. J.; Park, J. Y.; Kim, J. S.; Lee, H.; Hong, K. S.; Lee, I.; Jeong, S. Y.; Lee, S.-W.; Ha, J.-H.; Ahn, B.-C.; Lee, J. Combined Fluorescence and Magnetic Resonance Imaging of Primary Macrophage Migration to Sites of Acute Inflammation Using Near-Infrared Fluorescent Magnetic Nanoparticles. *Mol. Imaging Biol.* **2015**, *17*, 643–651.
- Karp, J.; Zhao, W. *Micro- and Nanoengineering of the Cell Surface*; William Andrew **2014**, *3*, 44-58.
- Kellam, B.; De Bank, P. A.; Shakesheff, K. M. Chemical Modification of Mammalian Cell Surfaces. *Chem. Soc. Rev.* **2003**, *32*, 327.
- Kidd, S.; Spaeth, E.; Dembinski, J. L.; Dietrich, M.; Watson, K.; Klopp, A.; Battula, V. L.; Weil, M.; Andreeff, M.; Marini, F. C. Direct Evidence of Mesenchymal Stem Cell Tropism for Tumor and Wounding Microenvironments Using In Vivo Bioluminescent Imaging. *Stem Cells* **2009**, *27*, 2614–2623.
- Kinge, S.; Crego-Calama, M.; Reinhoudt, D. N. Self-Assembling Nanoparticles at Surfaces and Interfaces. *Chem. Phys. Chem.* **2008**, *9*, 20–42.
- Klyachko, N. L.; Polak, R.; Haney, M. J.; Zhao, Y.; Gomes Neto, R. J.; Hill, M. C.; Kabanov, A. V.; Cohen, R. E.; Rubner, M. F.; Batrakova, E. V. Macrophages with Cellular Backpacks for Targeted Drug Delivery to the Brain. *Biomaterials* **2017**, *140*, 79–87.

- Kölmel, D. K.; Kool, E. T. Oximes and Hydrazones in Bioconjugation: Mechanism and Catalysis. *Chem. Rev.* **2017**, *117*, 10358-10376.
- Komohara, Y.; Jinushi, M.; Takeya, M. Clinical Significance of Macrophage Heterogeneity in Human Malignant Tumors. *Cancer Sci.* **2014**, *105*, 1–8.
- Koniev, O.; Wagner, A. Developments and Recent Advancements in the Field of Endogenous Amino Acid Selective Bond Forming Reactions for Bioconjugation. *Chem. Soc. Rev.* **2015**, *44*, 5495–5551.
- Lai, Q.-G.; Yuan, K.-F.; Xu, X.; Li, D.; Li, G.-J.; Wei, F.-L.; Yang, Z.-J.; Luo, S.-L.; Tang, X.-P.; Li, S. Transcription Factor Osterix Modified Bone Marrow Mesenchymal Stem Cells Enhance Callus Formation during Distraction Osteogenesis. *Oral Surg. Oral Med. Oral Pathol. Oral Radiol. and Endodontol.* **2011**, *111*, 412–419.
- Lammers, T.; Kiessling, F.; Hennink, W. E.; Storm, G. Drug Targeting to Tumors: Principles, Pitfalls and (Pre-) Clinical Progress. *J. Control. Release* **2012**, *161*, 175–187.
- Laughlin, S. T.; Bertozzi, C. R. Metabolic Labeling of Glycans with Azido Sugars and Subsequent Glycan-Profiling and Visualization via Staudinger Ligation. *Nat. Protoc.* **2007**, *2*, 2930–2944.
- Layek, B.; Sadhukha, T.; Prabha, S. Glycoengineered Mesenchymal Stem Cells as an Enabling Platform for Two-Step Targeting of Solid Tumors. *Biomaterials* **2016**, *88*, 97–109.
- Lee, D. Y.; Park, S. J.; Nam, J. H.; Byun, Y. A New Strategy Toward Improving Immunoprotection in Cell Therapy for Diabetes Mellitus: Long-Functioning PEGylated Islets *In Vivo*. *Tissue Eng.* **2006**, *12*, 615–623.
- Leng, L.; Wang, Y.; He, N.; Wang, D.; Zhao, Q.; Feng, G.; Su, W.; Xu, Y.; Han, Z.; Kong, D.; Cheng, Z.; Xiang, R.; Li, Z. Molecular Imaging for Assessment of Mesenchymal Stem Cells Mediated Breast Cancer Therapy. *Biomaterials* **2014**, *35*, 5162–5170.
- Leoni, V.; Gatta, V.; Palladini, A.; Nicoletti, G.; Ranieri, D.; Dall’Ora, M.; Grosso, V.; Rossi, M.; Alviano, F.; Bonsi, L.; Nanni, P.; Lollini, P.-L.; Campadelli-Fiume, G. Systemic Delivery of HER2-Retargeted Oncolytic-HSV by Mesenchymal Stromal Cells Protects from Lung and Brain Metastases. *Oncotarget* **2015**, *6*, 34774–34787.
- Leuzzi, V.; Micheli, R.; D’Agnano, D.; Molinaro, A.; Venturi, T.; Plebani, A.; Soresina, A.; Marini, M.; Ferremi Leali, P.; Quinti, I.; Pietrogrande, M. C.; Finocchi, A.; Fazzi, E.; Chessa, L.; Magnani, M. Positive Effect of Erythrocyte-Delivered Dexamethasone in Ataxia-Telangiectasia. *Neurol. Neuroimmunol.* **2015**, *2*, 3.
- Lewis, C. E.; Pollard, J. W. Distinct Role of Macrophages in Different Tumor Microenvironments. *Cancer Res.* **2006**, *66*, 605–612.
- Li, J.; Yu, J.; Zhao, J.; Wang, J.; Zheng, S.; Lin, S.; Chen, L.; Yang, M.; Jia, S.; Zhang, X.; Chen, P. R. Palladium-Triggered Deprotection Chemistry for Protein Activation in Living Cells. *Nat. Chem.* **2014**, *6*, 352–361.

- Li, L.; Guan, Y.; Liu, H.; Hao, N.; Liu, T.; Meng, X.; Fu, C.; Li, Y.; Qu, Q.; Zhang, Y.; Ji, S.; Chen, L.; Chen, D.; Tang, F. Silica Nanorattle–Doxorubicin-Anchored Mesenchymal Stem Cells for Tumor-Tropic Therapy. *ACS Nano* **2011**, *5*, 7462–7470.
- Li, S.; Feng, S.; Ding, L.; Liu, Y.; Zhu, Q.; Qian, Z.; Gu, Y. Nanomedicine Engulfed by Macrophages for Targeted Tumor Therapy. *Int. J. Nanomed.* **2016**, *11*, 4107–4124.
- Li, Z.; Huang, H.; Tang, S.; Li, Y.; Yu, X.-F.; Wang, H.; Li, P.; Sun, Z.; Zhang, H.; Liu, C.; Chu, P. K. Small Gold Nanorods Laden Macrophages for Enhanced Tumor Coverage in Photothermal Therapy. *Biomaterials* **2016**, *74*, 144–154.
- Lin, M.; Chen, Y.; Zhao, S.; Tang, R.; Nie, Z.; Xing, H. A Biomimetic Approach for Spatially Controlled Cell Membrane Engineering Using Fusogenic Spherical Nucleic Acid. *Angew. Chem. Intl. Ed.* **2022**, *61*, 1-9.
- Liu, S.; Ginestier, C.; Ou, S. J.; Clouthier, S. G.; Patel, S. H.; Monville, F.; Korkaya, H.; Heath, A.; Dutcher, J.; Kleer, C. G.; Jung, Y.; Dontu, G.; Taichman, R.; Wicha, M. S. Breast Cancer Stem Cells Are Regulated by Mesenchymal Stem Cells through Cytokine Networks. *Cancer Res.* **2011**, *71*, 614–624.
- Livnah, O.; Bayer, E. A.; Wilchek, M.; Sussman, J. L. Three-Dimensional Structures of Avidin and the Avidin-Biotin Complex. *Proc. Natl. Acad. Sci., U. S. A.* **1993**, *90*, 5076–5080.
- Longley, D. B.; Harkin, D. P.; Johnston, P. G. 5-Fluorouracil: mechanisms of action and clinical strategies. *Nat. Rev. Cancer* **2003**, *3*, 330–338.
- Lu, J.; Jiang, F.; Lu, A.; Zhang, G. Linkers Having a Crucial Role in Antibody–Drug Conjugates. *Int. J. Mol. Sci.* **2016**, *17*, 561.
- Ma, C.; Xia, F.; Kelley, S. O. Mitochondrial Targeting of Probes and Therapeutics to the Powerhouse of the Cell. *Bioconjug. Chem.* **2020**, *31*, 2650–2667.
- Mader, E. K.; Butler, G.; Dowdy, S. C.; Mariani, A.; Knutson, K. L.; Federspiel, M. J.; Russell, S. J.; Galanis, E.; Dietz, A. B.; Peng, K.-W. Optimizing Patient Derived Mesenchymal Stem Cells as Virus Carriers for a Phase I Clinical Trial in Ovarian Cancer. *J. Transl. Med.* **2013**, *11*, 20.
- Maeda, H. Macromolecular Therapeutics in Cancer Treatment: The EPR Effect and Beyond. *J Control Release* **2012**, *164*, 138–144.
- Magnani, M.; Rossi, L.; D’Ascenzo, M.; Panzani, I.; Bigi, L.; Zanella, A. Erythrocyte Engineering for Drug Delivery and Targeting. *Biotechnol. Appl. Biochem.* **1998**, *28*, 1–6.
- Mahal, L. K.; Yarema, K. J.; Bertozzi, C. R. Engineering Chemical Reactivity on Cell Surfaces Through Oligosaccharide Biosynthesis. *Science* **1997**, *276*, 1125–1128.
- Mantovani, A.; Allavena, P. The Interaction of Anticancer Therapies with Tumor-Associated Macrophages. *J. Exp. Med.* **2015**, *212*, 435–445.
- Matsumura, Y.; Kataoka, K. Preclinical and Clinical Studies of Anticancer Agent-incorporating Polymer Micelles. *Cancer Sci.* **2009**, *100*, 572–579.

- Miliotou, A. N.; Papadopoulou, L. C. CAR T-Cell Therapy: A New Era in Cancer Immunotherapy. *Curr. Pharm. Biotechnol.* **2018**, *19*, 5–18.
- Miller, M. A.; Zheng, Y.; Gadde, S.; Pfirschke, C.; Zope, H.; Engblom, C.; Kohler, R. H.; Iwamoto, Y.; Yang, K. S.; Askevold, B.; Kolishetti, N.; Pittet, M.; Lippard, S. J.; Farokhzad, O. C.; Weissleder, R. Tumour-Associated Macrophages Act as a Slow-Release Reservoir of Nano-Therapeutic Pt(IV) pro-Drug. *Nat. Commun.* **2015**, *6*, 8692.
- Miyake, M.; Lawton, A.; Goodison, S.; Urquidi, V.; Gomes, G. E.; Zhang, G.; Ross, S.; Kim, J.; Rosser, C.J. Chemokine (CXC) ligand 1 (CXCL1) protein expression is increased in aggressive bladder cancers. *BMC Cancer.* **2013**, *13*, 1-7.
- Mooney, R.; Roma, L.; Zhao, D.; Van Haute, D.; Garcia, E.; Kim, S. U.; Annala, A. J.; Aboody, K. S.; Berlin, J. M. Neural Stem Cell-Mediated Intratumoral Delivery of Gold Nanorods Improves Photothermal Therapy. *ACS Nano* **2014**, *8*, 12450–12460.
- Mooney, R.; Weng, Y.; Garcia, E.; Bhojane, S.; Smith-Powell, L.; Kim, S. U.; Annala, A. J.; Aboody, K. S.; Berlin, J. M. Conjugation of PH-Responsive Nanoparticles to Neural Stem Cells Improves Intratumoral Therapy. *J Control Release* **2014**, *191*, 82–89.
- Mooney, R.; Weng, Y.; Tirughana-Sambandan, R.; Valenzuela, V.; Aramburo, S.; Garcia, E.; Li, Z.; Gutova, M.; Annala, A. J.; Berlin, J. M.; Aboody, K. S. Neural Stem Cells Improve Intracranial Nanoparticle Retention and Tumor-Selective Distribution. *Future Oncol.* **2014**, *10*, 401–415.
- Motaln, H.; Schichor, C.; Lah, T. T. Human Mesenchymal Stem Cells and Their Use in Cell-Based Therapies. *Cancer* **2010**, *116*, 2519–2530.
- Mura, S.; Nicolas, J.; Couvreur, P. Stimuli-Responsive Nanocarriers for Drug Delivery. *Nat. Mater.* **2013**, *12*, 991–1003.
- Murad, K. L.; Mahany, K. L.; Brugnara, C.; Kuypers, F. A.; Eaton, J. W.; Scott, M. D. Structural and Functional Consequences of Antigenic Modulation of Red Blood Cells with Methoxypoly(Ethylene Glycol). *Blood* **1999**, *93*, 2121–2127.
- Murciano, J.-C.; Medinilla, S.; Eslin, D.; Atochina, E.; Cines, D. B.; Muzykantov, V. R. Prophylactic Fibrinolysis through Selective Dissolution of Nascent Clots by TPA-Carrying Erythrocytes. *Nat. Biotechnol.* **2003**, *21*, 891–896.
- Murdoch, C.; Giannoudis, A.; Lewis, C. E. Mechanisms Regulating the Recruitment of Macrophages into Hypoxic Areas of Tumors and Other Ischemic Tissues. *Blood* **2004**, *104*, 2224–2234.
- Muro, S. Challenges in Design and Characterization of Ligand-Targeted Drug Delivery Systems. *J. Control. Release* **2012**, *164*, 125–137.
- Muthana, M.; Giannoudis, A.; Scott, S. D.; Fang, H.-Y.; Coffelt, S. B.; Morrow, F. J.; Murdoch, C.; Burton, J.; Cross, N.; Burke, B.; Mistry, R.; Hamdy, F.; Brown, N. J.; Georgopoulos, L.; Hoskin, P.; Essand, M.; Lewis, C. E.; Maitland, N. J. Use of Macrophages to Target Therapeutic Adenovirus to Human Prostate Tumors. *Cancer Res.* **2011**, *71*, 1805–1815.

- Muthana, M.; Kennerley, A. J.; Hughes, R.; Fagnano, E.; Richardson, J.; Paul, M.; Murdoch, C.; Wright, F.; Payne, C.; Lythgoe, M. F.; Farrow, N.; Dobson, J.; Conner, J.; Wild, J. M.; Lewis, C. Directing Cell Therapy to Anatomic Target Sites in Vivo with Magnetic Resonance Targeting. *Nat. Commun.* **2015**, *6*, 8009.
- Muthana, M.; Rodrigues, S.; Chen, Y.-Y.; Welford, A.; Hughes, R.; Tazzyman, S.; Essand, M.; Morrow, F.; Lewis, C. E. Macrophage Delivery of an Oncolytic Virus Abolishes Tumor Regrowth and Metastasis after Chemotherapy or Irradiation. *Cancer Res.* **2013**, *73*, 490–495.
- Muzykantov, V. R. Drug Delivery by Red Blood Cells: Vascular Carriers Designed by Mother Nature. *Expert Opin. Drug Deliv.* **2010**, *7*, 403–427.
- Neuwelt, E.; Abbott, N. J.; Abrey, L.; Banks, W. A.; Blakley, B.; Davis, T.; Engelhardt, B.; Grammas, P.; Nedergaard, M.; Nutt, J.; Pardridge, W.; Rosenberg, G. A.; Smith, Q.; Drewes, L. R. Strategies to Advance Translational Research into Brain Barriers. *Lancet Neurol.* **2008**, *7*, 84–96.
- Newick, K.; O'Brien, S.; Moon, E.; Albelda, S. M. CAR T Cell Therapy for Solid Tumors. *Annu. Rev. Med.* **2017**, *68*, 139–152.
- Ni, Z.; Zhou, L.; Li, X.; Zhang, J.; Dong, S. Tetrazine-Containing Amino Acid for Peptide Modification and Live Cell Labeling. *PLoS ONE* **2015**, *10*, e0141918.
- Oliveira, M. B.; Hatami, J.; Mano, J. F. Coating Strategies Using Layer-by-Layer Deposition for Cell Encapsulation. *Chem. Asian J.* **2016**, *11*, 1753–1764.
- Owen, J. L.; Mohamadzadeh, M. Macrophages and Chemokines as Mediators of Angiogenesis. *Front. Physiol.* **2013**, *4*.
- Pang, L.; Qin, J.; Han, L.; Zhao, W.; Liang, J.; Xie, Z.; Yang, P.; Wang, J. Exploiting Macrophages as Targeted Carrier to Guide Nanoparticles into Glioma. *Oncotarget* **2016**, *7*, 37081–37091.
- Park, J. S.; Suryaprakash, S.; Lao, Y.-H.; Leong, K. W. Engineering Mesenchymal Stem Cells for Regenerative Medicine and Drug Delivery. *Methods* **2015**, *84*, 3–16.
- Park, J.; Andrade, B.; Seo, Y.; Kim, M.-J.; Zimmerman, S. C.; Kong, H. Engineering the Surface of Therapeutic “Living” Cells. *Chem. Rev.* **2018**, *118*, 1664–1690.
- Parveen, S.; Mishra, R.; Sahoo, S. K. Nanoparticles: A Boon to Drug Delivery, Therapeutics, Diagnostics and Imaging. *Nanomed. Nanotechnol. Biol. Med.* **2012**, *8*, 147–166.
- Patil, U. S.; Qu, H.; Caruntu, D.; O'Connor, C. J.; Sharma, A.; Cai, Y.; Tarr, M. A. Labeling Primary Amine Groups in Peptides and Proteins with *N*-Hydroxysuccinimidyl Ester Modified Fe₃O₄@SiO₂ Nanoparticles Containing Cleavable Disulfide-Bond Linkers. *Bioconjug. Chem.* **2013**, *24*, 1562–1569.
- Perrigue, P. M.; Silva, M. E.; Warden, C. D.; Feng, N. L.; Reid, M. A.; Mota, D. J.; Joseph, L. P.; Tian, Y. I.; Glackin, C. A.; Gutova, M.; Najbauer, J.; Aboody, K. S.; Barish, M. E.

- The Histone Demethylase Jumonji Coordinates Cellular Senescence Including Secretion of Neural Stem Cell-Attracting Cytokines. *Mol. Cancer Res.* **2015**, *13*, 636–650.
- Pierigè, F.; Serafini, S.; Rossi, L.; Magnani, M. Cell-Based Drug Delivery. *Adv. Drug Deliv. Rev.* **2008**, *60*, 286–295.
- Pixley, F. J.; Stanley, E. R. CSF-1 Regulation of the Wandering Macrophage: Complexity in Action. *Trends Cell Biol.* **2004**, *14*, 628–638.
- Polak, R.; Lim, R. M.; Beppu, M. M.; Pitombo, R. N. M.; Cohen, R. E.; Rubner, M. F. Liposome-Loaded Cell Backpacks. *Adv. Healthcare Mater.* **2015**, *4*, 2832–2841.
- Pollard, J. W. Tumour-Educated Macrophages Promote Tumour Progression and Metastasis. *Nat. Rev. Cancer* **2004**, *4*, 71–78.
- Porada, C. D.; Almeida-Porada, G. Mesenchymal Stem Cells as Therapeutics and Vehicles for Gene and Drug Delivery. *Adv. Drug Deliv. Rev.* **2010**, *62*, 1156–1166.
- Porada, C.; Zanjani, E.; Almeida-Porada, G. Adult Mesenchymal Stem Cells: A Pluripotent Population with Multiple Applications. *Curr. Stem Cell Res. Ther.* **2006**, *1*, 365–369.
- Portnow, J.; Synold, T. W.; Badie, B.; Tirughana, R.; Lacey, S. F.; D’Apuzzo, M.; Metz, M. Z.; Najbauer, J.; Bedell, V.; Vo, T.; Gutova, M.; Frankel, P.; Chen, M.; Aboody, K. S. Neural Stem Cell-Based Anticancer Gene Therapy: A First-in-Human Study in Recurrent High-Grade Glioma Patients. *Clin. Cancer Res.* **2017**, *23*, 2951–2960.
- Pulaski, B. A.; Ostrand-Rosenberg, S. Mouse 4T1 Breast Tumor Model. *Curr. Protoc. Immunol.* **2000**, *39*, 20.
- Qian, B.; Deng, Y.; Im, J. H.; Muschel, R. J.; Zou, Y.; Li, J.; Lang, R. A.; Pollard, J. W. A Distinct Macrophage Population Mediates Metastatic Breast Cancer Cell Extravasation, Establishment and Growth. *PLoS ONE* **2009**, *4*, 6562.
- Qian, B.-Z.; Li, J.; Zhang, H.; Kitamura, T.; Zhang, J.; Campion, L. R.; Kaiser, E. A.; Snyder, L. A.; Pollard, J. W. CCL2 Recruits Inflammatory Monocytes to Facilitate Breast-Tumour Metastasis. *Nature* **2011**, *475*, 222–225.
- Qian, B.-Z.; Pollard, J. W. Macrophage Diversity Enhances Tumor Progression and Metastasis. *Cell* **2010**, *141*, 39–51.
- Rabuka, D.; Forstner, M. B.; Groves, J. T.; Bertozzi, C. R. Noncovalent Cell Surface Engineering: Incorporation of Bioactive Synthetic Glycopolymers into Cellular Membranes. *J. Am. Chem. Soc.* **2008**, *130*, 5947–5953.
- Rajabzadeh, N.; Fathi, E.; Farahzadi, R. Stem Cell-Based Regenerative Medicine. *Stem Cell Investig.* **2019**, *6*, 19.
- Rakic, P. Evolution of the Neocortex: A Perspective from Developmental Biology. *Nat. Rev. Neurosci.* **2009**, *10*, 724–735.
- Rana, S.; Bajaj, A.; Mout, R.; Rotello, V. M. Monolayer Coated Gold Nanoparticles for Delivery Applications. *Adv. Drug Deliv. Rev.* **2012**, *64*, 200–216.

- Richardsen, E.; Uglehus, R. D.; Johnsen, S. H.; Busund, L.-T. Macrophage-Colony Stimulating Factor (CSF1) Predicts Breast Cancer Progression and Mortality. *Anticancer Res.* **2015**, 865–874.
- Ries, C. H.; Cannarile, M. A.; Hoves, S.; Benz, J.; Wartha, K.; Runza, V.; Rey-Giraud, F.; Pradel, L. P.; Feuerhake, F.; Klaman, I.; Jones, T.; Jucknischke, U.; Scheiblich, S.; Kaluza, K.; Gorr, I. H.; Walz, A.; Abiraj, K.; Cassier, P. A.; Sica, A.; Gomez-Roca, C.; de Visser, K. E.; Italiano, A.; Le Tourneau, C.; Delord, J.-P.; Levitsky, H.; Blay, J.-Y.; Rüttinger, D. Targeting Tumor-Associated Macrophages with Anti-CSF-1R Antibody Reveals a Strategy for Cancer Therapy. *Cancer Cell* **2014**, 25, 846–859.
- Rodriguez, L. G.; Wu, X.; Guan, J.-L. Wound-Healing Assay. *Cell Migr.* **2004**, 294, 023–030.
- Rosenblum, D.; Joshi, N.; Tao, W.; Karp, J. M.; Peer, D. Progress and Challenges towards Targeted Delivery of Cancer Therapeutics. *Nat. Commun.* **2018**, 9, 1410
- Rossi, N. A. A.; Constantinescu, I.; Kainthan, R. K.; Brooks, D. E.; Scott, M. D.; Kizhakkedathu, J. N. Red Blood Cell Membrane Grafting of Multi-Functional Hyperbranched Polyglycerols. *Biomaterials* **2010**, 31, 4167–4178.
- Saha, K.; Agasti, S. S.; Kim, C.; Li, X.; Rotello, V. M. Gold Nanoparticles in Chemical and Biological Sensing. *Chem. Rev.* **2012**, 112, 2739–2779.
- Salgaller, M. L.; Tjoa, B. A.; Lodge, P. A.; Ragde, H.; Kenny, G.; Boynton, A.; Murphy, G. P. Dendritic Cell-Based Immunotherapy of Prostate Cancer. *Crit. Rev. Immunol.* **1998**, 18, 109–119.
- Sampathkumar, S.-G.; Li, A. V.; Jones, M. B.; Sun, Z.; Yarema, K. J. Metabolic Installation of Thiols into Sialic Acid Modulates Adhesion and Stem Cell Biology. *Nat. Chem. Biol.* **2006**, 2, 149–152.
- Sancho-albero, M.; Rubio-ruiz, B.; Pérez-lópez, A. M.; Sebastián, V.; Martín-duque, P.; Arruebo, M.; Santamaría, J.; Unciti-broceta, A. Cancer-Derived Exosomes Loaded with Ultrathin Palladium Nanosheets for Targeted Bioorthogonal Catalysis. *Nat. Catal.* **2019**, 2, 864–872.
- Sarkar, D.; Spencer, J. A.; Phillips, J. A.; Zhao, W.; Schafer, S.; Spelke, D. P.; Mortensen, L. J.; Ruiz, J. P.; Vemula, P. K.; Sridharan, R.; Kumar, S.; Karnik, R.; Lin, C. P.; Karp, J. M. Engineered Cell Homing. *Blood* **2011**, 118, 184–191.
- Sarkar, D.; Vemula, P. K.; Teo, G. S. L.; Spelke, D.; Karnik, R.; Wee, L. Y.; Karp, J. M. Chemical Engineering of Mesenchymal Stem Cells to Induce a Cell Rolling Response. *Bioconj. Chem.* **2008**, 19, 2105–2109.
- Saxon, E.; Bertozzi, C. R. Cell Surface Engineering by a Modified Staudinger Reaction. *Science* **2000**, 287, 2007–2010.
- Schiwon, M.; Weisheit, C.; Franken, L.; Gutweiler, S.; Dixit, A.; Meyer-Schwesinger, C.; Pohl, J.-M.; Maurice, N. J.; Thiebes, S.; Lorenz, K.; Quast, T.; Fuhrmann, M.; Baumgarten, G.; Lohse, M. J.; Opendakker, G.; Bernhagen, J.; Bucala, R.; Panzer, U.; Kolanus, W.;

Gröne, H.-J.; Garbi, N.; Kastenmüller, W.; Knolle, P. A.; Kurts, C.; Engel, D. R. Crosstalk between Sentinel and Helper Macrophages Permits Neutrophil Migration into Infected Uroepithelium. *Cell* **2014**, *156*, 456–468.

Schmaljohann, D. Thermo- and pH-Responsive Polymers in Drug Delivery. *Adv. Drug Deliv. Rev.* **2006**, *58*, 1655–1670.

Schnarr, K.; Mooney, R.; Weng, Y.; Zhao, D.; Garcia, E.; Armstrong, B.; Annala, A. J.; Kim, S. U.; Aboody, K. S.; Berlin, J. M. Gold Nanoparticle-Loaded Neural Stem Cells for Photothermal Ablation of Cancer. *Adv. Health. Mater.* **2013**, *2*, 976–982.

Scott, M. D.; Chen, A. M. Beyond the Red Cell: Pegylation of Other Blood Cells and Tissues. *Transfus. Clin. Biol.* **2004**, *11*, 40–46.

Shahar, T.; Rozovski, U.; Hess, K. R.; Hossain, A.; Gumin, J.; Gao, F.; Fuller, G. N.; Goodman, L.; Sulman, E. P.; Lang, F. F. Percentage of Mesenchymal Stem Cells in High-Grade Glioma Tumor Samples Correlates with Patient Survival. *Neurooncol.* **2017**, *19*, 660–668.

Shi, P.; Ju, E.; Yan, Z.; Gao, N.; Wang, J.; Hou, J.; Zhang, Y.; Ren, J.; Qu, X. Spatiotemporal Control of Cell–Cell Reversible Interactions Using Molecular Engineering. *Nat. Commun.* **2016**, *7*, 13088.

Simon, G. H.; Daldrup-Link, H. E.; Kau, J.; Metz, S.; Schlegel, J.; Piontek, G.; Saborowski, O.; Demos, S.; Duyster, J.; Pichler, B. J. Optical Imaging of Experimental Arthritis Using Allogeneic Leukocytes Labeled with a Near-Infrared Fluorescent Probe. *Eur. J. Nucl. Med. Mol. Imaging* **2006**, *33*, 998–1006.

Sletten, E. M.; Bertozzi, C. R. Bioorthogonal Chemistry: Fishing for Selectivity in a Sea of Functionality. *Angew. Chemie Int. Ed.* **2009**, *48*, 6974–6998.

Smith, B. R.; Ghosn, E. E. B.; Rallapalli, H.; Prescher, J. A.; Larson, T.; Herzenberg, L. A.; Gambhir, S. S. Selective Uptake of Single-Walled Carbon Nanotubes by Circulating Monocytes for Enhanced Tumour Delivery. *Nat. Nanotechnol.* **2014**, *9*, 481–487.

Sousa, S.; Brion, R.; Lintunen, M.; Kronqvist, P.; Sandholm, J.; Mönkkönen, J.; Kellokumpu-Lehtinen, P.-L.; Lanttia, S.; Tynnininen, O.; Joensuu, H.; Heymann, D.; Määttä, J. A. Human Breast Cancer Cells Educate Macrophages toward the M2 Activation Status. *Breast Cancer Res.* **2015**, *17*, 101.

Spiller, K. L.; Koh, T. J. Macrophage-Based Therapeutic Strategies in Regenerative Medicine. *Adv. Drug Deliv. Rev.* **2017**, *122*, 74–83.

Springer, C. J.; Niculescu-Duvaz, I. Prodrug-Activating Systems in Suicide Gene Therapy. *J. Clin. Invest.* **2000**, *105*, 1161–1167.

Steinberg, G. K.; Kondziolka, D.; Wechsler, L. R.; Lunsford, L. D.; Coburn, M. L.; Billigen, J. B.; Kim, A. S.; Johnson, J. N.; Bates, D.; King, B.; Case, C.; McGrogan, M.; Yankee, E. W.; Schwartz, N. E. Clinical Outcomes of Transplanted Modified Bone Marrow-Derived Mesenchymal Stem Cells in Stroke: A Phase 1/2a Study. *Stroke* **2016**, *47*, 1817–1824.

- Stephan, M. T.; Moon, J. J.; Um, S. H.; Bershteyn, A.; Irvine, D. J. Therapeutic Cell Engineering with Surface-Conjugated Synthetic Nanoparticles. *Nat. Med.* **2010**, *16*, 1035–1041.
- Sternberg, N.; Georgieva, R.; Duft, K.; Bäuml, H. Surface-Modified Loaded Human Red Blood Cells for Targeting and Delivery of Drugs. *J. Microencapsul.* **2012**, *29*, 9–20.
- Studený, M.; Marini, F. C.; Champlin, R. E.; Zompetta, C.; Fidler, I. J.; Andreeff, M. Bone Marrow-Derived Mesenchymal Stem Cells as Vehicles for Interferon- β Delivery into Tumors. *Cancer Res.* **2002**, *62*, 3603–3608.
- Su, S.; Liu, Q.; Chen, J.; Chen, J.; Chen, F.; He, C.; Huang, D.; Wu, W.; Lin, L.; Huang, W.; Zhang, J.; Cui, X.; Zheng, F.; Li, H.; Yao, H.; Su, F.; Song, E. A Positive Feedback Loop between Mesenchymal-like Cancer Cells and Macrophages Is Essential to Breast Cancer Metastasis. *Cancer Cell* **2014**, *25*, 605–620.
- Su, Y.; Xie, Z.; Kim, G. B.; Dong, C.; Yang, J. Design Strategies and Applications of Circulating Cell-Mediated Drug Delivery Systems. *ACS Biomater. Sci. Eng.* **2015**, *1*, 201–217.
- Suetsugu, A.; Katz, M.; Fleming, J.; Truty, M.; Thomas, R.; Saji, S.; Moriwaki, H.; Bouvet, M.; Hoffman, R. M. Non-Invasive Fluorescent-Protein Imaging of Orthotopic Pancreatic-Cancer-Patient Tumorgraft Progression in Nude Mice. *Anticancer Res.* **2012**, *32*, 3063–3068.
- Sugimoto, S.; Iwasaki, Y. Surface Modification of Macrophages with Nucleic Acid Aptamers for Enhancing the Immune Response against Tumor Cells. *Bioconjug. Chem.* **2018**, *29*, 4160–4167.
- Sun, X.; Wang, C.; Gao, M.; Hu, A.; Liu, Z. Remotely Controlled Red Blood Cell Carriers for Cancer Targeting and Near-Infrared Light-Triggered Drug Release in Combined Photothermal-Chemotherapy. *Adv. Funct. Mater.* **2015**, *25*, 2386–2394.
- Sykes, E. A.; Chen, J.; Zheng, G.; Chan, W. C. W. Investigating the Impact of Nanoparticle Size on Active and Passive Tumor Targeting Efficiency. *ACS Nano* **2014**, *8*, 5696–5706.
- Taciak, B.; Białasek, M.; Braniewska, A.; Sas, Z.; Sawicka, P.; Kiraga, Ł.; Rygiel, T.; Król, M. Evaluation of Phenotypic and Functional Stability of RAW 264.7 Cell Line through Serial Passages. *PLoS ONE* **2018**, *13*, 1–13.
- Teramura, Y.; Kaneda, Y.; Totani, T.; Iwata, H. Behavior of Synthetic Polymers Immobilized on a Cell Membrane. *Biomaterials* **2008**, *29*, 1345–1355.
- The Cancer Genome Atlas Network. Comprehensive Molecular Portraits of Human Breast Tumours. *Nature* **2012**, *490*, 61–70.
- Tonga, G. Y.; Jeong, Y.; Duncan, B.; Mizuhara, T.; Mout, R.; Das, R.; Kim, S. T.; Yeh, Y.-C.; Yan, B.; Hou, S.; Rotello, V. M. Supramolecular Regulation of Bioorthogonal Catalysis in Cells Using Nanoparticle-Embedded Transition Metal Catalysts. *Nat. Chem.* **2015**, *7*, 597.

- Tran Cao, H. S.; Reynoso, J.; Yang, M.; Kimura, H.; Kaushal, S.; Snyder, C. S.; Hoffman, R. M.; Bouvet, M. Development of the Transgenic Cyan Fluorescent Protein (CFP)-Expressing Nude Mouse for “Technicolor” Cancer Imaging. *J. Cell. Biochem.* **2009**, *107*, 328–334.
- Van de L’Isle, M. O. N.; Ortega-Liebana, M. C.; Unciti-Broceta, A. Transition Metal Catalysts for the Bioorthogonal Synthesis of Bioactive Agents. *Curr. Opin. Chem. Biol.* **2021**, *61*, 32–42.
- Vaupel, P.; Rallino, F.; Okunieff, P. Blood Flow, Oxygen and Nutrient Supply, and Metabolic Microenvironment of Human Tumors: A Review. *Cancer Res.* **1989**, *49*, 6449–6465.
- Völker, T.; Dempwolff, F.; Graumann, P. L.; Meggers, E. Progress towards Bioorthogonal Catalysis with Organometallic Compounds. *Angew. Chemie Int. Ed.* **2014**, *53*, 10536–10540.
- Völker, T.; Meggers, E. Transition-Metal-Mediated Uncaging in Living Human Cells—an Emerging Alternative to Photolabile Protecting Groups. *Curr. Opin. Chem. Biol.* **2015**, *25*, 48–54.
- Wagers, A. J.; Weissman, I. L. Plasticity of Adult Stem Cells. *Cell* **2004**, *116*, 639–648.
- Wan, D. H.; Ma, X. Y.; Lin, C.; Zhu, D. H.; Li, X.; Zheng, B. Y.; Li, J.; Ke, M. R.; Huang, J. D. Noncovalent Indocyanine Green Conjugate of C-Phycocyanin: Preparation and Tumor-Associated Macrophages-Targeted Photothermal Therapeutics. *Bioconjug. Chem.* **2020**, *31*, 1438–1448.
- Wang, C.; Sun, X.; Cheng, L.; Yin, S.; Yang, G.; Li, Y.; Liu, Z. Multifunctional Theranostic Red Blood Cells for Magnetic-Field-Enhanced in Vivo Combination Therapy of Cancer. *Adv. Mater.* **2014**, *26*, 4794–4802.
- Wang, Q.; Cheng, H.; Peng, H.; Zhou, H.; Li, P. Y.; Langer, R. Non-Genetic Engineering of Cells for Drug Delivery and Cell-Based Therapy. *Adv. Drug Deliv. Rev.* **2015**, *91*, 125–140.
- Wang, T. P.; Hwang, Y. J.; Chen, Y. H. Versatile Phosphoramidation Reactions for Nucleic Acid Conjugations with Peptides, Proteins, Chromophores, and Biotin Derivatives. *Bioconj. Chem.* **2010**, *21*, 1642–1655.
- Wang, W.; Zhang, X.; Huang, R.; Hirschi, C. M.; Wang, H.; Ding, Y.; Rotello, V. M. In Situ Activation of Therapeutics through Bioorthogonal Catalysis. *Adv. Drug Deliv. Rev.* **2021**, *176*, 113893.
- Weischenfeldt, J.; Porse, B. Bone Marrow-Derived Macrophages (BMM): Isolation and Applications. *Cold Spring Harb. Protoc.* **2008**, *2008* (12).
- Weiss, J. T.; Dawson, J. C.; Macleod, K. G.; Rybski, W.; Fraser, C.; Torres-Sánchez, C.; Patton, E. E.; Bradley, M.; Carragher, N. O.; Unciti-Broceta, A. Extracellular Palladium-Catalysed Dealkylation of 5-Fluoro-1-Propargyl-Uracil as a Bioorthogonally Activated Prodrug Approach. *Nat. Commun.* **2014**, *5*, 3277.

- Weissleder, R.; Nahrendorf, M.; Pittet, M. J. Imaging Macrophages with Nanoparticles. *Nature Mater.* **2014**, *13*, 125–138.
- Wilchek, M.; Bayer, E. A. Introduction to Avidin-Biotin Technology. *Methods Enzymol.* **1990**, *184*, 5–13.
- Wilhelm, S.; Tavares, A. J.; Dai, Q.; Ohta, S.; Audet, J.; Dvorak, H. F.; Chan, W. C. W. Analysis of Nanoparticle Delivery to Tumours. *Nat. Rev. Mater.* **2016**, *1*, 16014.
- Wilson, J. T.; Krishnamurthy, V. R.; Cui, W.; Qu, Z.; Chaikof, E. L. Noncovalent Cell Surface Engineering with Cationic Graft Copolymers. *J. Am. Chem. Soc.* **2009**, *131*, 18228–18229.
- Wu, J.; Wang, X.; Wang, Q.; Lou, Z.; Li, S.; Zhu, Y.; Qin, L.; Wei, H. Nanomaterials with Enzyme-like Characteristics (Nanozymes): Next-Generation Artificial Enzymes (II). *Chem. Soc. Rev.* **2019**, *48*, 1004–1076.
- Wyckoff, J. B.; Wang, Y.; Lin, E. Y.; Li, J.; Goswami, S.; Stanley, E. R.; Segall, J. E.; Pollard, J. W.; Condeelis, J. Direct Visualization of Macrophage-Assisted Tumor Cell Intravasation in Mammary Tumors. *Cancer Res.* **2007**, *67*, 2649–2656.
- Xie, Q.-P.; Huang, H.; Xu, B.; Dong, X.; Gao, S.-L.; Zhang, B.; Wu, Y.-L. Human Bone Marrow Mesenchymal Stem Cells Differentiate into Insulin-Producing Cells upon Microenvironmental Manipulation in Vitro. *Differen.* **2009**, *77*, 483–491.
- Xie, R.; Hong, S.; Feng, L.; Rong, J.; Chen, X. Cell-Selective Metabolic Glycan Labeling Based on Ligand-Targeted Liposomes. *J. Am. Chem. Soc.* **2012**, *134*, 9914–9917.
- Xie, Z.; Zhang, Y.; Liu, L.; Weng, H.; Mason, R. P.; Tang, L.; Nguyen, K. T.; Hsieh, J.-T.; Yang, J. Development of Intrinsically Photoluminescent and Photostable Polylactones. *Adv. Mater.* **2014**, *26*, 4491–4496.
- Yan, F.; Li, X.; Li, N.; Zhang, R.; Wang, Q.; Ru, Y.; Hao, X.; Ni, J.; Wang, H.; Wu, G. Immunoproapoptotic Molecule ScFv-Fdt-TBid Modified Mesenchymal Stem Cells for Prostate Cancer Dual-Targeted Therapy. *Cancer Lett.* **2017**, *402*, 32–42.
- Yang, M.; Li, L.; Jiang, P.; Moossa, A. R.; Penman, S.; Hoffman, R. M. Dual-Color Fluorescence Imaging Distinguishes Tumor Cells from Induced Host Angiogenic Vessels and Stromal Cells. *Proc. Natl. Acad. Sci. U. S. A.* **2003**, *100*, 14259–14262.
- Yang, M.; Reynoso, J.; Bouvet, M.; Hoffman, R. M. A Transgenic Red Fluorescent Protein-Expressing Nude Mouse for Color-Coded Imaging of the Tumor Microenvironment. *J. Cell. Biochem.* **2009**, *106*, 279–284.
- Yang, M.; Reynoso, J.; Jiang, P.; Li, L.; Moossa, A. R.; Hoffman, R. M. Transgenic Nude Mouse with Ubiquitous Green Fluorescent Protein Expression as a Host for Human Tumors. *Cancer Res.* **2004**, *64*, 8651–8656.

Yu, W.; Chen, J.; Xiong, Y.; Pixley, F. J.; Yeung, Y.-G.; Stanley, E. R. Macrophage Proliferation Is Regulated through CSF-1 Receptor Tyrosines 544, 559, and 807. *J. Biol. Chem.* **2012**, *287*, 13694–13704.

Yusop, R. M.; Unciti-Broceta, A.; Johansson, E. M. V; Sánchez-Martín, R. M.; Bradley, M. Palladium-Mediated Intracellular Chemistry. *Nat. Chem.* **2011**, *3*, 239–243.

Zhang, X.; Fedeli, S.; Gopalakrishnan, S.; Huang, R.; Gupta, A.; Luther, D. C.; Rotello, V. M. Protection and Isolation of Bioorthogonal Metal Catalysts by Using Monolayer-Coated Nanozymes. *ChemBioChem* **2020**, *21*, 2759–2763.

Zhang, X.; Huang, R.; Gopalakrishnan, S.; Cao-milán, R.; Rotello, V. M. Bioorthogonal Nanozymes: Progress towards Therapeutic Applications. *Trends Chem.* **2019**, *1*, 90–98.

Zhang, X.; Landis, R. F.; Keshri, P.; Cao-Milán, R.; Luther, D. C.; Gopalakrishnan, S.; Liu, Y.; Huang, R.; Li, G.; Malassiné, M.; Uddin, I.; Rondon, B.; Rotello, V. M. Intracellular Activation of Anticancer Therapeutics Using Polymeric Bioorthogonal Nanocatalysts. *Adv. Healthc. Mater.* **2021**, 2001627.

Zhang, X.; Liu, Y.; Gopalakrishnan, S.; Castellanos-Garcia, L.; Li, G.; Malassine, M.; Uddin, I.; Huang, R.; Luther, D. C.; Vachet, R. W.; Rotello, V. M. Intracellular Activation of Bioorthogonal Nanozymes through Endosomal Proteolysis of the Protein Corona. *ACS Nano* **2020**, *14*, 4767–4773.

Zhang, Y.; Cheng, S.; Zhang, M.; Zhen, L.; Pang, D.; Zhang, Q.; Li, Z. High-Infiltration of Tumor-Associated Macrophages Predicts Unfavorable Clinical Outcome for Node-Negative Breast Cancer. *PLoS ONE* **2013**, *8*, 1-8.

Zhao, D.; Najbauer, J.; Annala, A. J.; Garcia, E.; Metz, M. Z.; Gutova, M.; Polewski, M. D.; Gilchrist, M.; Glackin, C. A.; Kim, S. U.; Aboody, K. S. Human Neural Stem Cell Tropism to Metastatic Breast Cancer. *Stem Cells* **2012**, *30*, 314–325.

Zhao, Y.; J. Haney, M. Active Targeted Macrophage-Mediated Delivery of Catalase to Affected Brain Regions in Models of Parkinson's Disease. *J. Nanomed. Nanotechnol.* **2011**, *4*, 1-8.